12-2021

IDENTIFYING AN OPTIMIZATION TECHNIQUE FOR MAKER USAGE TO ADDRESS COVID-19 SUPPLY SHORTFALLS

Michael J. Wilson
University of Tennessee, Knoxville, mwils107@vols.utk.edu

To the Graduate Council:

I am submitting herewith a dissertation written by Michael J. Wilson entitled "IDENTIFYING AN OPTIMIZATION TECHNIQUE FOR MAKER USAGE TO ADDRESS COVID-19 SUPPLY SHORTFALLS." I have examined the final electronic copy of this dissertation for form and content and recommend that it be accepted in partial fulfillment of the requirements for the degree of Doctor of Philosophy, with a major in Industrial Engineering.

Andrew Yu, Major Professor

We have read this dissertation and recommend its acceptance:

Zhongshun Shi, James Simonton, Feng Yuan Zhang

Accepted for the Council:

Dixie L. Thompson

Vice Provost and Dean of the Graduate School

(Original signatures are on file with official student records.)

Identifying an Optimization Technique for Maker Usage to Address Covid-19 Supply Shortfalls

A Dissertation Presented for the

Doctor of Philosophy

Degree

The University of Tennessee, Knoxville

Michael J. Wilson
December 2021

ISBN:

ISBN-13:

ACKNOWLEDGEMENTS

Throughout my PhD classes, my research, and the writing of this dissertation I have received significant support and assistance.

I would like to thank my dissertation advisor, Dr. Andrew Yu, whose guidance, and feedback was instrumental in the composition of this research. It was through Dr. Yu's willingness to constantly answer my questions that I was able to focus on my research.

I would like to thank all my colleagues at Austin Peay State University that assisted and advised me during my PhD classes and my research. I would especially like to thank Dr. Raman Sahi who always made time to tutor me in mathematical and statistical classes and answer questions. Without her assistance and tutelage, I would not have been able to complete many of my classes successfully.

Most importantly, I would like to thank my family. My children Braxton and Alex, you have always been and will always be an inspiration to me. I could not be prouder of you both. I would like to thank my parents who raised me to love science and to always ask why. Some of my fondest memories as a child were fishing with my dad and going to museums with my mom. Lastly, I would like to thank my wife, Tara, whose love, and support have saved my life both figuratively and literally. You kept me going when I wanted to quit. I love you.

ABSTRACT

Fused Deposition Modeling (FDM) can be purchased for under five hundred dollars. The availability of these inexpensive systems has created a large hobbyist (or maker) community. For makers, FDM printing is used numerous uses.

With the onset of the COVID-19 pandemic, the needs for Personal Protective Equipment (PPE) skyrocketed. COVID-19 mitigation strategies such as social distancing, businesses closures, and shipping delays created significant supply shortfalls. The maker community stepped in to fill gaps in PPE supplies.

In the case of 3DP, optimization remains the domain of commercial entities. Optimization is, at best, ad-hoc for makers. With the need to PPE supplies and COVID-19 related supply delays, optimization techniques would be of great value to makers.

The objective functions in this research is throughput and cost with quality factored into both. There are several parameters common to both throughput and surface roughness, including layer thickness, print speed, infill density, raster width, and wall thickness. This research will utilize a 2-level fractional factorial design.

Least Squares Regression (OLS) will be completed on throughput and cost independently. Quality will be considered a component of both. For example, an OLS will be completed for the throughput to determine the effects of the process parameters on throughput. Using a 95% confidence interval, a process parameter with a P-value smaller that .05 will show that the process parameter has a significant effect on the throughput. Upon completion of each OLS model ϵ-Contraint methodology will be used

to jointly optimize the process parameters. Validation trials will be completed to test the optimized process parameters. The results will be documented and discussed.

PREFACE

The basis of this research stems from my work early in the COVID-19 pandemic. I was part of a team to use 3D printers to create face shields for first responders and medical personnel. One of the ongoing problems throughout the project was securing resources. With production and shipping from China heavily impacted, we needed to do more with less. At the height of the project, tools and methods to easily optimize print parameters would have been invaluable. Unfortunately, many optimization techniques remain the domain of engineers and industry.

The focus of this research is to identify optimization methods that can be accessed by the maker community. In a review of the literature, ϵ-constraints methodology has not previously been utilized. This method and the use of open-source tools to execute the analysis offer an option for makers.

TABLE OF CONTENTS

LIST OF TABLES

LIST OF FIGURES

ABBREVIATIONS

List of Key Abbreviations

- 3D - Three-Dimensional
- 3DP - Three-Dimensional Printing
- aid - Actual Infill Density
- alh - Actual Layer Height
- AM - Additive Manufacturing
- ANOVA - Analysis of Variance
- aps - Actual Print Speed
- arw - Actual Raster Width
- awt - Actual Wall Thickness
- CAD - Computer Aided Design
- CR6 - Creality CR6 SE Printer
- DOE - Design of Experiments
- FDM - Fused Deposition Modeling
- id - Infill Density
- lh - Layer Height
- OLS - Ordinary Least Squares Regression
- PLA - Polylactic Acid Filament
- PPE - Personal Protective Equipment
- ps - Print Speed
- RC - Release Candidate

- RSM - Response Surface Methodology
- rw - Raster Width
- SWX1 - Artillery Sidewinder X1 Printer
- TEMA - Tennessee Emergency Management Agency
- THEC - Tennessee Higher Education Commission
- wt - Wall Thickness

1 — CHAPTER ONE - INTRODUCTION AND GENERAL INFORMATION

1.1 — INTRODUCTION TO AM

Traditional manufacturing utilizes subtractive processes. The part geometry is created by removing material. Subtractive processes include injection molding, metal casting, and conventional machining processes (Bhushan & Caspers, 2017). Although there are numinous types of additive manufacturing (AM), commonly referred to as 3D printing, most methods deposit a material and build an object layer-by-layer (Yoon et al., 2014). Typically, a model of the object is created is a computer aided design (CAD) software. This model is then “printed”.

AM can be utilized for a wide range of manufacturing initiatives; current literature highlights several applications. According to (Ngo, Kashani, Imbalzano, Nguyen, & Hui, 2018), there are several trending applications for AM. These applications include:

- Biomaterials
- Aerospace
- Buildings
- Protective Structures

AM offers several benefits over traditional manufacturing. These benefits include:

- Reduced Materials (Bhushan & Caspers, 2017)

- Rapid Prototyping - the results of a print test is an actual part (Kruth, Mercelis, Van Vaerenbergh, Froyen, & Rombouts, 2005)
- Multi-material parts and biomedical objects including organs (Bose, Vahabzadeh, & Bandyopadhyay, 2013)
- Idea for Small orders (Bhushan & Caspers, 2017)

Although AM is a promising technology, it has several drawbacks. As noted previously, AM can be efficient and cost effective for small orders. Because of excessive print times, AM can be less effective that traditional manufacturing. The layer-by-layer approach to AM can also be problematic in terms of quality control (Bhushan & Caspers, 2017), cost control, and large volume projects.

AM offers the manufacturing industry many benefits both economically and in processing. Of particular interest is the usage of 3D printers to create prototypes and for small-scale production.

With the rise in AM, the number of hobbyist/prosumer 3D printers available. This availability coincides with the maker movement.

1.2 — The Maker Community and COVID-19

The description of the maker movement is broad. The definition is based on an individual's ability to be a creator of things. This individual is a maker. This growing community of hobbyists and professionals with diverse skills, backgrounds, and interests make their own functional devices. These devices can be technological, or craft based, such as home decor (Papavlasopoulou, Giannakos, & Jaccheri, 2017).

By using shared tools, technology, and experience makers have the potential act as producers in the sharing economy. Makers can also increase entrepreneurship, advanced manufacturing, and spur economic growth (Browder, Aldrich, & Bradley, 2019).

According to Browder et al. (2019), three features set the maker movement apart from past eras of craft making:

"(1) a high level of social exchange and collaboration among diverse actors, (2) enhanced knowledge creation and sharing in physical or virtual spaces, and (3) the production of material artifacts using technological resources previously restricted to corporate research and development (R&D) facilities"

When 3D printers are used by hobbyists, makers, and enthusiast, most use a typical workflow (Figure 1). The decision on a successful print is a visual inspection. A visual inspection is subjective and makes true optimization difficult.

The maker community can be limited by the lack of printable material. Traditional Design of Experiments (DOE) requires numerous runs and samples to identify an optimal solution. For example, to investigate optimizing for quality, cost, and speed using 4 print parameters, approximately 160 models would need to be printed. In a setting outside of industry. This is a prohibitive cost. A new workflow is described in Figure 2.

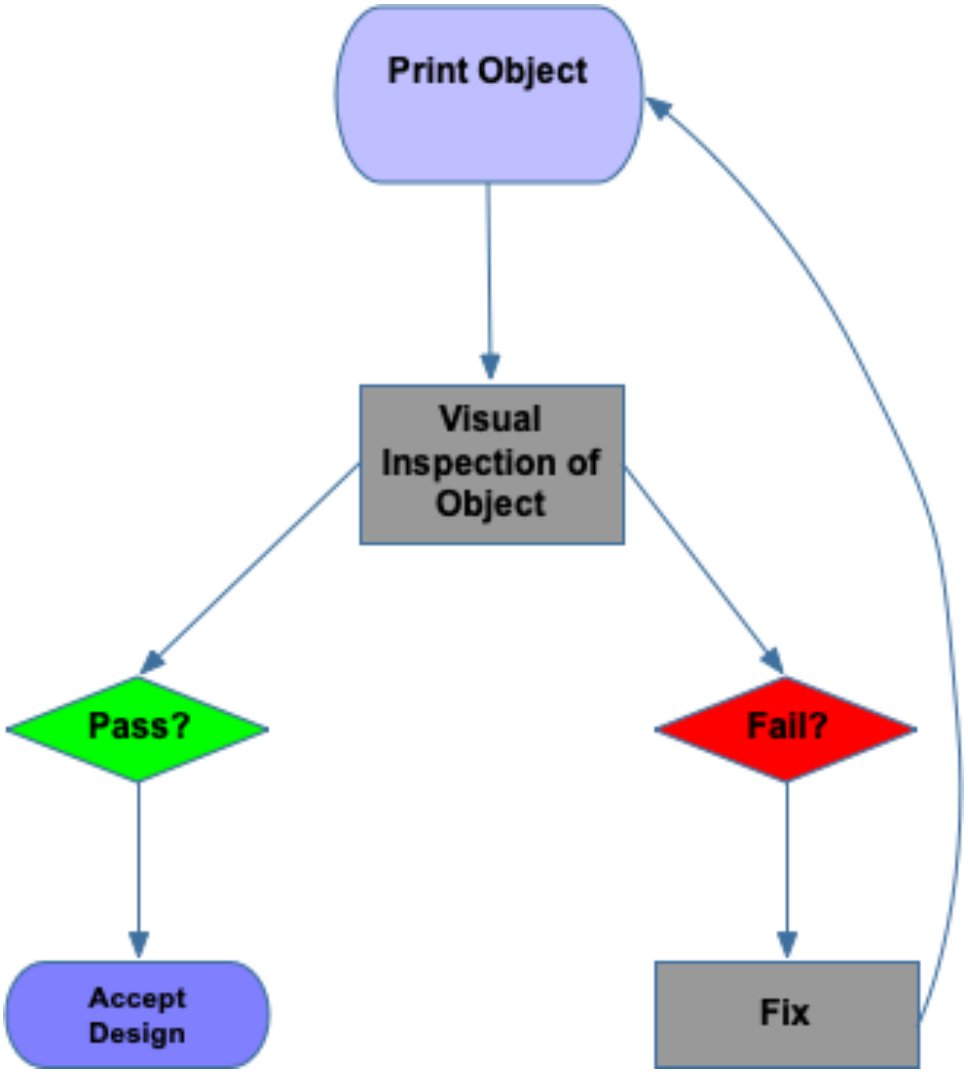

Figure 1: Example of the Typical 3DP workflow for a maker

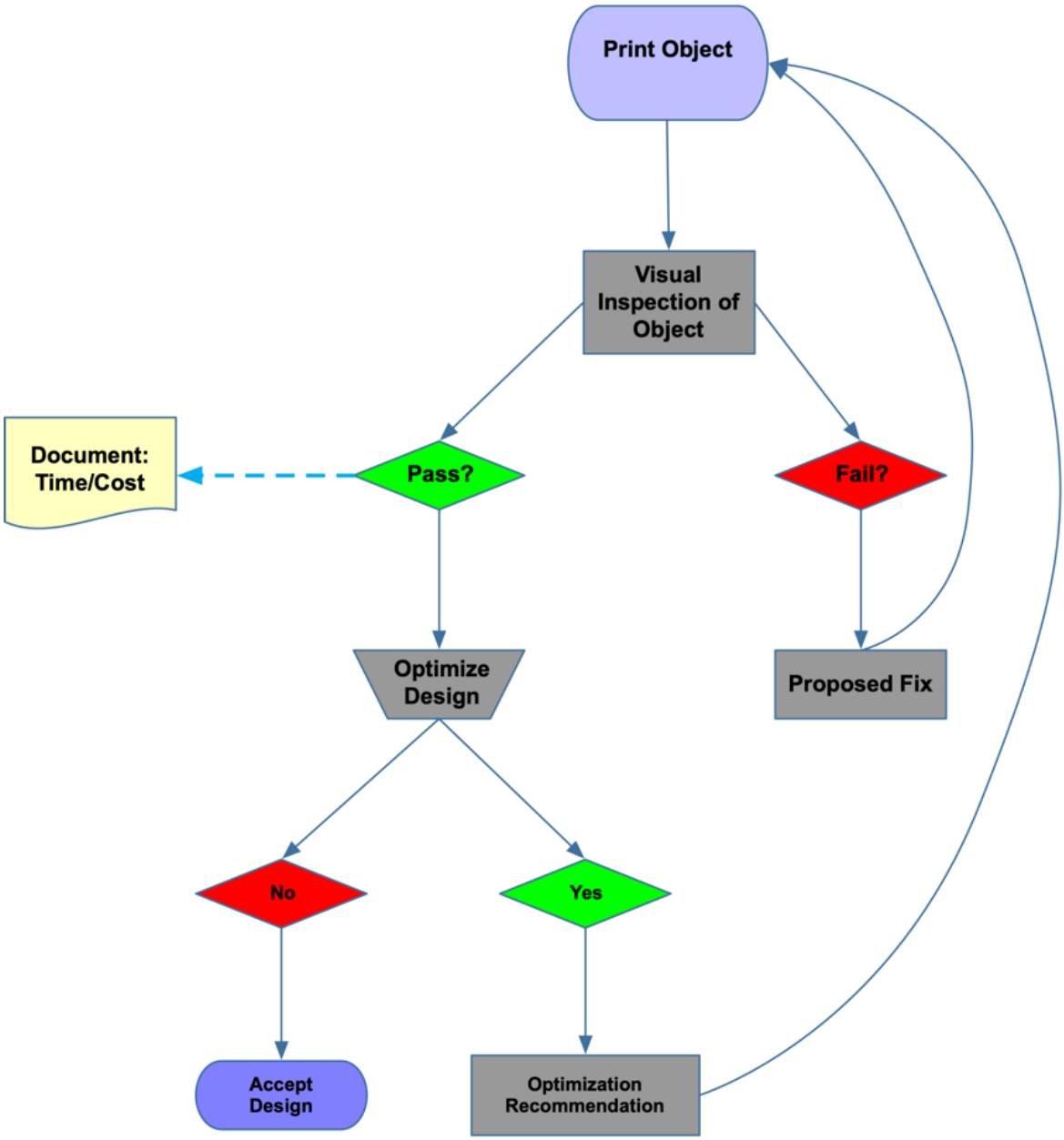

Figure 2: New Workflow to Integrate Optimization

A methodology is required to allow makers to incrementally optimize the print process while at the same time being cost effective and conducive to the continued use of a visual inspection. The use of the augmented Epsilon-Constraint method is a possible solution. This methodology can offer makers the ability to optimize and can be particularly important considering such issues as this created by COVID-19.

1.3 — COVID-19 AND SUPPLY ISSUES

In 2019 the first cases of the novel coronavirus (2019-nCoV) or the severe acute respiratory syndrome corona virus 2 (SARS-CoV-2), commonly known as COVID-19, were reported in Wuhan City of Hubei Province of China (Singhal, 2020). The virus primarily targets the human respiratory system. The most common COVID-19 symptoms are fever, cough, sore throat, fatigue, muscle/body/headaches, new loss of taste or smell, congestion or runny nose, nausea or vomiting, and diarrhea (CDC, 2020). The symptoms range from mild to severe. At present, COVID-19 is particularly deadly for those with compromised immune systems and those over 70 years of age. Examples of a “compromised immune system” includes individuals with hypertension, diabetes, cardiovascular disease, and malignancy. The literature currently estimates that approximately 20% of patients develop severe respiratory illness, with the overall mortality between 2-4% (Shi et al., 2020), (Sohrabi et al., 2020).

As of 5 March 2020, 7 of the hardest hit countries from COVID-19 were the US, China, Japan, Germany, Britain, France, and Italy (Baldwin & Mauro, 2020). According to Baldwin and Mauro (2020), these countries account for the following:

- 60% of world supply and demand (GDP)

- 65% of world manufacturing
- 41% of world manufacturing exports

As of June 2020, unemployment in the US is approximately 11%. As a comparison, the rate is over 7% higher than the previous June (BLS, 2020). Initial social distancing efforts exacerbated already tight supplies of PPE. Baldwin and Mauro (2020) describe the “triple hit” on world manufacturing:

1. Direct supply disruptions have hindered production is industrial powerhouses of China, USA, and Germany.
2. The supply-chain has faced “supply-chain contagion” as direct supply shocks. Manufacturers in less hard-hit nations find it harder and more costly to acquire imported industrial outputs.
3. Demand disruptions caused by drops in aggregate demand and “wait-and-see” spending by consumers and industry.

Overall, the effects on global industry and the rapid growth in COVID-19 cases created shortages in many goods including PPE.

1.3.1 — Supplies of PPE

China represents much of the world’s personal protective equipment (PPE) production. In the case of the United States, 48% of all PPE used is sourced from China. In January and February, production from China dipped 15% (Bown, 2020). PPE shortages have been documented accrues the globe, including in the US, Italy, South Korea, and the United Kingdom (Emanuel et al., 2020). Innovative solutions are required to mitigate this shortfall. Additive manufacturing is one such solution.

The maker community and makerspaces could provide the resources needed to meet the PPE supply shortfalls caused by COVID-19.

During the COVID-19 pandemic there have been numinous instances of makers assisting with the production of medical supplies. These ad hoc efforts to supply PPE are just a small example of maker efforts happening across the globe. In most cases, the efforts were spontaneous and lacked centralized coordination an optimization. An important component of future endeavors would be the optimization of production. Techniques developed in the field of Industrial Engineering could be integrated into maker efforts to streamline processes and maximize output.

1.4 — Optimization

“Tennessee colleges are teaming up to mass produce face shields for medical workers battling the coronavirus outbreak. In days, colleges throughout the state have used 3D printers to produce more than 1,500 pieces of personal protective equipment, with plans to create thousands more. Hospitals are clamoring for masks, face shields and other tools as the explosive spread of COVID-19 continues to strain their supply chains.” - Adam Tamburin, Tennessean, 2020

It is estimated that there are 47,000 3D printers in the United States (US) (Feldman, 2020). Many of these printers became inactive as companies and organizations transitioned to work-from-home and social distancing in the wake of COVID-19 (Feldman, 2020). This number does not include maker owned 3D printers. It is estimated that there are at least 300 publicly accessible makerspaces, libraries,

YMCAs, community colleges, and universities (Holman, 2015). Many organizations used the idle printers to answer the PPE shortage.

With the growing shortage of PPE, many organizations and individual makers began producing PPE to meet demand. Novak and Loy (2020) identified many of the early production projects in February and March 2020. The researchers identified over 91 maker projects of which 60% were producing PPE (Novak & Loy, 2020a). The PPE beginning produced included:

- Face Shields (62%)
- Masks (20%)
- Goggles (9%)
- Mask Adjusters (5%)
- Other (4%)

Universities in Tennessee participated in the production of PPE. In the case mentioned in the Tennessean (2020), “Tennessee colleges mass producing face shields to guard against coronavirus using 3D printers”, the Tennessee Universities were producing PPE face shields. In all, over 18,000 face shields were produced.

The mobilization of the maker community can be considered a bright spot in perilous times of the COVID-19 pandemic. Many of the 3D models utilized to produce PPE require hours to print (Tino et al., 2020). Even with multiple printers, the previously mention TN project was limited by the print time of the face shields. The face shields typically took between 1.5 to 3.5 hours to print (Wesemann, Pieralli, Fretwurst, Nold, & Nelson…, 2020). Optimization could be used to increase the throughput of shields while

at the same time maintaining quality and limiting the materials and labor required to complete a build.

1.4.1 — Makers and Optimization

Makers across the globe have utilized 3D printers to meet the PPE challenges posed by COVID-19. In the case of face shields, there is a vast array of models and versions available for maker production. Added to these selections are the numerous options for FDM printers. Selecting a model, best suited for a given printer can be challenging. The choices with this selection have an overall effect on the throughput of a project and is particularly critical during a disaster. Utilizing various industrial engineering methodologies, it is possible to improve throughput while at the same time retaining quality and keeping costs down. This study will focus on the optimization of the production of face shields (Figure 3).

1.4.2 — Overview of a Face Shield

A face shield (Figure 3) is composed of a FDM printed frame, a piece of elastic, and a cut sheet of clear acetate.

The most time consume component of production is the frame.

1.4.3 — Discussion of Variables

To optimize throughput several variables, need to be investigated (Popescu, Zapciu, Amza, Baciu, & Marinescu, 2018). Throughput, cost, and quality can all be affected through the manipulation of various 3D print parameters. Some examples include:

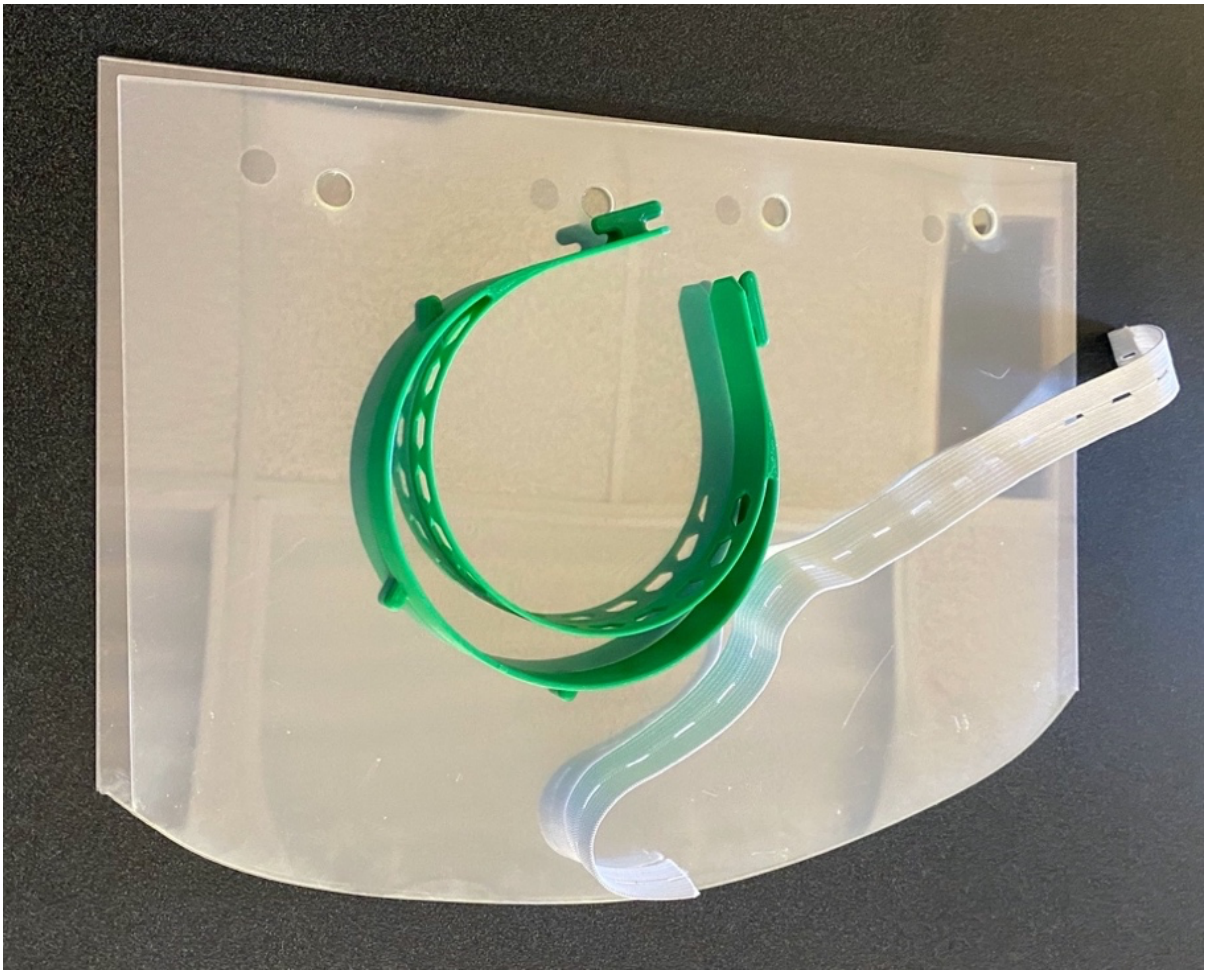

Figure 3: Face Shield Components

- Slicing Parameters - includes a variety of variables including infill, layer height, nozzle diameter, etc.
- Build Orientation - Fit of the frame on the build surface
- Temperature Conditions

The study “Parametric Analysis of the Build Cost for FDM Additive Processed Parts Using Response Surface Methodology” (Mohamed, Masood, & Bhowmik, 2016b) identifies a cost model that is applicable for determine the cost for printing FDM parts. The model developed is:

$$B_{cost} = C_M + C_S + (M_r + T_{Build})$$

Where:

- B_{cost} = Build cost ($)
- C_M = Model material cost ($)
- C_S = Support material cost ($)
- M_r = Machine running cost (Hour)
- T_{Build} = Built time (Hour)

To complete this formulation, the various FDM input factors will need to be identified. In the case of Mohamed et al (2016), the following inputs selected were:

- Layer thickness
- Air gap
- Raster angle
- Build orientation

- Road width
- Number of contours

This study will review various studies and identify the ideal FDM input factors. The independent variables will be identified and used as a starting point to identify other key independent variables. The selection of variables will also be influenced by the various slicer programs typically used by makers, with a focus on the free/open-source tools.

Various levels of the variables can be tested to identify the cost production variables. Design of experiments and ANOVA will be utilized to test the results. A quadratic equation can then be used to optimize the build variables to lowest cost.

1.5 — Chapter 1 Summary

The various methodologies for optimization are ideal for researchers but are outside of the experience and knowledge of the typical maker. This study will focus on the use of easy to understand and accessible optimization techniques. Figure 4 represents the various problems outlined previously.

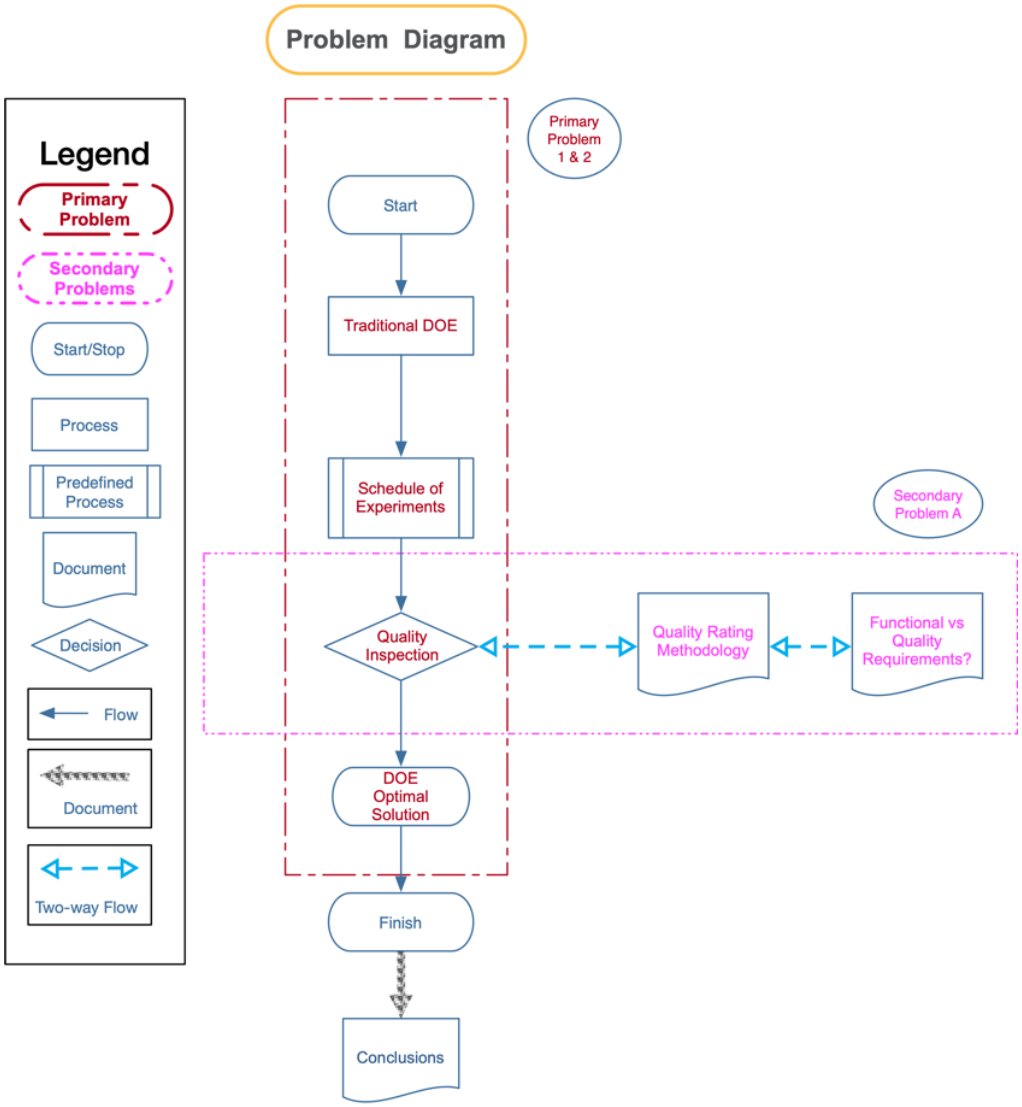

Figure 4: Diagram of Problem

2 — CHAPTER TWO - LITERATURE REVIEW

2.1 — 3DP INTRODUCTION

Traditional manufacturing utilizes subtractive processes. The part geometry is created by removing material. Subtractive processes include injection molding, metal casting, and conventional machining processes (Bhushan & Caspers, 2017). Although there are numinous types of 3D printing (3DP) processes, most methods deposit a material and build an object layer-by-layer (Yoon et al., 2014). Typically, a model of the object is created is a computer aided design (CAD) software. This model is then "printed".

Some of the first patents for 3D printing technologies were granted in the 1970s (Bradshaw, Bowyer, & Haufe, 2010b). At present there is a wide range of available 3D printing technologies. With the growth in the industry 3D printing devices, machines previously only available to industry have begun to appear is in universities and private citizen's garages (Ludwig, Stickel, Boden, & Pipek, 2014). As noted by Ludwig et al. (2014):

"…entry level 3D printers and machines such as RepRaps or MakerBots have become more and more common in various professional and non-professional settings such as universities and small businesses as well as in the hobbyist and semi-professional Maker scene."

In this research, 3DP will be reviewed based on two subcategories additive manufacturing (AM) and the prosumer 3D printing (P3D). The AM will be used to

describe the professional 3D printing industry and Industrial and manufacturing processes. P3D will be used to refer to the semi-professional market, hobbyists, university, and school 3DP.

2.1.1 — HISTORY OF 3DP

The initial 3D printers were valued as rapid prototyping tools. Not only could a part be modeled, but once printed the result was the actual part. At present, AM is often used for small batch products that would require extensive machining for traditional manufacturing techniques.

The first commercial use of additive manufacturing in 1987 by the company 3D Systems. 3D Systems' SLA-1 was a stereolithography (SL) system that used a laser to solidify thin layers of ultraviolet (UV) light-sensitive liquid polymer (Wohlers & Gornet, 2014).

In the 1990s, several new AM technologies were commercialized (Wohlers & Gornet, 2014). These included:

- Fused Deposition Modeling (FDM) from Stratasys
- Solid Ground Curing (SGC) from Cubital
- Laminated Object Manufacturing (LOM) from Helisys
- Selective Laser Sintering (SLS)

In Fused Deposition Modeling (FDM), a plastic material, in filament form, is extruded through a nozzle that contains resistive heaters. As the nozzle traces the part's cross-

sectional geometry, the melted material is deposited layer-by-layer (Novakova-Marcincinova & Kuric, 2012).

With Solid Ground Curing (SGC) also known as Resin Printers, each layer is generated by creating a negative image mask of the cross section of the part on an electrostatically charged glass plate. a thin layer of UV-sensitive liquid polymer is spread across the surface of the workspace. The workspace is then flooded with UV light creating a layer in one pass (Gu, Zhang, Zeng, & Ferguson, 2001).

Laminated Object Manufacturing (LOM) can be considered a hybrid on additive manufacturing. Layers are sequentially laminated together (additive) via adhesive activated by a heating plate. Excess material is then cut away utilizing a special tool (subtractive).

Selective laser sintering (SLS) uses thermal energy supplied by a laser to consolidate successive layers of a power material. Each successive layer of the power material is deposited, typically thickness of 20 till 150 μm, across the workspace. The laser traces the part's cross-sectional geometry and melts the powder in the path. The excess powder is removed from the workspace (Kruth et al., 2005).

The methodologies listed previously represent the common 3D systems still in use. Although LOM and SLS printers can cost in the hundreds of thousands, many FDM can be purchased for under five hundred dollars.

The availability of these inexpensive systems has created a large hobbyist community particularly for the FDM printing.

2.1.2 — Introduction to AM

Additive Manufacturing (AM) utilizes processes to produce objects from digital models. The models are rendered into a series of 2D cross-sections of a finite thickness. The cross sections are fed into the AM machine, adding each layer-by-layer to produce the finished object (Gibson, Rosen, & Stucker, 2014). The layering process defines the geometry and the material properties of the object. The AM machine feedstock is transformed via the AM process into the finished part (Thompson et al., 2016).

AM can be utilized for a wide range of manufacturing initiatives; current literature highlights several applications. According to (Ngo et al., 2018), there are several trending applications for AM. These applications include:

- Biomaterials
- Aerospace
- Buildings
- Protective Structures

There is rapid development of AM technologies. AM technology is continuously improving with the ability to print end user designs using diverse metallic and nonmetallic materials (Thompson et al., 2016). The literature notes many of the advantages and benefits of AM over traditional manufacturing processes (Table 1).

Table 1: Advantages of AM (Durakovic, 2018)

Advantages	Explanation
Cost and geometry complexity	The cost of printing complex objects is cheaper than the cost of printing simple designs AM allows designers to create complex geometric shapes that are not possible using traditional manufacturing
Functional complexity	Besides printing single parts, with AM it is possible to create functional objects. Examples could include gears, hinges, and bicycle chains.
Material complexity	AM allows a designer to create parts that are made from multiple materials. This type of design allows for an object to have different physical properties in specific areas.
Hierarchical complexity	AM designs can utilize a variety of internal structure. These structures allow for a part to have varied physical properties such as strength, stiffness, and weight
Low manufacturing skills	The printing process is not complicated. To print, an individual simply needs to be able to design a model. The availability of pre-made models also lowers the need for training.
Reduced material waste	AM only uses the material needed to print a model. AM generates very little waste material

Table 1 Continued

Advantages	Explanation
Part and material variety	A designer can alter an existing model to create parts that are similar. The only requirement is CAD software.
Quality control	Quality control methodologies are well documented in the literature.

Although AM and 3D printing is a promising technology, it has several drawbacks. As noted previously, 3DP can be efficient and cost effective for small orders. Because of excessive print times, AM can be less effective that traditional manufacturing. The layer-by-layer approach to 3DP can also be problematic in terms of quality control (Bhushan & Caspers, 2017), cost control, and large volume projects. The use of 3D printers in homes and schools can also create problems with intellectual property (Nitti, 2019).

2.1.3 — Trends in AM

The literature documents numerous uses for AM technology. The trending applications (Ngo et al., 2018) in AM include:

- Biomaterials
- Buildings
- Protective Structures
- Aerospace
- Low Cost 3DP

Biomaterials

Biomaterials are defined as natural or synthetic materials that can be used in the repair of damaged limbs and body parts by interacting with living body. In (Bose, Ke, Sahasrabudhe, & Bandyopadhyay, 2018), the example of a total hip replacement is described. With traditional manufacturing techniques, a hip replacement requires a complex combination of materials and structures. To achieve this blend, multiple steps are required. Once manufacturing is complete, post-processing steps are often

required. In all steps specific pattern making or tooling is needed which increases the expense (Bose, Ke, Sahasrabudhe, & Bandyopadhyay, 2018).

AM is ideally suited for small, custom orders (Bhushan & Caspers, 2017). The typical biomaterial pattern meets these criteria. Unlike traditional manufacturing where each step creates expense, in AM the costs are associated with the cost of the AM machine and the raw materials (Bose, Ke, Sahasrabudhe, & Bandyopadhyay, 2018). As noted by Bose et al. (2018),

"Comparing the process setup, there are no costs involved in specific pattern making or tooling. After AM based processing, machining may be needed to get the desired surface finish. Key advantage towards AM of biomedical devices lies in patient-specific device manufacturing. In some AM approaches, secondary processing such as depositing a bio-ceramic coating on a metallic hip stem can also be integrated."

Buildings

The traditional construction industry faces numerous challenges including resources, environmental, and productivity. The construction industry utilizes a considerable quantity of resources and stresses the environment (Wu, Wang, & Wang, 2016). In the United States, buildings use 36 percent of the total energy consumed, 30 percent of the raw materials consumed and 12 percent of potable water (Klotz, Horman, & Bodenschatz, 2007). Additionally, construction poses numerous productivity challenges. In a comparison of the construction industry productivity in 20 countries, the United States scored the worst (Nasir, Ahmed, Haas, & Goodrum, 2014).

In the research, several benefits of 3D printing in construction are noted (Wu, Wang, & Wang, 2016). These benefits include:

- Reduced Waste
- Design Flexibility
- Reduced Manpower
- Other improvements in economic, environmental and constructability

These benefits directly address the challenges in the traditional construction industry.

Protective Structures

A trending application of AM manufacturing includes the development of protective structures. Examples of protective structures include vehicle and personal protection armor. The ability to rapidly prototype complex structures allows researchers to explore the protective properties of parallel panels filled with the most disparate lattice cores and other novel snap-through concepts. This research is ideal for the development of materials with high stiffness-to-weight and strength-to-weight ratios (Ngo et al., 2018).

An interesting trend in protective structure research is the investigation of bio-inspired design (BID). BID looks at protective structures in nature such as fish scales, fruit peels, abdominal armor, and bones to create protective structures. AM processes are ideal for the creation of these complex structures (Mehta, Ocampo, Tovar, & Chaudhari, 2016).

AEROSPACE

The aerospace industry requires strong, light, and durable components. Additive manufacturing is ideally suited to meet these requirements. It is estimated that the aerospace industry currently accounts for over 12% of global additive manufacturing applications. At present AM in aerospace is a $1.5 billion dollar industry. It is expected to grow to $100 billion in the next 20 years (Kumar & Nair, 2017). Although rapid prototyping is a common aerospace use case, metallic AM processes are often used for end-use parts. With metallics, much of the research focuses on Powder Bed Technologies and Deposition Technologies (Dordlofva, Lindwall, Torlind, & others, 2016). AM is an ideal fit for aerospace due to the need for complex components in low volumes (Gibson, Rosen, & Stucker, 2010). This is demonstrated by the fact that the international space station has a 3D printer for creating parts and components as needed (Tofail et al., 2018).

A critical challenge in utilizing AM in aerospace is that of variation. Variation is AM produced products include those observed from part-to-part as well as machine-to-machine. It is critical to identify and minimize variations including internal defects, surface roughness and geometry tolerances (Dordlofva, Lindwall, Torlind, & others, 2016).

LOW-COST 3D PRINTING

Adrian Bowyer in 2004 realized that fused filament deposition (FDM) 3D printing provides the opportunity to manufacture a significant portion of its own parts. From this realization, the Replicating Rapid- prototype (RepRap) community was born. RepRap is

currently a collection of open-source design, software, and hardware. Although RepRap printers have a slightly lower quality that commercial units, RepRap Based devices are a fraction of the cost (Bradshaw, Bowyer, & Haufe, 2010b).

The cost (and usability) of RepRap based 3D printers has dropped significantly. For under five hundred dollars, a user can purchase a machine for home use. While costs for devices have fallen, there has been an exponential growth of databases for printable objects (Halassi, Semeijn, & Kiratli, 2019). These databases are repositories of pre-built items (models) that can be printed. In many cases, these models are free and open-source. With the open-source models, a user can make changes and customize the items for their direct use case. A consumer that is now also a producer can be called a "prosumer" (Rayna, Striukova, & Darlington, 2015). According to Rayna et al., (2015),

"One of the most obvious consequences for businesses of the advent of Internet is the increased participation of users in the production process. This increased participation has been particularly visible since the birth of Web 2.0 technologies and for some of the most successful Web 2.0 outlets (e.g. Facebook, Instagram, Flickr, Twitter), the content provided by users accounts for most of the value of the service. This increased user participation blurs the line between consumption and production activities since users both consume and produce content. No longer 'pure' consumers, users have become prosumers."

With the growth of school and home 3D printers (Bradshaw et al., 2010b), the usages include the following:

- Spare Parts

- Craft and Hobby Items
- Educational Instruction
- Prototyping
- Fashion Related Items
- Maker Spaces

RepRap based printers have led the development of various tools and processes to design and print models.

2.1.4 — 3D Printing Tools and Terminology

The RepRap based 3DP stack includes the following components:

- *Firmware* - is the software that works with the printer microcontroller (Romero et al., 2014). The firmware computes and controls the movements of the printer, sensors, and heaters, by interpreting a sliced model. There are several alternatives firmware alternatives, these include Sprinter, Teacup, and Marlin. Marlin is the most used firmware for the prosumer 3D printer (Stănciulescu, Schulze, & Wąsowski, 2015).
- *Printer Controller* - The print controller represents the interface for the user to interact with the printer. It allows the user to issue commands, set temperatures, set speed, and send files to print (Stănciulescu, Schulze, & Wąsowski, 2015).
- *GCODE Generator* - Commonly referred to as a “slicer”, the GCODE generator transforms a model into GCODE for printing. The GCODE can then be transferred to the machine, controls the speed of extrusion, optimizes the tool path for printing and controls the orientation of the object and the formation of

layers (Šljivic, Pavlovic, & Kraišnik…, 2019). There are numerous slicer programs available including commercial and open-source products.

Slicing Software

As noted by Baumann et al. (2016), the typical 3DP workflow includes the following:

- Creating (or downloading) and exporting the 3D model to print. The format of the exported or downloaded model is commonly standard tessellation language (STL) format.
- Calculation of the printer tool path and characteristics based on the sliced STL file. The sliced file is in GCODE format.
- Printing based on the GCODE file.

The slicing software or slicer is used to convert a model to control commands suited for the 3D printer. It should be noted that the GCODE commands are 3D printer specific. A slicer must be configured to produce GCODE for the printer to be used (Baumann, Schuermann, Odefey, & Pfeil, 2017).

There are numerous commercial and free slicers available. Some of them include:

- Simplify3D (Commercial)
- PrusaSlicer (Open-Source, Free)
- Slic3r (Open-Source, Free)
- UltiMaker Cura (Open-Source, Free)

Ultimaker Cura, referred to as Cura is one on the most popular slicers available. It offers a robust set of features and supports numerous 3D printers. The printer support is in the

form of profiles. Each printer profile is a set of community tested print parameters ideally suited for a printer's hardware. The feature set of Cura allows the user to control and change numerous 3DP parameters. These changes are reflected in the resultant GCODE.

2.1.5 — AM SUMMARY

AM offers the manufacturing industry many benefits both economically and in processing. Of particular interest is the usage of 3D printers to create prototypes and for small-scale production. These uses, particularly in low-cost printing, are important. Low-cost printing offers the ability of anyone to become a 3DP prosumer. Although this type of printing is promising, there remains challenges for the prosumer/maker. One of the significant challenges is that of optimization.

2.2 — PPE AND COVID-19

On 24 August 2020, the number of cases based on the largest economies is detailed in Table 2.

As of June 2020, unemployment in the US is approximately 11%. As a comparison, the rate is over 7% higher than the previous June (BLS, 2020). Initial social distancing efforts exacerbated already tight supplies of PPE.

Baldwin and Mauro (2020) describe the "triple hit" on world manufacturing:

4. Direct supply disruptions have hindered production is industrial powerhouses of China, USA, and Germany.

Table 2: Large Economies and Number of COVID-19 Cases (WHO, 2020)

Country	GDP	Manufacturing	Exports	Manufactured Exports	COVID-19 Cases	Rank
US	24%	16%	8%	8%	5,612,163	1
China	16%	29%	13%	18%	90,182	33
Japan	6%	8%	4%	5%	62,507	44
Germany	5%	6%	8%	10%	233,575	19
UK	3%	2%	2%	3%	325,646	13
France	3%	2%	3%	4%	228,224	20
India	3%	3%	2%	2%	3,106,348	3
Italy	2%	2%	3%	3%	259,345	17
Brazil	2%	1%	1%	1%	3,582,362	2
Canada	2%	0%	2%	2%	124,629	25

5. The supply-chain has faced “supply-chain contagion” as direct supply shocks cause manufacturers in less hard-hit nations find it harder and more costly to acquire imported industrial outputs.
6. Demand disruptions due to drops in overall demand and “wait-and-see” spending by consumers and industry.

China represents much of the world’s personal protective equipment (PPE) production. In the case of the United States, 48% of all PPE used is sourced from China. In January and February, production from China dipped 15% (Bown, 2020). PPE shortages have been documented accrues the globe, including in the US, Italy, South Korea, and the United Kingdom (Emanuel et al., 2020). Innovative solutions are required to mitigate this shortfall. Without these solutions, rationing will become more prominent.

Transmission of COVID-19 to healthcare workers has been widely documented (Singhal, 2020). PPE is critical to protecting both healthcare workers and patients. The PPE should include contact and airborne precautions (Cascella, Rajnik, Cuomo, & Dulebohn…, 2020). Specifically, PPE includes the following:

- N95 or FFP3 masks
- Eye Protection
- Gowns
- Gloves

2.2.1 — COVID-19 PREVENTION

Transmission of COVID-19 to health care workers (HCW) caring for the sick was identified on 20th January 2020 (Singhal, 2020). Using history as a guide, 21% of all

those affected by the 2002 SARS outbreak were HCW workers (Chang, Xu, Rebaza, Sharma, & Cruz, 2020). With the rapid spread of COVID-19, personal protective equipment (PPE) for HCW is critical. The PPE should include contact and airborne precautions (Cascella, Rajnik, Cuomo, & Dulebohn…, 2020). Specifically, PPE should include the following:

- N-95 or FFP3 masks
- Eye Protection
- Face Shields
- Gowns
- Gloves

COVID-19 has created shocks to the global economy. The demand and supply shocks has impacted such industries as transportation, manufacturing, mining, and services (Rio-Chanona, Mealy, & Pichler…, 2020). These shocks have put significant constrains on the global supply of PPE and other medical supplies.

2.2.2 — American Medical Association Ideas

According to the Journal of the American Medical Association (2020), the PPE shortage is described in these terms:

"PPE, formerly ubiquitous and disposable in the hospital environment, is now a scarce and precious commodity in many locations when it is needed most to care for highly infectious patients. An increase in PPE supply in response to this new demand will

require a large increase in PPE manufacturing, a process that will take time many health care systems do not have, given the rapid increase in ill COVID-19 patients."

Which this in mind, JAMA issued a call for ideas to solve the PPE shortages on 20 March 2020 (Livingston, Desai, & Berkwits, 2020). The call received over 280,000 views and 291 comments. Numerous ideas were shared including creating and repurposing supplies using 3D printers (Table 3).

Rationing and the downgrade of safety regulations are a recipe for disaster. Two studies from early in the pandemic show that 1% of HCW have been infected. Not all of these HCW had previously worked with COVID-19 patients (Kluytmans-van den Bergh et al., 2020) and (Lai et al., 2020). As of April 2020, an estimated 9,200 US HCW have been infected with the virus.

Innovative solutions must be found to provide safe and effective PPE. The engagement and use of makerspaces, university 3D print labs, and the DIY community offers a possible path forward.

2.3 — The Maker Community and Makerspaces

The definition for the maker movement is broad. It is based on an person's ability to be a creator of things, This person is known as a maker. This growing community of hobbyists and professionals with diverse skills, backgrounds, and interests make their own functional products. These devices can be technological, or craft based, such as home decor (Papavlasopoulou et al., 2017). According to Browder et al. (2019), the maker movement differentiates itself by three features:

Table 3: JAMA Summary of Recommendations for PPE Conservation and Management (Livingston, Desai, & Berkwits, 2020)

Domain	Idea
Import	
	Purchase from international suppliers: China proposed as a primary market given manufacturing capacity, experience with and decline in COVID-19 incidence
Reclaim	
	Dentists, farmers, construction, high schools, universities, veterinarians, salons, manufacturing, aerospace, industrial “clean labs”
	Individual HCW procurement in towns and communities
	Charitable movements
	Public or private buybacks
	Public or private bounties
Reuse	
	Rotate through 72-h cycles given current understanding of surface viability
	Reusable elastomeric respirators (have exchangeable filter cartridges)
	Disinfectants
	Heat (eg, autoclave), UV, ozone, ethylene oxide, hydrogen peroxide, bleach, isopropyl alcohol, gamma or e-beam radiation, microwave, copper sulfate, methylene blue with light, sodium chlorine, iodine, zinc oxide impregnation (gowns), hypochlorous acid, commercial laundering (for cloth)

Table 3 Continued

Domain	Idea
Repurpose	
	Prefabricated masks: snorkel and scuba, 3D printed, welder's, civilian military grade gas masks, ski buffs
	Eye and face shields: sports eye protectors, motorcycle helmets with visors, balaclavas
	Gowns: plastic ponchos or poly bags, bedbug sheet material
	Adhesive bandage as nasal PPE
Create supply	
	Sewn fabric masks and gowns, coffee filter masks, home HVAC filter masks
Extend supply	
	Plastic face shields (water bottle cutouts, thermoplastic sheets, A4 acetate sheets, Ziploc bags) to preserve face masks and eyewear
Reduce nonessential services	
	Cancel elective and ambulatory procedures; reduce questionable contact and isolation precautions (eg, MRSA/VRE, influenza, cellulitis)

Table 3 Continued

Domain	Idea
Reduce patient contact	
	Utilize mobile and out-of-room monitoring and device controls, e-consults, extended dwell IVs, batching medications or self-administration, barrier visits
Alter staffing	
	Reduce student and trainee patient contacts
Use nonhuman services	
	Nonhuman services (drones and robots) for delivery of test kits for self-testing, robots for equipment movement within hospitals, decontamination protocols
Stratify use by patient risk	
	Cohort patients and reduce PPE use for those at low risk (ideally requires testing to accurately stratify low and high risk)
Employ immune workers	

Table 3 Continued

Domain	Idea
	HCWs recovered from clinical illness or with demonstrated immunity care preferentially for COVID-19 patients without PPE
Use government solutions	
	Regionalize care and supply, import international supply, ration supply, loosen import regulations, commandeer business to accelerate supply
Manage supply	
	Reduce bulk packaging, Pyxis-like controlled distribution, nongovernment regional coordination of PPE distribution
Miscellaneous	
	Convert RV trailers to negative pressure spaces; phase change material to improve comfort and reduce reuse of gowns

- A high level of collaboration and social exchange among a diverse community
- Enhanced knowledge creation and sharing both physically and virtually
- The production of material items using technology that had previously only been the domain of corporate research and development (R&D) facilities

The diverse maker community is composed of includes do-it-yourself (DIY) hobbyists, engineers, artists, hackers, students and educators, the self-employed, prototyping entrepreneurs, technology and corporate innovators, and a new type of manufacturers (Browder et al., 2019). A physical space for this community to share ideas is called a “makerspace”.

A makerspace, sometimes referred to as a hackerspace or fablab, is a community workshops where members can access tools and workspace. The benefit of the makerspace is the shared access to expensive tools and human capital. This capital is the sharing of knowledge and ideas (Holm, 2015). Makerspaces can be commercial enterprises with membership fees, public spaces in libraries, or workshops in schools designed for student access. In an informal 2015 survey, it was estimated that there are at least 300 publicly accessible makerspaces in the United States. Furthermore 120,000 libraries, 2,600 YMCAs, and 1,200 community colleges provide access to other shared resources (Holman, 2015). Additionally, makerspaces have been gaining popularity at universities. The research has identified two significant benefits, the benefits of physical modeling and the growth of communities of practice (Forest, Moore, Jariwala, & Fasse…, 2014).

2.3.1 — The Maker Community and COVID-19

During the COVID-19 pandemic there have been numinous instances of makers assisting with the production of medical supplies. Some examples include:

- “This Is Truly a Last Resort. Makers Are 3D Printing Ventilator Parts and Sewing Masks Amid a Critical Shortage in Medical Supplies” (Clark, 2020).
- “Can The U.S. Crowdsource Its Way Out of a Mask Shortage? No, but it Still Helps” (Westervelt, 2020)
- “3D Printer Groups Continue Working Round the Clock to Help 2020 PPE Shortage” (McCue, 2020)
- “How Library Maker Spaces Can #FlattentheCurve” (Vecchione & Woltjer, 2020)
- “Tennessee Colleges Mass Producing Face Shields to Guard Against Coronavirus Using 3D Printers” (Tamburin, 2020)

These ad hoc efforts to supply PPE are just a small example of maker efforts happening across the globe. In most cases, the efforts were spontaneous and lacked centralized coordination and optimization. An important component of future endeavors would be the optimization of production. Techniques developed in the field of Industrial Engineering could be integrated into maker efforts to streamline processes and maximize output.

2.4 — Introduction to Optimization

Optimization can be defined as “an act, process, or methodology of making something (such as a design, system, or decision) as fully perfect, functional, or effective as possible; specifically : the mathematical procedures (such as finding the maximum of a

function) involved in this" (Merriam-Webster, n.d.). In the case of design of experiments, optimization is the process of determining the region in the important factors that will lead to the best possible response (Montgomery, 2017). In the case of manufacturing, a system must be characterized. Characterization is the process of the identification of the factors that have the most influence on the response of interest (Montgomery, 2017). In the case of makers responding to COVID-19 PPE shortages, the critical responses are print speed, cost, and quality. In the following sections, this research will identify the critical factors that contribute to the responses of speed, cost, and quality.

2.4.1 — Optimization for Makers

It is estimated that there are 47,000 3D printers in the United States (US) (Feldman, 2020). This number does not include printers an estimated that there are at least 300 publicly accessible makerspaces, libraries, YMCAs, community colleges, and universities (Holman, 2015). Many of these printers became inactive as companies and organizations transitioned to work-from-home and social distancing in the wake of COVID-19 (Feldman, 2020). Many organizations used the idle printers to answer the PPE shortage.

With the growing shortage of PPE, many organizations and individual makers began producing PPE to meet demand. Novak and Loy (2020) identified many of the early production projects in February and March 2020. The researchers identified over 91 maker projects of which 60% were producing PPE (Novak & Loy, 2020a). The PPE beginning produced included:

- Face Shields (62%)

- Masks (20%)
- Goggles (9%)
- Mask Adjusters (5%)
- Other (4%)

“Tennessee colleges are teaming up to mass produce face shields for medical workers battling the coronavirus outbreak. In days, colleges throughout the state have used 3D printers to produce more than 1,500 pieces of personal protective equipment, with plans to create thousands more. Hospitals are clamoring for masks, face shields and other tools as the explosive spread of COVID-19-19 continues to strain their supply chains.” - Adam Tamburin, Tennessean, 2020 (Tamburin, 2020)

Universities in Tennessee participated in the production of PPE. In the case mentioned in the Tennessean (2020), “Tennessee colleges mass producing face shields to guard against coronavirus using 3D printers”, the Tennessee Universities were producing PPE face shields. In all, over 18,000 face shields were produced.

The mobilization of the maker community can be considered a bright spot in perilous times of the COVID-19 pandemic. Several barriers remain for 3D printing to become a permanent fixture in the PPE supply chain. These barriers include:

- PPE Fit/Comfort
- Regulations
- Throughput
- Geometry of Design

The most significant barrier is that of throughput and, to a lesser degree, geometry of design (Novak & Loy, 2020b).

Many of the 3D models utilized to produce PPE require hours to print (Tino et al., 2020). Even with multiple printers, the previously mention TN project was limited by the print time of the face shields. The face shields typically took between 1.5 to 3.5 hours to print (Wesemann et al., 2020). Optimization could be used to increase the throughput of shields.

Optimization for Makers

Makers across the globe have utilized 3D printers to meet the PPE challenges posed by COVID-19. In the case of face shields, there is a vast array of models and versions available for maker production. Added to these selections are the numerous options for FDM printers. Selecting a model, best suited for a given printer can be challenging. The choices with this selection have an overall effect on the throughput of a project and is particularly critical during a disaster. Utilizing various industrial engineering methodologies, it is possible to improve throughput while at the same time retaining quality and reducing costs. The determination of quality is made via a visual inspection Figure 5.

This study will focus on the production of face shields (Figure 3).

Overview of a Face Shield

A face shield (Figure 6) is composed of a FDM printed frame, a piece of elastic, and a cut sheet of clear acetate.

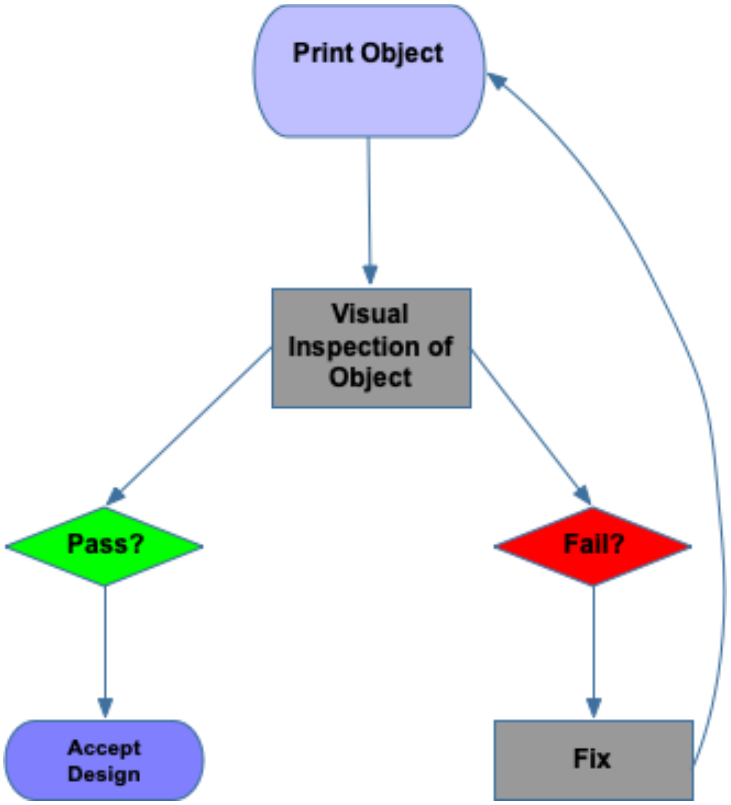

Figure 5: Example of the Typical 3DP workflow for a maker

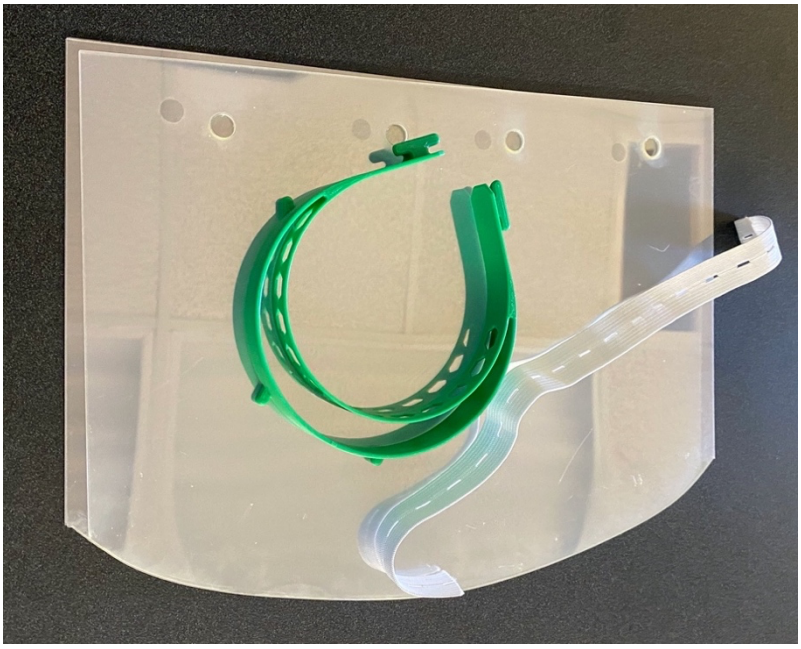

Figure 6: Face Shield Components

The most time consume component of production is the 3D printed frame.

2.4.2 — Discussion of Parameters

To optimize throughput several variables must be investigated (Popescu et al., 2018). These include:

- Slicing Parameters - includes a variety of variables including infill, layer height, nozzle diameter, etc.
- Build Orientation - Fit of the frame on the build surface
- Temperature Conditions

Each of the variables impacts the 3D print throughput as well as the frame quality. There are several studies that have investigated the effect of these variables on FDM printers. These include and are not limited to:

- “A Systematic Survey of FDM Process Parameter Optimization and Their Influence on Part Characteristics” (Dey & Yodo, 2019) - a review of various process parameter studies.
- “Build orientation analysis for minimum cost determination in FDM” (Ingole, Deshmukh, Kuthe, & Ashtankar, 2011) - a study that attempts to develop a universal cost model for varying geometries.
- “Mathematical modeling and FDM process parameters optimization using response surface methodology based on Q-optimal design” (Mohamed, Masood, & Bhowmik, 2016a) - utilizes Q-optimal response surface methodology to determine the functional relationship between the processing conditions and the process quality characteristics.

- “FDM process parameters influence over the mechanical properties of polymer specimens: A review” (Popescu et al., 2018) - is a literature search identifying various parameters and variable effecting cost.
- “Design for Scalability and Strength Optimization for Components Created Through FDM Process” (Qureshi, Mahmood, & Wong…, 2015) - a study that uses Taguchi’s design of experiment to analyze the effect of these process parameters on physical characteristics.

The identification of optimal print parameters is a significant problem for makers (Figure 4). Dey and Yodo, (2019) conducted an in-depth survey of various studies looking at printing parameters and their effects on part characteristics (Table 4). This research will serve as a basis for determine the process parameters to optimize for makers.

In the studies reviewed by Dey and Yodo, (2019) (Figure 7), the common variables affecting build time and quality is layer thickness, print speed, infill density and raster width. Layer thickness (Figure 8) is the thickness of a layer deposited by nozzle and is affected by extrusion speed and can depend upon the type of the nozzle (Gurrala & Regalla, 2012). Print Speed is the mm/s that the printer head deposits filament. Infill density (or percentage) is the percentage of an infill pattern that fills voids in print. The raster width is the thickness of lines in a print (Figure 9). Build orientation (Figure 8) is the geometry of the model as it is printed on the build plate (Figure 10).

Table 4: List of Various Parameters from Previous Studies (Dey & Yodo, 2019)

Part Characteristics	Process Parameters
Strength	Build orientation and raster orientation
Elastic performance	Layer thickness, raster orientation, raster width, air gap
Throwing distance of a bow	Layer thickness, raster orientation, raster width, air gap
Residual stress and part distortion	Layer thickness, print speed, raster width
Ultimate tensile, yield, flexural, and impact strength	Raster orientation
Tensile, flexural, and impact strength	Layer thickness, build orientation, raster orientation, raster width, air gap
Tensile, flexural, and impact strength	Layer thickness, build orientation, raster orientation, raster width, air gap
Tensile, flexural, and impact strength, and deflection test	Raster orientation
Viscosity and modulus	Build style, raster orientation, raster width
Dynamic stress–strain response	Build orientation
Tensile strength and elastic modulus	Raster orientation and layer thickness

Table 4 Continued

Part Characteristics	Process Parameters
Build time, dimensional accuracy, warp deformation	Width compensation, layer thickness, extrusion velocity and filling velocity
Ultimate tensile strength, modulus of elasticity, elongation	Raster orientation and layer thickness
Ultimate shear strength, 0.2% yield strength, proportional limit, shear modulus, and fracture strain	Layer thickness, infill density and postprocessing heat-treatment time
Part cost, tensile, compressive and flexural properties	Infill Pattern
Tensile strength and fatigue performance	Raster orientation
Tensile and shear properties	Raster Orientation and Build orientation
Young's modulus, yield strength, tensile strength, dimensional accuracy	Build orientation, infill density, print speed, layer thickness, infill thickness, infill pattern, extrusion temperature
Tensile strength, failure strain, modulus Poisson's ratio, thermal expansion	Build orientation
Tensile, flexural and impact strength	Build orientation, layer thickness, raster orientation, raster width, air gap

Table 4 Continued

Part Characteristics	Process Parameters
Hardness, flexural modulus, tensile tensile strength, and surface roughness	Layer thickness, build orientation, support material, model interior
Tensile, dynamic, and thermoelectric properties	Infill pattern and infill density
Elongation, and tensile, flexural, and impact strength	Print speed, layer thickness, extrusion temperature, infill temperature, infill density
Ultimate tensile and yield strength, modulus of elasticity and elongation	Infill density, extrusion temperature, raster orientation, and layer thickness
Compressive properties, porosity	Air gap, raster width, build orientation, build layer, and build profile
Build time, support material volume	Layer thickness, raster and build orientation, raster width, shell
Impact strength	Build orientation
Storage modulus, Storage modulus, loss modulus, mechanical dumping	Layer thickness, air gap, raster orientation, build orientation, road width, and number of shells
Layer height, raster height, width	Thermal conductivity

Table 4 Continued

Part Characteristics	Process Parameters
Tensile strength, strength, modulus of rupture, impact resistance	Raster orientation
Build time and support volume	Layer thickness, air gap, raster and build orientation, and shell width
Material volume	Layer thickness, air gap, road and shell width
Lattice structure	
Tensile strength, energy consumption and build time	Extrusion temperature, raster orientation, infill density

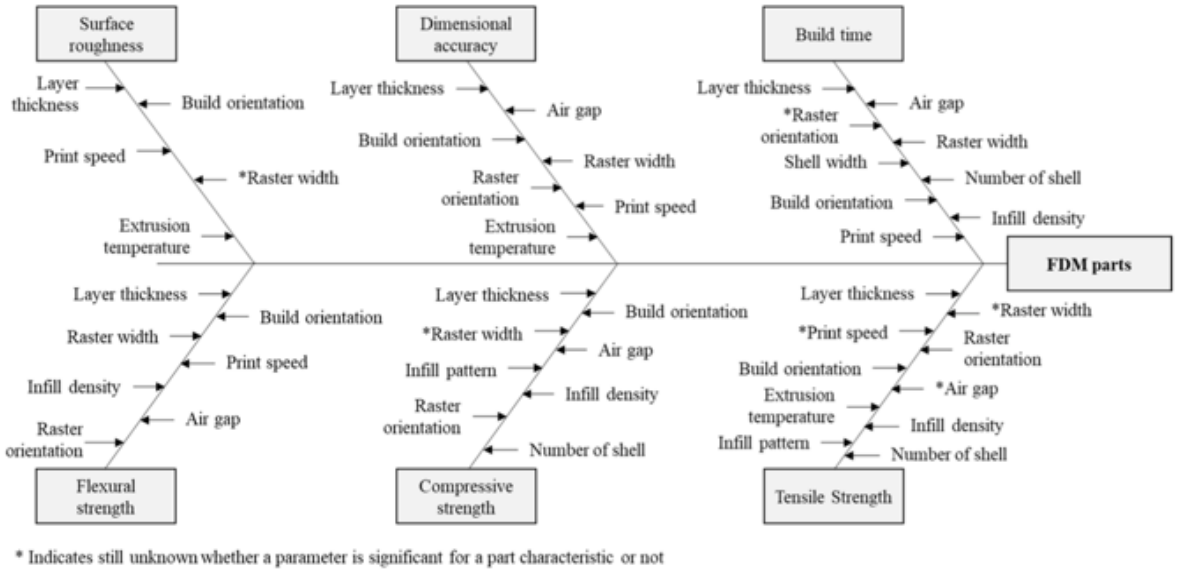

Figure 7: Breakdown of Characteristics vs Parameters (Dey & Yodo, 2019)

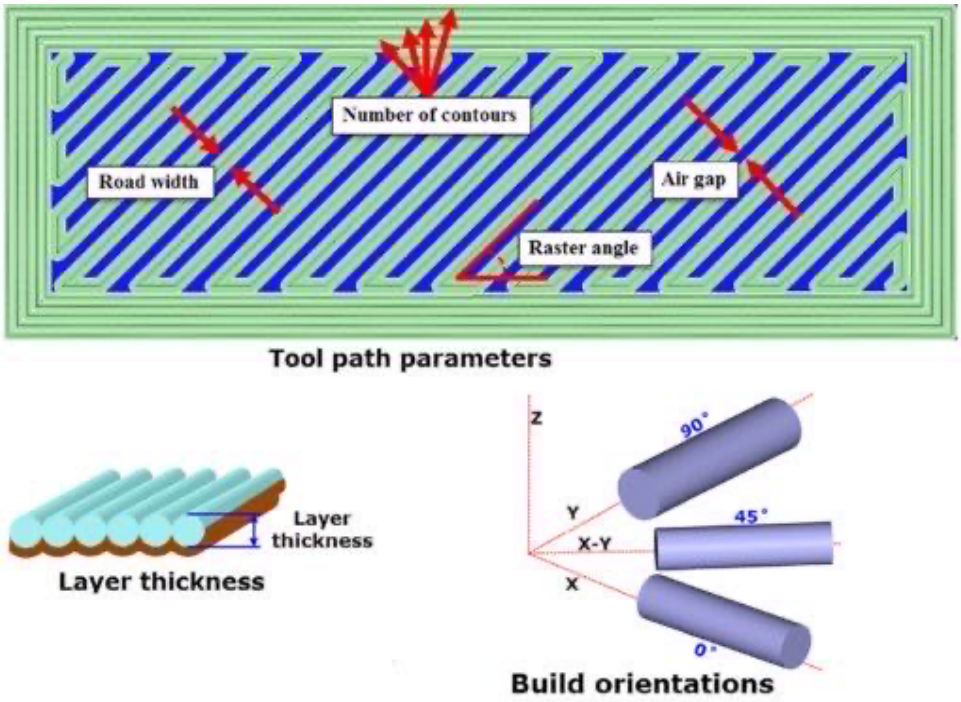

Figure 8: Examples of Process Parameters (Mohamed, Masood, & Bhowmik, 2018)

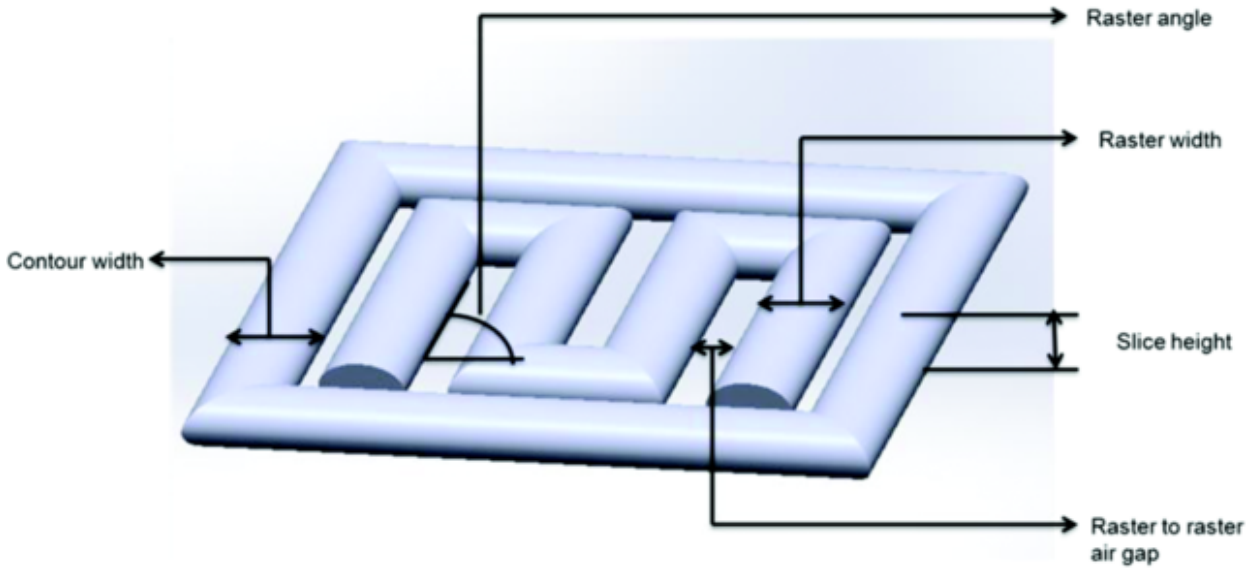

Figure 9: Examples of Width and Angle Parameters (theone8480, 2018)

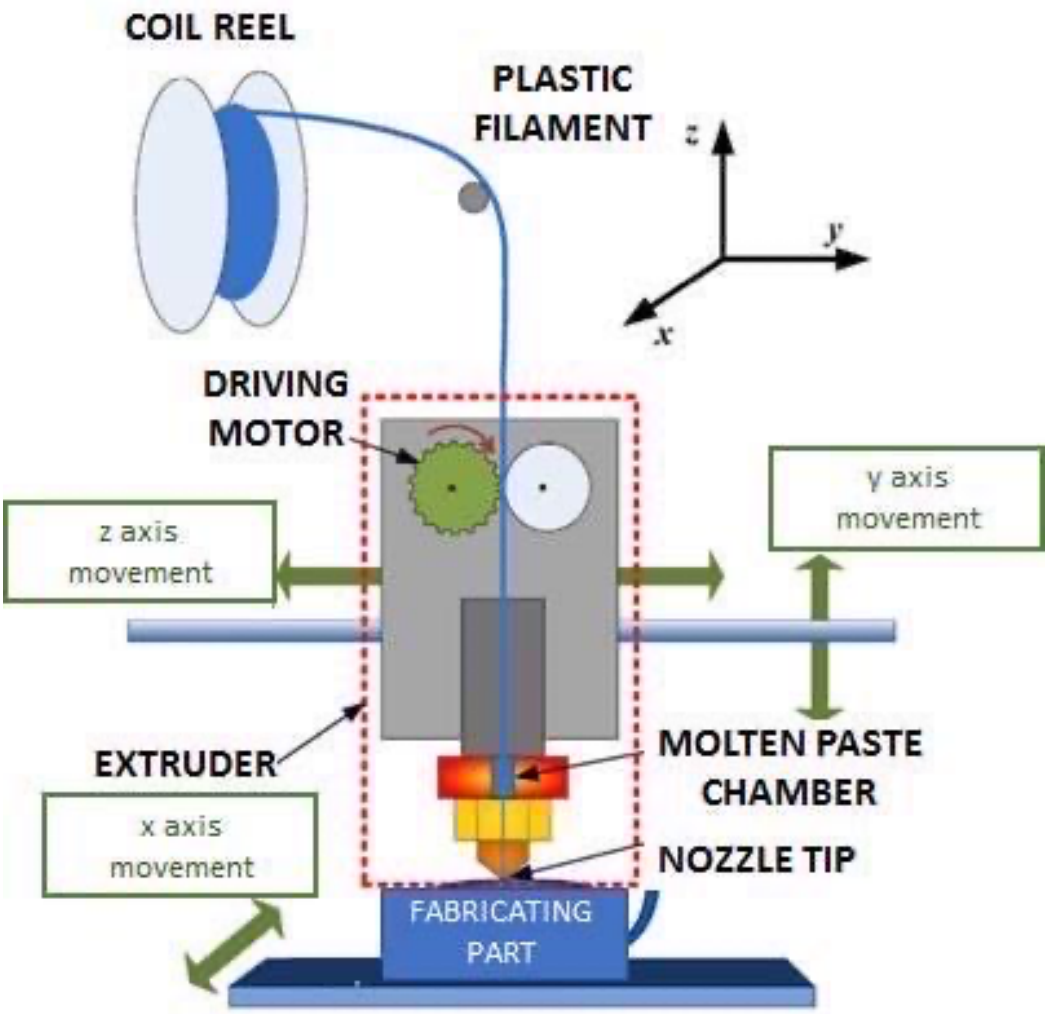

Figure 10: Diagram of FDM Printer (Zaharin, Rani, & Ginta…, 2018)

2.4.3 — Optimization Summary

The various methodologies for optimization are ideal for researchers but are outside of the experience and knowledge of the typical maker. This study will focus on the review and identification of methods and processes that could be used by makers increase throughput to meet supply shortfalls in a disaster. The literature demonstrates that common factors that affect print speed, cost, and quality include:

- layer thickness
- print speed
- infill density
- raster width

It should be noted that a key component of the maker workflow is a visual inspection Figure 5. This inspection is used to determine the quality of the printed object. An overview of visual quality control can be found in the 4.2 — Inspection for Quality Control section.

3 — CHAPTER THREE - PROBLEM DEFINITION

3.1 — RESEARCH SCOPE

As noted previously, makers from across the globe have utilized 3D printers to meet the PPE challenges posed by COVID-19. According to Salmi et al., (2020), some of the items that were produced via 3DP include:

- Testing Supplies
- Ventilator parts
- Face Masks
- Face Shields

Salmi et al., (2020) estimates that the pandemic demand for face shields is in excess of 1 billion units. According to Novak and Loy (2020), from February to March 2020, 62% of PPE projects were focused on the production of face shields. Of all the PPE project surveyed, over 60% utilized FDM printers. In many cases, maker production represented volunteer efforts to create PPE that was in short supply. The quick production (throughput) of PPE was critical to alleviate short falls but because of the strain on unpaid volunteers utilizing their own resources, it was critical to minimize the need for materials (print stock) and cost on the maker community. Optimization could be used to increase the throughput of shields while at the same time maintaining quality and limiting the materials and cost required to complete a build.

This study is to focus on the adaptation of an optimization technique for injection modeling to optimize FDM print parameters. The primary objective is to define an

optimization technique to maximize throughput while at the same time maintaining quality, and cost reduction. A key component for the maker build process is a visual inspection which is described in Figure 11.

As a secondary objective, this research will develop a methodology for scoring quality based on functionality and surface quality. Finally, as a tertiary objective, the study will structure the optimization model in an accessible manner for makers.

As stated previously, the primary objective is to increase throughput, while reducing costs and maintaining an acceptable quality. Based on the work of Dey and Yodo, (2019), there are numerous parameters that can affect quality, speed, and cost. Of particular interest for this study are the following FDM process parameters including:

- Layer Thickness - refers to the amount of material deposited by the FDM along the vertical axis. The layer thickness is less that the nozzle diameter. The thicker the layers, the faster the print speed. The thickness directly contributes to surface roughness and build strength/flexibility (Solomon, Sevvel, & Gunasekaran, 2020).
- Print Speed - is the speed of the nozzle as it traverses the build surface depositing material (Solomon, Sevvel, & Gunasekaran, 2020). Besides throughput, print speed has been found to have a significant impact on deformation of the active layer (Kačergis, Mitkus, & Sinapius, 2019).
- Infill Density - Solomon et al. (2020) states that, “Infill density denotes the material volume printed on the given component. Infill density directly dominates the printed component’s properties. Lesser density affects the mechanical properties considerably whereas the denser component possesses better

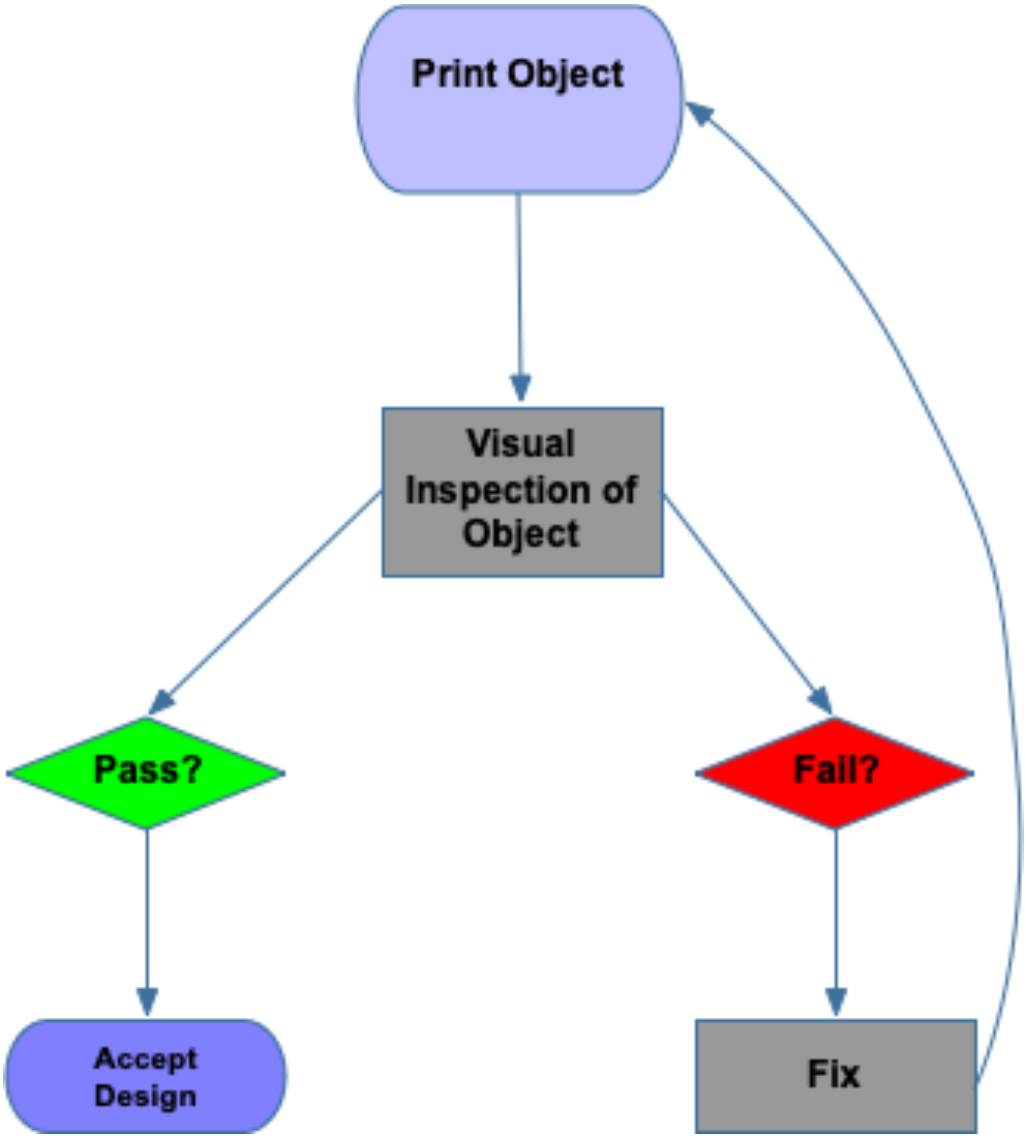

Figure 11: Example of the Typical 3DP Workflow for a Maker

mechanical properties than the earlier one but needs more time to prepare the component."

- Raster Width (Infill Line Width) - can be described as the tool path width of the pattern used to fill the interior regions of a model (Gurrala & Regalla, 2012). Raster width is particularly impactful on a part's surface roughness (Patil, Singh, Raykar, & Bhamu, 2021).
- Wall Thickness - refers to the thickness of the external walls of a printed model. This parameter can affect surface roughness, stability, and throughput (LIANG & LI, 2017).

The following sections will describe the research problems addressed in this study and will also describe the research methodology.

3.2 — Problem Definition

As manufactures have shut down or been disrupted by COVID-19 overall demand for PPE and other medical equipment has skyrocketed while the availability of raw materials has decreased and constrained production (Paul & Chowdhury, 2020). The effects on global industry and the rapid growth in COVID-19 cases has created shortages in many goods including PPE.

With the growing shortages of PPE, many organizations and individual makers began producing PPE to meet demand. Most of the 3D models utilized to produce PPE require hours to print (Tino et al., 2020). Face shields typically took between 1.5 to 3.5 hours to print (Wesemann et al., 2020). In some cases, COVID-19 created delays in shipping of 3D filament. To meet PPE demand, it was critical to produce as many face shields as

possible with minimal material. Optimization could be used to increase the throughput of shields while at the same time maintaining quality and limiting the materials and cost required to complete a build.

For makers, there are several issues that can be identified when utilizing FDM printers Figure 12. The issues can be categorized as primary and secondary problems and are as follows:

- Primary Problems - Speed, Cost, and Quality
    1. What parameters should be optimized to increase speed, reduce costs, and achieve satisfactory quality?
    2. What is the contribution of each parameter to the increase speed, reduce costs, and achieve satisfactory quality?
- Secondary Problems
    1. Because of the subjective nature of quality inspection, what is an acceptable methodology to quantify the quality of a 3D printed model?
    2. Accessibility of the optimization methodologies remains the domain of engineers. Can the optimization method utilized in this study be made accessible to makers?
    3. Does the additive nature of FDM allow for the quick elimination of print parameters?

3.2.1 — Primary Problems

What parameters should be optimized to increase speed, reduce costs, and achieve satisfactory quality?

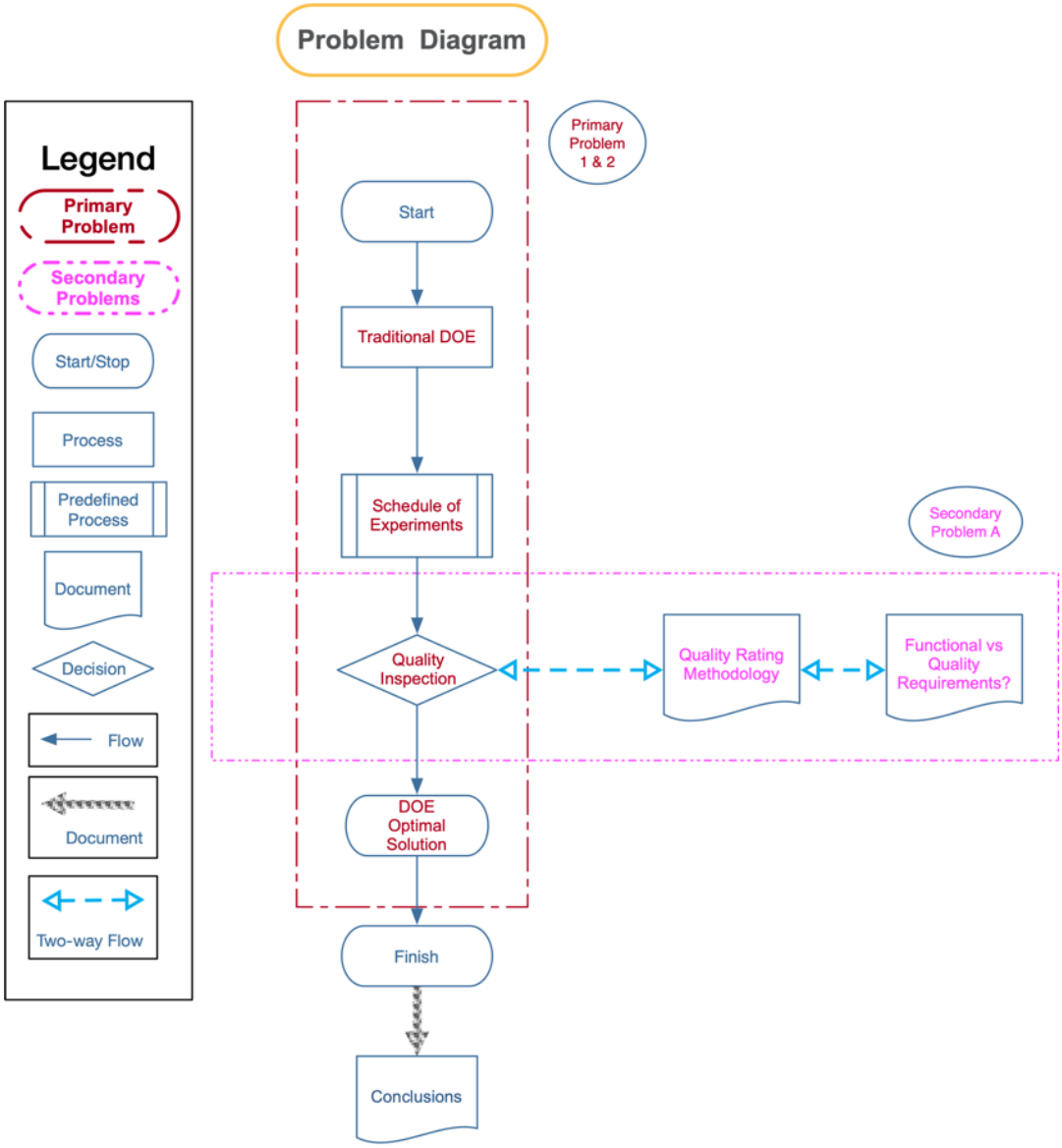

Figure 12: Diagram of the Problems Outline in this Research

In the studies reviewed by Dey and Yodo, (2019) (Figure 7), the common variables affecting build time and quality is layer thickness, print speed, infill density and raster width. Layer thickness (Figure 8) is the thickness of a layer deposited by nozzle and is affected by extrusion speed and can depend upon the type of the nozzle (Gurrala & Regalla, 2012). Print Speed is the mm/s that the printer head deposits filament. Infill density (or percentage) is the percentage of an infill pattern that fills voids in print. The raster width is the thickness of lines in a print. Build orientation (Figure 8) is the geometry of the model as it is printed on the build plate (Figure 10).

It is proposed that this research look at the effects of the following variables on print speed and quality:

- Layer Thickness
- Print Speed
- Infill Density
- Raster Width
- Wall Thickness

What is the contribution of each parameter to the increase speed, reduce costs, and achieve satisfactory quality?

For this study, I propose that the methodology utilized by Tranter et al. (2017) (Figure 4) with modifications to address research gaps identified by Dey and Yodo (2019). In the study, Tranter et al. (2017) optimized for energy consumption and quality in injection molding be adapted to optimizing for throughput, cost, and quality in FDM printing.

A study by Tranter et al., (2017) offers a possible solution developing a cost and quality model that could be utilized by makers. The study is an investigation into the reduction of energy consumption in injection molding while maintaining a part's quality. According to the paper the "work focused on study on the effects of selected process parameters of the injection molding process on energy consumption and quality of the molded parts. This is to achieve an optimal process parameter configuration that would reduce the energy consumption, whilst still maintaining production of parts of good quality."

The design of the experiment in the Tranter et al., (2017) paper utilized design of experiments to test the design parameters to determine the relationship with the process output. The study focused on the following:

- A Melt Temperature, T_m
- B Mold Temperature, $T_m o$
- C Holding Pressure, P_h
- D Holding Time, th
- E Cooling Time, tc

The researchers utilized a 2-level fractional factorial design in which process parameters had a specified upper (+1) and lower (-1) levels. With 16 trails, the 25-1 design, no main effects were confounded with any other main effect or 2-factor interaction. This allowed them to be estimated separately from one another without the requirement for conducting a full factorial (32 trails) (Tranter, Refalo, & Rochman, 2017). A total of 10 parts were created per trail.

Once the trials were completed, Analysis of Variance (ANOVA) was utilized to determine the effects of the process parameters on the energy consumption. 5 of the 10 samples generated per trial were selected at random and then a quality determination procedure was applied. ANOVA was employed again to determine the effects of the process parameters on the part quality. Once the energy and quality data were collected response optimization was used to jointly optimize the process parameters (Tranter, Refalo, & Rochman, 2017).

The results of the research show that the outlined process can be used to optimize for energy and quality. The researchers also state that their methodology could be used in other studies using other materials and energy requirements (Tranter, Refalo, & Rochman, 2017).

3.2.2 — SECONDARY PROBLEMS

Because of the subjective nature of quality inspection, what is an acceptable methodology to quantify the quality of a 3D printed model?

For makers using FDM printing, the quantification of quality offers challenges, shown as A in Figure 4. As noted previously, quality will be rated based on a visual inspection. In the case of makers and low cost 3DP, the literature does not offer guidance for a previously used system. As part of this work, a rating system will be developed. The rating system will provide a unified methodology for scoring quality. This rating system could be extended to other projects and uses.

Previous studies have used a visual inspection to check the functional and non-function aspects of a 3D printed model (Ramananantoandro et al., 2014 and Li et al., 2017). The

functionality of a print can be considered an objective measurement. With the production of face shields the 3D printed band is functional if it has both flexibility and precision.

The band must be flexible to fit on a person's head. A simple stretching of the band by hand will suffice. Problems with the band could be inflexible or brittle. In either case,

- Flexibility - Band is flexible (ie it can fit on the head)
- Precision of print

The simplistic design of the face shield lends itself to a less rigorous need for exact headband measurements and dimensions. Basically, a headband does not need to have exact measurements to work. However, measurements should be considered as part of the inspection process. To assess the measurements and dimensions of the headbands, a stencil with flex marks will be created. The assessor can then compare the headband to the stencil and use the flex marks as a means to determine functionality. For the functionality of the band, characteristics 1-2 should be considered binary.

In the case of aesthetics, a subjective assessment is required. This study will utilize a visuotactile perception classification based on the work of Ramananantoandro et al. (2014), an assessor classifies an object based upon a scale of 1-5(1 being the worst value and 5 the best). The three characteristics to be classified are as follows:

- Hedonic tactile appreciation - this characteristic is the preference of the object based upon touch (Ramananantoandro, Larricq, & Eterradossi, 2014).

- Tactile roughness perception - this characteristic is the determination of roughness based upon touch (Ramananantoandro, Larricq, & Eterradossi, 2014).
- Visual impression of roughness - this characteristic is the determination of surface roughness based upon sight only (Ramananantoandro, Larricq, & Eterradossi, 2014).

The scores will be captured via a “scoring card” (Figure 13).

Accessibility of the optimization methodologies remains the domain of engineers. Can the optimization method utilized in this study be made accessible to makers?

As the proposed methodology (3.2.1 — Primary Problems) is applied, efforts will be made to allow makers to easily utilize the optimization process in future projects. Jupiter Notebooks off a possible free and open-source solution to reproduce the methodology in an accessible manner.

Does the additive nature of FDM allow for the quick elimination of print parameters?

“Everyone then who hears these words of mine and does them will be like a wise man who built his house on the rock. And the rain fell, and the floods came, and the winds blew and beat on that house, but it did not fall, because it had been founded on the rock. And everyone who hears these words of mine and does not do them will be like a foolish man who built his house on the sand. And the rain fell, and the floods came, and the winds blew and beat against that house, and it fell, and great was the fall of it.”
Matthew 7: 24-27

Purpose:

Criteria (clearly spelled out as positive statements)	weight	Option 1		Option 2		Option 3		Option 4	
		rating	weighted score	rating	weighted score	rating	weighted score	rating	weighted score
Criterion 1	250	0%	0	0%	0	0%	0	0%	0
Criterion 2	200	0%	0	0%	0	0%	0	0%	0
Criterion 3	150	0%	0	0%	0	0%	0	0%	0
Criterion 4	100	0%	0	0%	0	0%	0	0%	0
Criterion 5	80	0%	0	0%	0	0%	0	0%	0
Criterion 6	80	0%	0	0%	0	0%	0	0%	0
Criterion 7	50	0%	0	0%	0	0%	0	0%	0
Criterion 8	50	0%	0	0%	0	0%	0	0%	0
Criterion 9	40	0%	0	0%	0	0%	0	0%	0
Totals	1000		0		0		0		0

Rating: Excellent ★★★★★(100%); Good ★★★★(75%); satisfactory ★★★ (50%); mediocre ★★ (25%); poor ★ (0%)

Figure 13: Sample Aesthetic Scoring Form

FDM printing is additive in nature, the quote above regarding foundations has struck a chord with me. I will be investigating the possibility that if a single print parameter can cause a print to be non-functional or to be of poor quality be itself, will future experimental runs that include that parameter with the same settings cause functionality and quality issues in a run.

For example, it is proposed that this research look at the effects of the following variables on print speed and quality:

- Layer Thickness
- Print Speed
- Infill Density
- Raster Width
- Wall Thickness

In experiment Run 2, Layer Thickness is set to .28 and all other parameters are set to the default. The prints from Run 2 are judged to be of poor quality. How is the quality of any other runs that include the Layer Thickness set to .28? Can a single print parameter, such as Layer Thickness be a foundation of sand?

3.3 — Research Scope and Definition Summary

Research Scope

This research has several objectives, primary, secondary, and tertiary. The objectives are as follows:

- Primary - define an optimization technique to maximize throughput while at the same time maintaining quality, and cost reduction.
- Secondary - develop a methodology for scoring quality based on functionality and surface quality.
- Tertiary
  - Structure the optimization model in an accessible manner for makers.
  - Determine the possibility of eliminating print parameters from the experimental design due to the additive nature of FDM.

To achieve the project objectives, this study will address the following research problems.

Primary Problems - Speed, Cost, and Quality

Utilizing the research, several print parameters will be used to optimize FDM printing. this research looks at the effects of the following variables on print speed and quality:

- Layer Thickness
- Print Speed
- Infill Density
- Raster Width
- Wall Thickness

This work will represent the use of existing engineering approaches used in processes outside of FDM, as identified in Tranter et al., (2017), to optimization while maintaining quality in FDM printing. Additionally, rather than the use of response surface

methodology to determine the optimal settings, this study will use the numerical optimization of ϵ -Contraint methodology.

Secondary Problems

Previous studies have used a visual inspection to check the functional and non-function aspects of a 3D printed model (Ramananantoandro et al., 2014 and Li et al., 2017). This study will lean on Ramananantoandro et al., (2014) and Li et al., (2017) to develop an inspection methodology for FDM printing.

Accessibility of the optimization methodologies remains the domain of engineers. Can the optimization method utilized in this study be made accessible to makers? This study will utilize Jupiter notebooks as a method to make the various analysis more accessible. Jupiter notebooks can be described as a document format for publishing code, results and explanations in a readable form that can be executed (Kluyver et al., 2016). The notebook is is designed to allow for reproducible computational workflows (Yin et al., 2017). In the case of these experiments, the notebooks are designed to allow the results to be calculated in a repeatable manner. Additionally, the notebooks will allow for the results and code to be utilized in future research with minimal effort.

4 — CHAPTER FOUR - EXPERIMENTAL DESIGN AND SOLUTION APPROACH

4.1 — DESIGN OF EXPERIMENT (DOE)

According to the “NIST/SEMATECH e-Handbook of Statistical Methods”, Design of experiments (DOE) can be defined as:

“Design of experiments (DOE) is a systematic, rigorous approach to engineering problem-solving that applies principles and techniques at the data collection stage so as to ensure the generation of valid, defensible, and supportable engineering conclusions. In addition, all of this is carried out under the constraint of a minimal expenditure of engineering runs, time, and money.”

DOE can be categorized in 4 general engineering domains (Natrella, 2010). The domains include:

- Comparison - the researcher is interested in how changes in a single variable affect the system.
- Screening and Characterization - this process allows the researcher to understand the system. It also allows for the creation of a ranked list of factors and their influence on the overall results.
- Modeling - the modeling process allows the researcher to create an equation that accurately and with high predictive power to emulate the system.

- Optimization - a researcher is interested in the determination of the optimal settings of the system factors. The settings of these factors will then optimize the process response.

This study will focus on the engineering domain of optimization.

In the case of makers responding to COVID-19 PPE shortages, the critical responses are print speed, cost, and quality. This research will leverage DOE to identify the critical factors that contribute to the responses of speed, cost, and quality. Once the factors have been identified, processes described in the following sections will be utilized to minimize costs, maximize speed, and maintain quality.

4.1.1 — An Example of DOE

In Tranter et al. (2017) the research team optimized for energy consumption and quality in injection molding. This method could be adapted to optimize for throughput, cost, and quality in FDM printing. The study is an investigation into the reduction of energy consumption in injection molding while maintaining a part's quality. According to the paper the "work focused on study on the effects of selected process parameters of the injection molding process on energy consumption and quality of the molded parts. This is to achieve an optimal process parameter configuration that would reduce the energy consumption, whilst still maintaining production of parts of good quality."

The design of the experiment in the Tranter et al., (2017) paper utilized design of experiments to test the design parameters to determine the relationship with the process output. The study focused on the following:

- A Melt Temperature, T_m
- B Mold Temperature, $T_m o$
- C Holding Pressure, P_h
- D Holding Time, th
- E Cooling Time, tc

The researchers utilized a 2-level fractional factorial design in which process parameters had a specified upper (+1) and lower (-1) levels. With 16 trails, the 25-1 design, no main effects were confounded with any other main effect or 2-factor interaction. This allowed them to be estimated separately from one another without the requirement for conducting a full factorial (32 trails) (Tranter, Refalo, & Rochman, 2017). A total of 10 parts were created per trail.

Once the trials were completed, 4.1.3 — Analysis of Variance (ANOVA) was utilized to determine the effects of the process parameters on the energy consumption. 5 of the 10 samples generated per trial were selected at random and then a quality determination procedure was applied. ANOVA was employed again to determine the effects of the process parameters on the part quality. Once the energy and quality data were collected response optimization was used to jointly optimize the process parameters (Tranter, Refalo, & Rochman, 2017).

The results of the research show that the outlined process can be used to optimize for energy and quality. The researchers also state that their methodology could be used in other studies using other materials and energy requirements (Tranter, Refalo, & Rochman, 2017).

4.1.2 — FRACTIONAL FACTORIAL DESIGN

In a factorial design, the factors are varied together rather than one at a time. Factorial design is ideal for dealing with several factors. In the case of Tranter (2017), the factors of interest were:

- A Melt Temperature, T_m
- B Mold Temperature, $T_m o$
- C Holding Pressure, P_h
- D Holding Time, th
- E Cooling Time, tc

Tranter (2017) utilized a 2-level fractional factorial design. The level notation can be described as the following (Christensen, 1996):

"A useful notation for factorial experiments identifies the number of factors and the number of levels of each factor. For example, the alcohol–sleeping pill experiment has 4 treatments because there are 2 levels of alcohol times 2 levels of sleeping pills. This is described as a 2 × 2 factorial experiment. If we had 3 levels of alcohol and 4 doses (levels) of sleeping pills we would have a 3×4 experiment involving 12 treatments."

Fractional factorial design utilizes confounding. This is a method to design factorial experiments allowing incomplete blocks. By using fractional replication, fewer treatments are needed as compared to full factorial. A basic concept in experimental

design is making sure that there is adequate replication to provide a satisfactory estimate of error (Christensen, 1996).

4.1.3 — Analysis of Variance (ANOVA)

The Analysis of Variance (ANOVA) was developed by Sir Ronald Fisher for the analysis of results in agricultural experiments (Fisher, 1992). According to Larson (2008), "ANOVA can be defined as a statistical technique used to analyze variation in a response variable measured under conditions defined by discrete factors. ANOVA is frequently used to test equality among several means by comparing variance among groups relative to variance within groups."

In the case of Tranter (2017), ANOVA was utilized to analyze the effects of the process parameters on both energy consumption and quality. With energy consumption, ANOVA allowed the researchers to study their effect of energy use based on the process parameters. The same ANOVA process was also utilized to determine the effects of the parameters on the part quality. Upon determining the effects of the process parameters, response optimization was conducted to jointly optimize the parameters (Tranter, Refalo, & Rochman, 2017).

4.1.4 — Ordinary Least Squares Regression

Ordinary Least Squares Regression (OLS) is a common linear analysis model. OLS models the relationship between a dependent value and a collection of independent variables (Pohlman & Leitner, 2003). The value of the dependent variable is defined by the linear combination of the independent variables as defined by:

$$Y = \beta_0 + \beta_1 * X_1 + \beta_2 * X_2 + \beta_k * X_k + \epsilon$$

where:

- Y is the dependent variable
- βs are the regression coefficients
- X is the column vector of the independent variables
- ϵ is the vector of errors of the prediction.

The errors are assumed to be normally distributed and expected to be zero with a common variance (Pohlman & Leitner, 2003).

In the case of this study, the OLS equation is expected to be like:

$$Cost = \beta_0 + \beta_1 * x_1 + \beta_2 * x_2 + \beta_3 * x_3 + \beta_4 * x_4 + \beta_5 * x_5$$

and

$$Time = \beta_0 + \beta_1 * x_1 + \beta_2 * x_2 + \beta_3 * x_3 + \beta_4 * x_4 + \beta_5 * x_5$$

where:

- $Cost$ and $Time$ are the dependent variable
- βs are the regression coefficients
- x_1 is the column vector of the layer height (lh)
- x_2 is the column vector of the print speed (ps)
- x_3 is the column vector of the infill density (id)
- x_4 is the column vector of the raster width (rw)
- x_5 is the column vector of the wall thickness (wt)

In Figure 14, the “coef” column represents the β values.

4.1.5 — Response Optimization and Epsilon-Constraint

Tranter (2017) utilized response optimization to determine the ideal process parameters to optimize for multiple responses. When optimizing for a single response, a solution can be easily obtained. In the Tranter study, the objective was to minimize energy consumption while at the same time maximizing part quality. In cases where there are multiple objectives to optimize, multiple response optimization offers a solution.

Multiple response optimization or response surface methodology (RSM) is set of mathematical and statistical techniques that can be used in cases where modeling and analysis require multiple responses of interest is to be optimized. A desirability function allows the researcher to optimize of all responses simultaneously by combining the various objectives into a single objective function. This function represents the relationship of all responses that are to be optimized (Akçay & Anagün, 2013).

As noted in Dey and Yodo (2019):

“In most of the existing research, the optimum combination of process parameters was determined from experimental studies instead of applying numerical optimizations. Thus, an optimum solution is one of the combinations from the experimental data. However, the actual optimal solutions might be different.”

This study will utilize ϵ-constraint methodology. ϵ-constraint is a class of multiple objective programming. These types of problems focus on the mathematical optimization of multiple objective functions where the objectives need to be optimized

OLS Regression Results

Dep. Variable:	time	R-squared:	0.985
Model:	OLS	Adj. R-squared:	0.982
Method:	Least Squares	F-statistic:	287.3
Date:	Wed, 28 Jul 2021	Prob (F-statistic):	1.17e-52
Time:	19:27:13	Log-Likelihood:	-593.61
No. Observations:	80	AIC:	1219.
Df Residuals:	64	BIC:	1257.
Df Model:	15		
Covariance Type:	nonrobust		

	coef	std err	t	P>|t|	[0.025	0.975]
Intercept	3.886e+04	4869.801	7.980	0.000	2.91e+04	4.86e+04
alh	-9.373e+04	1.1e+04	-8.494	0.000	-1.16e+05	-7.17e+04
aps	-101.9583	81.061	-1.258	0.213	-263.896	59.980
aid	6178.6667	1.31e+04	0.470	0.640	-2.01e+04	3.24e+04
arw	2096.5000	3353.230	0.625	0.534	-4602.347	8795.347
awt	-8507.9167	3197.582	-2.661	0.010	-1.49e+04	-2120.012
alh:aps	302.8333	168.294	1.799	0.077	-33.372	639.039
alh:aid	-4.994e+04	1.68e+04	-2.968	0.004	-8.36e+04	-1.63e+04
alh:arw	1.009e+04	4207.345	2.399	0.019	1688.613	1.85e+04
alh:awt	2.909e+04	4207.345	6.913	0.000	2.07e+04	3.75e+04
aps:aid	301.9000	201.953	1.495	0.140	-101.547	705.347
aps:arw	-137.1250	50.488	-2.716	0.008	-237.987	-36.263
aps:awt	-18.6750	50.488	-0.370	0.713	-119.537	82.187
aid:arw	5830.0000	5048.814	1.155	0.252	-4256.165	1.59e+04
aid:awt	-1.288e+04	5048.814	-2.552	0.013	-2.3e+04	-2798.835
arw:awt	1626.2500	1262.203	1.288	0.202	-895.291	4147.791

Omnibus:	117.964	Durbin-Watson:	1.973
Prob(Omnibus):	0.000	Jarque-Bera (JB):	3766.256
Skew:	4.734	Prob(JB):	0.00
Kurtosis:	35.252	Cond. No.	3.13e+04

Figure 14: Example OLS Results

simultaneously or sequentially. In many instances in the literature, the Pareto or efficient frontier function can be used to illustrate the trade-offs among conflicts between the multiple objectives (Wattanasaeng & Ransikarbum, 2021). According to Wattanasaeng and Ransikarbum (2021):

"The advantages of ϵ-constraint programming includes being able to obtain exact Pareto solutions, instead of approximated solutions, using a series of single-objective subproblems in which all but one objective is transformed into constraints."

Mathematically, ϵ-constraint programming can be described as the following:

Minimize/Maximize Z: $f_i(x)$

subject to: $x \in X$

$f_i(x) \leq \epsilon_j; \forall_i \in \{1, \ldots, k\} \backslash \{j\}$

For example, following the ϵ-constraint workflow (Figure 15), in the case of a problem with two objectives (f_1 and f_2), the researcher would keep f_1 as an objective Minimize $f_1(x)$ and treat f_2 as a constraint - $f_2(x) \leq \epsilon_2$ and then keep f_2 as an objective Minimize $f_2(x)$ and treat f_1 as a constraint - $f_1(x) \leq \epsilon_1$.

4.2 — Inspection for Quality Control

Numerous definitions for visual inspection are defined in the literature. The FAA (1997) defines it as the following:

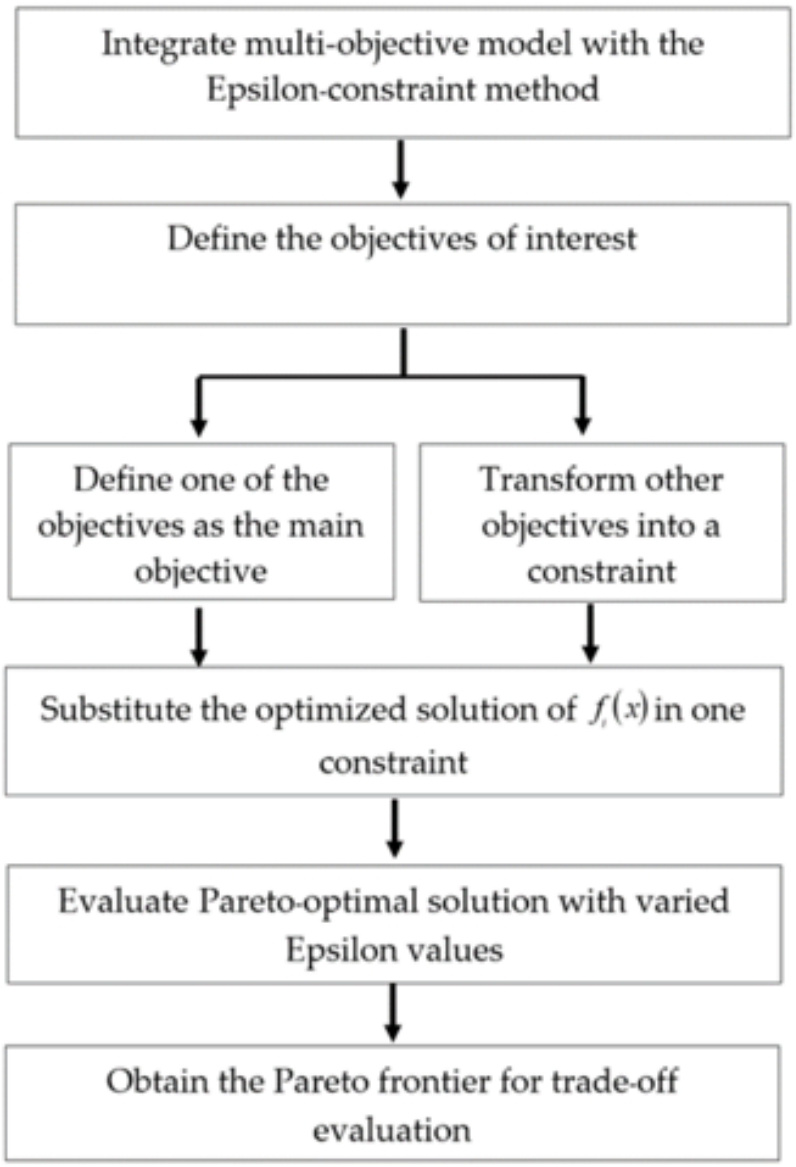

Figure 15: ϵ-Constraint Workflow (Wattanasaeng & Ransikarbum, 2021)

“Visual inspection is defined as the process of using the unaided eye, alone or in conjunction with various aids, as the sensing mechanism from which judgments may be made about the condition of a unit to be inspected.”

In the case of this study, visual inspection will be conducted with the unaided eye (FAA, 1997).

Numerous studies outline the generic steps for a visual inspection. These steps remain the same for manual, automated, and hybrid visual inspection systems. The generic functions include (Salvendy, 2001):

- Initiate - Defined as the preparatory work to perform the inspection. Initiation could include accessing a scoring system, gathering inspection equipment, and other work (Drury & Watson, 2002).
- Access - Defines as access to the inspection area or item to be inspected at an appropriate level (Drury & Watson, 2002).
- Search - Defines as moving the inspection object to adequately inspect the object (Drury & Watson, 2002).
- Decision - Form a indication regarding the object and compare to a standard (Drury & Watson, 2002).
- Response - On indication confirmation, document the result and complete the inspection (Drury & Watson, 2002).

With the development of a visual inspection system, it is important to note the logical errors that can be made while utilizing the generic steps. Drury and Watson (2002)

outline some examples of the errors that can occur with each of the generic steps. These include:

- Initiate
  - Incorrect equipment
  - Incorrect calibration
- Access
  - Item damaged in presentation
  - Incorrect Item
- Search
  - Error Indication Missed
  - Error Indication Misidentified
- Decision
  - Incorrect Measurement
  - Error Indication Misclassified
- Response
  - Response Action Incomplete
  - Wrong Response for Indication

By noting these errors, it is hoped that the visual inspection process can be completed in such a way as to minimize logical errors. The literature outlines some control actions that can be taken to minimize inspection errors. The actions include vigilance, environment, posture, speed, training, and documentation (Drury & Watson, 2002).

4.2.1 — VIGILANCE, ENVIRONMENT, POSTURE, SPEED, TRAINING, AND DOCUMENTATION

According to the literature, when an individual is performing a task, the individual's vigilance for task quality can be affected by the amount of time on task and the environment. Studies show that an individual has maximum vigilance during the first 15 minutes of a task and vigilance then drops by 10-15% in the first 30 minutes. A gradual decline in vigilance continues after the first 30 minutes (Warm, Parasuraman, & Matthews, 2008). Research shows that random noises increase the difficulty of tasks and decreases an individual's vigilance (Taylor, Melloy, Dharwada, Gramopadhye, & Toler, 2004).

The environment that the visual inspection is conducted in a component of success. As noted, previous the environment can impact an individuals' vigilance (Taylor, Melloy, Dharwada, Gramopadhye, & Toler, 2004). An environment for successful visual inspection should be both distraction free and comfortable (Melchore, 2011). Additionally, lighting is key to error detection. Inspection area should be well lit and glare/reflection free (Drury & Watson, 2002).

The comfort of the inspector can affect the quality of the inspection. A growing body of research demonstrates the importance of ergonomics. Drury and Watson (2002) enumerate many of these studies.

The velocity of the visual inspection can be affected by the the actual speed the inspection is performed. The science of human factors engineering is described as Speed/Accuracy Trade-Off (SATO). The quicker the inspection task is completed, the

more data limited and constrained is the inspector. This factor in conjunction with vigilance can be a large negative impact (Drury & Watson, 2002).

Training and documentation are linked factors. In the case of training, a common adage is “find the right person for the job”. Typically, the right person requires the right training. Unlike the previous factors, selection and training are ongoing costs. When developing a training regime, care must be taken to balance initial training with ongoing, update training (Drury & Watson, 2002).

A study by Webber and Drury (2000) identified that documentation was listed as a contributing factor in 46% or errors in maintenance and inspection. documentation need to be designed in accordance with proven guidelines that reduce errors and should be more usable to inspectors (Drury & Watson, 2002).

In this study, the generic steps for visual inspection will be utilized. Additionally, care will be taken to mitigate and control the human factor errors of vigilance, environment, posture, speed, training, and documentation.

4.2.2 — Functional vs Nonfunctional Quality

3DP and FDM technology has been used extensively for rapid prototyping of components, both simple and intricate. 3DP has also been used to create embossing tools, conductive polymers, pharmaceuticals, dielectric products, biomedical implants, medical supplies, spare parts, food, and toys (Mwema, Akinlabi, & Fatoba, 2020). In cases such as toys, spare parts, and PPE (face shields), quality must be measure based on functional and non-functional quality.

In the case of makers, a printed object must be functional and have acceptable aesthetics (non-functional quality). A visual inspection can be used to determine the if an object is functional. In the case of aesthetics, a visual inspection will yield a subjective observation. Previous research has utilized the visuotactile perception to rate objects (Li et al., 2017).

In a study by Ramananantoandro et al. (2014), visuotactile perception can be classified as the following:

- Hedonic tactile appreciation - this characteristic is the preference of the object based upon touch.
- Tactile roughness perception - this characteristic is the determination of roughness based upon touch.
- Visual impression of roughness - this characteristic is the determination of surface roughness based upon sight only.

The study had assessors rank objects based upon a scale of 1-5 (1 being the worst value and 5 the best). Ramananantoandro et al. (2014) utilized samples of wood and wood materials to determine surface roughness. Li et al., (2017) applied this technique to 3DP.

In Li et al., (2017), visuotactile perception was compared to measured roughness. Using the Ramananantoandro et al. (2014) methodology, the measured roughness matched well with the measured roughness. This methodology could be utilized in this research project.

4.3 — The Inspection Score

The visual inspection will consist of the following steps outlined in Figure 16.

This study will utilize a visuotactile perception classification based on the work of Ramananantoandro et al. (2014), An assessor classifies an object based upon a scale of 1-5 (1 being the worst value and 5 the best) expressed as percentages. The three characteristics to be classified are as follows:

- Hedonic tactile appreciation - this characteristic is the preference of the object based upon touch (Ramananantoandro et al., 2014).
- Tactile roughness perception - this characteristic is the determination of roughness based upon touch (Ramananantoandro et al., 2014).
- Visual impression of roughness - this characteristic is the determination of surface roughness based upon sight only (Ramananantoandro et al., 2014).

The weighted averages of the aesthetics assessment will be determined as follows:

7. Tactile Roughness Perception (200) - The face shield headband is meant to be worn on the head. Potentially, medical personnel could be wearing the face shield for long streets of time and comfort is key. The “feel” of the headband is the most important aesthetic factor.
8. Hedonic Tactile Appreciation (150) - Although not as important as the feel of the band, the look of the band can help increase perceptions.
9. Visual Impression of Roughness (100) - the visual inspection of roughness is given the least weight. This decision was made due to the possibility of varying colors of bands. In Ramananantoandro et al. (2014), it was noted that the color of

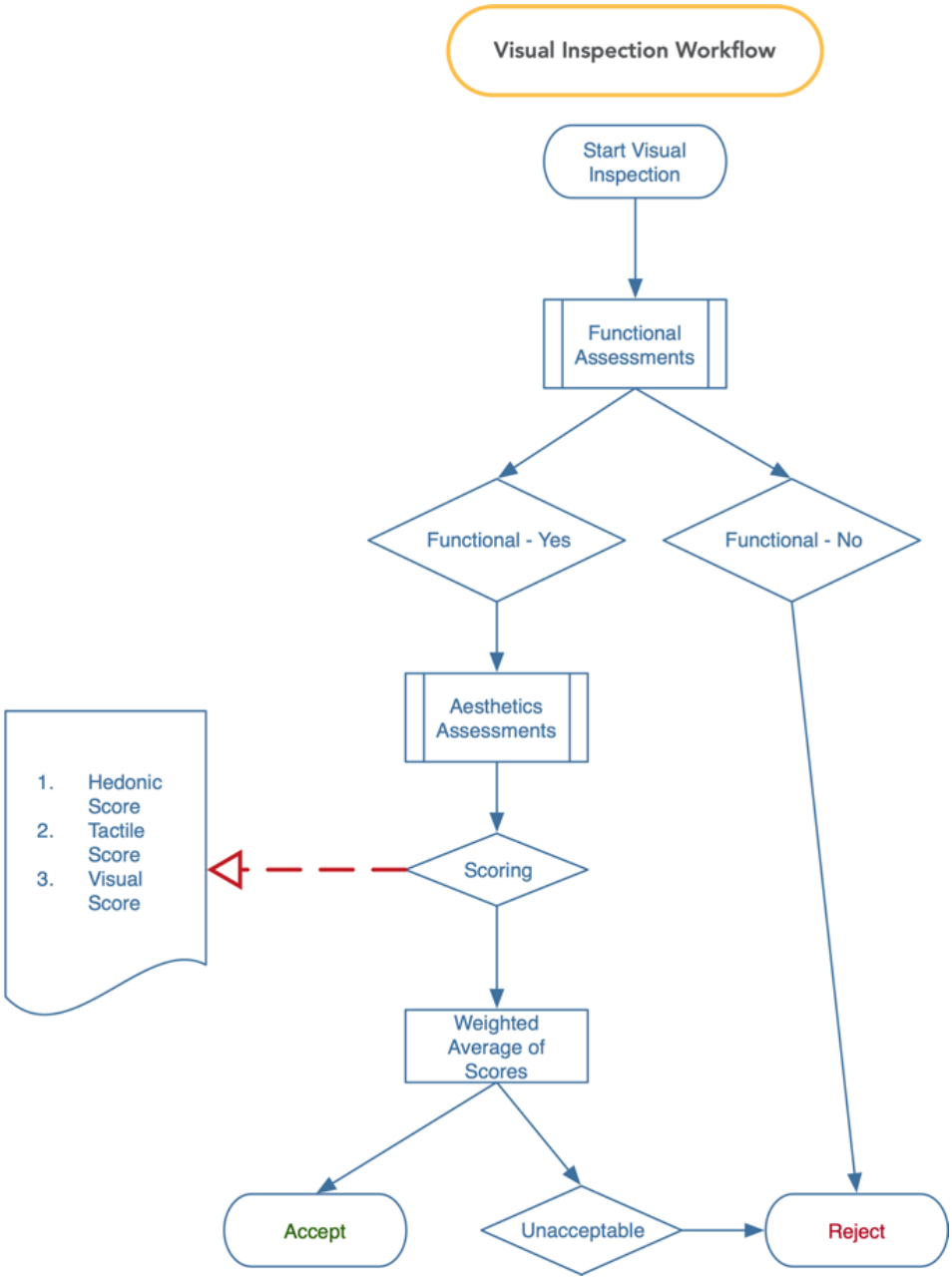

Figure 16: Steps in the Visual Inspection

wood samples had an impact on the impression of roughness. In an emergency, the production of items such as PPE should not be restricted to colors.

Figure 17 represents a template for the visual inspection. The scores will be utilized to help identify optimized print parameters.

The equations used to determine the weighted inspection score is as follows:

$$WS = W * R$$

Where:

- WS is Weighted Score
- W is Weight
- R is the rating expressed as a percentage

4.4 — Inspection Measurements

As noted previously, the simplistic design of the face shield lends itself to a less rigorous need for exact headband measurements and dimensions. Basically, a headband does not need to have exact measurements to work. However, measurements should be considered as part of the inspection process. To assess the measurements and dimensions of the headbands, the following techniques will be utilized:

- Print an “Index” headband. These headbands will be printed with the highest quality setting for the print parameters.
- Using the “Index” create a mold of the headband.
- Compare all subsequently printed headbands to the mold.

Purpose: Visual Inspection Score Card

Criteria	weight	Option 1		Option 2		Option 3		Option 4	
		rating	weighted score	rating	weighted score	rating	weighted score	rating	weighted score
Tactile Roughness Perception	200	0%	0	0%	0	0%	0	0%	0
Hedonic Tactile Appreciation	150	0%	0	0%	0	0%	0	0%	0
Visual Impression of Roughness	100	0%	0	0%	0	0%	0	0%	0
Totals	450		0		0		0		0

Rating: Excellent ★★★★★(100%); Good ★★★★(75%); satisfactory ★★★ (50%); mediocre ★★ (25%); poor ★ (0%)

Figure 17: Visual Inspection (Aesthetics) Score Card

- Consider any headband that does not fit the mold as non-functional

To create the mold, modeling clay was purchased. The clay was modeled into 9x9 cake pans. Once in the pans, the index print was pressed into the mold. The index mold was used for future comparisons (Figure 18).

In addition to the index mold, various measurements (Figure 19 and Figure 20) were utilized to determine the functionality of the headband. The measurements include:

1. Top “horns” at approximately 6cm
2. Bottom “horns” at approximately 12cm
3. Right hand elastic clip, at approximately 2.5cm

4.5 — Experimental Tools

This study will utilize several tools to meet the project objectives. These tools include:

- FDM Printer Selection
- Filament Selection
- 3DP Model Slicer
- Octoprint
- Face Shield Model
- Programming and DOE Modeling

FDM Printers

This study will utilize two low cost FDM printers to test the effects of the listed process parameters on throughput, cost, and quality. The printers to be used are the

Figure 18: Index Mold

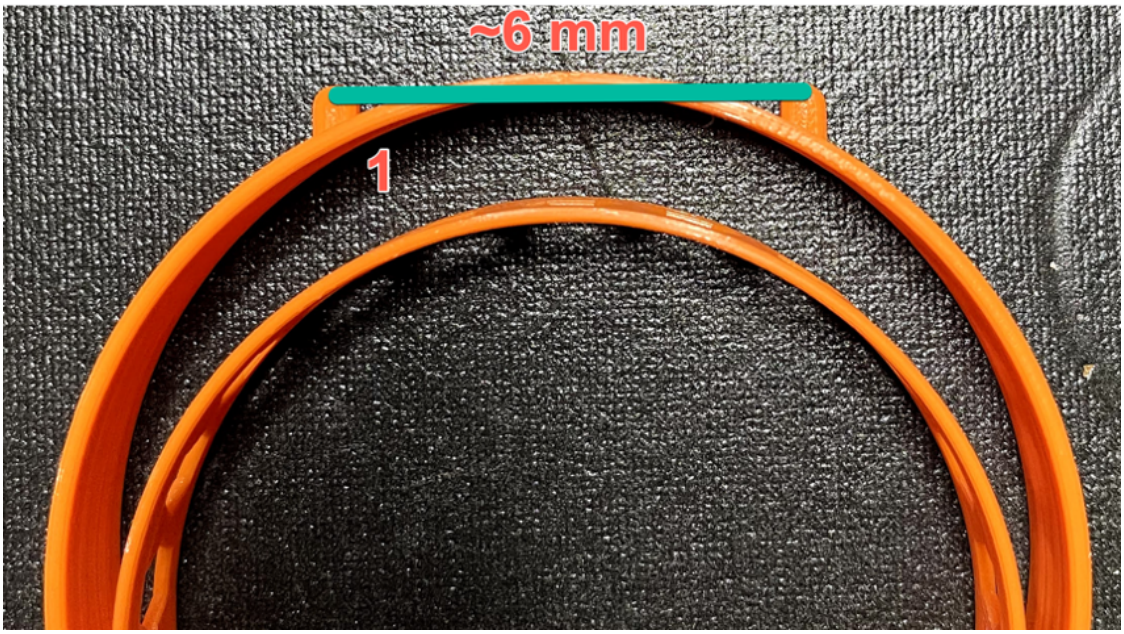

Figure 19: Image of Headband Measurements (Measure 1)

Figure 20: Image of Headband Measurements (Measure 2 and 3)

Artillery Sidewinder X1 and the Creality CR-6 SE. Both printers retail for under $500 and are widely available from numerous sites including Amazon.

Smart Plugs

To collect the cost of electricity to utilize the printers, BN-LINK WIFI Heavy Duty Smart Plug Outlets were use. These smart plugs allow for the remote monitoring of energy usage via a mobile application. Energy usage is captured as kilowatts per hour (KWh). The type of smart plug used offers a cost-effective method to monitor energy consumption.

Filament

There are numerous FDM filaments are used by makers. The best indicator of popular brands of filament, is sales data on Amazon.com. The brand of filament selected will be Hatchbox PLA. This study will review a common, inexpensive Polylactic Acid (PLA) filament. PLA is a natural polymer derived from plant starch, a large carbohydrate that plants synthesize during photosynthesis. For these reasons PLA is environmentally friendly (Valerga, Batista, Salguero, & Girot, 2018). A 1kg roll of PLA costs between $18-$30.

3DP Slicer

Before experimentation, it was required to determine the lower and upper limits of each of the process parameters. In order to determine the lower limits, software for 3DP slicing was selected. Cura is an open-source software developed by Ultimaker and a large community of developers. Although there are several other free and open-source

slicing software available, Cura has been shown to have good quality (Šljivic, Pavlovic, Kraišnik, & Ilić, 2019). Additionally, Cura is a popular choice for makers.

Cura allows a user to access numerous process parameters. Cura has built-in configurations for a large selection of popular 3D printers including the Creality CR-6 SE and the Artillery Sidewinder X1. These printer profiles have the default values for a all the process parameters accessible to Cura. The parameter defaults are those submitted by the Cura community and widely tested. The process parameter defaults will be used as the lower limits for the process parameters reviewed in this study. The upper limits will be set based on the defaults. The process parameters for both print filament and the selected printer can differ.

OCTOPRINT

Octoprint is a free, open-source set of software that allows a user to monitor and control all aspects of an FDM printer via a Raspberry Pi. In most cases, host software that sends commands to the printer must remain connected to the printer during the print. Octoprint allows the users to start print jobs by sending G-code to 3D printer connected via USB. The user interacts with Octoprint via a web interface. Some of the benefits of Octoprint are the ability to start and monitor prints remotely (MP, Shinde, Madaki, & Nadaf, 2019). Additionally, Octoprint has numerous plugins that extend functionality.

In the case of this study, several plugins will be utilized to capture key print metrics. These plugins include:

- Filament Manager - a plugin with numerous functions, including the ability to track material usage

- Cost Estimator - a plug-in that allows a user to estimate print cost for the loaded model.
- Print Job History - a plugin stores all print-job information of a print in a database that can be exported to excel.

Face Shield Model

The models to be printed are a basic face shield designed by Prusa Research (https://www.prusaprinters.org/prints/25857-prusa-face-shield). Prusa Research is a Czech company known for their popular FDM Prusa printers. Prusa developed the Release candidate 1 headband (covid19_headband_rc1.stl) in three days at the onset of the pandemic. The original model was certified by the Czech Ministry of Health (Research, 2020). A consortium of Tennessee Universities produced 18,000 face shields based on the Prusa RC1 headband (Tamburin, 2020). This research will utilize the Prusa RC1 headband as the model to be optimized.

Programming and DOE Modeling

This study will utilize the Python programming language. An open-source programming language, python was introduced in 1991 and is considered extremely stable and mature. Python is used extensively by data scientists and is currently one of the most popular programming languages in the world. A key aspect of the selection of python is the availability of DOE and other relevant scientific and data analysis packages.

As part of the analysis of data from the experiments, Jupyter Notebooks (http://jupyter.org/) using python were utilized. Jupyter notebooks can be described as a

document format for publishing code, results and explanations in a readable form that can be executed (Kluyver et al., 2016). The notebook is is designed to allow for reproducible computational workflows (Yin et al., 2017). In the case of these experiments, the notebooks are designed to allow the results to be calculated in a repeatable manner. Additionally, the notebooks will allow for the results and code to be utilized in future research with minimal effort.

4.6 — Experimental Process

The objective functions in this research are cost, throughput, and quality. In this project, cost is calculated as the sum of material and energy costs. Throughput is synonymous with build time. In this project, cost is calculated as the sum of material and energy costs. Quality, in the case of makers, is expressed as surface roughness.

The study “Parametric Analysis of the Build Cost for FDM Additive Processed Parts Using Response Surface Methodology” (Mohamed et al., 2016b) identifies a cost model that is applicable for determine the cost for printing FDM parts. The model developed is:

$$B_{cost} = C_M + C_S + (M_r + T_{Build})$$

Where:

- B_{cost} = Build cost ($)
- C_M = Model material cost ($)
- C_S = Support material cost ($)
- M_r = Machine running cost (Hour)
- T_{Build} = Built time (Hour)

As noted in Dey and Yodo, (2019) (Figure 21) and Pérez et al., (2018), there are several parameters common to both throughput and surface roughness. The process parameters include:

- Layer Thickness
- Print Speed
- Infill Density
- Raster Width
- Wall Thickness

As with Tranter et al. (2017), this research will utilize a 2-level fractional factorial design, in which process parameter had a specified upper (+1) and lower (-1) level. By using the upper and lower limits, this study will more closely align with the common maker workflow (Figure 22). The 2^{5-1} design will have a total of 16 trials, which was chosen on the basis that in a resolution −V design, no main effect or 2-factor interactions are confounded with any other main effect or 2-factor interactions, this will allow the parameters to be estimated separately from one another without the requirement for conducting a full factorial (32 trials) (Tranter et al., 2017).

As noted previously, the process parameters to be examined include:

- Layer Thickness (LH)
- Print Speed (PS)
- Infill Density (ID)
- Raster Width (RW) - Infill Line Width in Cura
- Wall Thickness (WT)

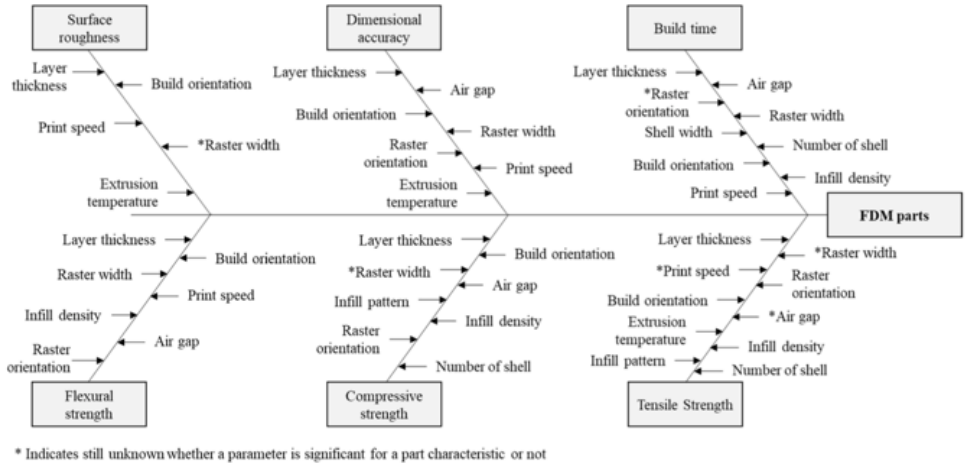

Figure 21: Breakdown of Characteristics vs Parameters (Dey and Yodo, 2019)

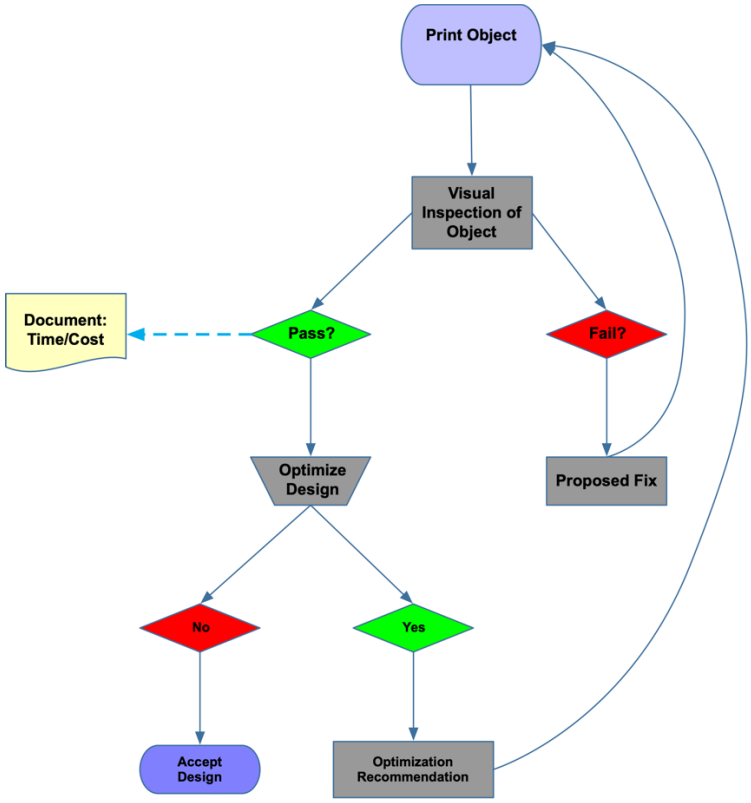

Figure 22: New Workflow to Integrate Optimization

The upper and lower limits of each process parameter is documented in Table 5. For the Print Speed (PS), the PS on the Creality CR-6 SE the upper limit is 60 and for the Sidewinder X1 the PS upper limit is 72. The experimental schedule is laid out in Table 6

After each trial, the throughput, quality, and cost values will be recorded. Ordinary Least Squares Regression (OLS) will be completed on throughput and cost independently. For example, an OLS will be completed for the throughput to determine the respective effects of the process parameters. Using a 95% confidence interval, a process parameter with a P-value smaller that .05 will show that the parameter has a significant effect on the throughput. Upon completion of each OLS analysis. The linear model identified will be reduced to represent only significant first and second order experimental effects. Several OLS runs may be required to reduce the linear equation. A function will be developed in python to utilize backward regression to complete the reduction.

ϵ-constraints optimization will be used to identify the combination of process parameters that will be required to satisfy all the objectives of throughput, cost, and quality. Once the ϵ-constraints optimization has been completed, a validation trial will be completed to test the optimized process parameters. The results will be documented and discussed in Chapter 6.

Table 5: Low and High Print Parameters

Factor	Process Parameter	Unit	Lower Value (-1)	Upper Level (+1)
A	LH	mm	0.16	0.28
B	PS (+20%)		50	60 (72)
C	ID	%	25	15
D	RW	mm	0.4	0.8
E	WT	mm	1.2	0.8

Table 6: Experimental Schedule

Trial Number	LH	PS	ID	RW	WT
1	-1	-1	-1	-1	-1
2	1	-1	-1	-1	-1
3	-1	-1	-1	-1	1
4	-1	1	-1	-1	-1
5	1	1	-1	-1	1
6	-1	-1	1	-1	-1
7	1	-1	1	-1	1
8	-1	1	1	-1	1
9	1	1	1	-1	-1
10	-1	-1	-1	1	-1
11	1	-1	-1	1	1
12	-1	1	-1	1	1
13	1	1	-1	1	-1
14	-1	-1	1	1	1
15	1	-1	1	1	-1
16	-1	1	1	1	-1
17	1	1	1	1	1

5 — CHAPTER FIVE - CASE STUDY

5.1 — CASE STUDY INTRODUCTION

In the early stages of the COVID-19 pandemic, there were numerous medical supply shortfalls. Examples include:

- Testing Supplies
- Ventilator parts
- Face Masks
- Face Shields

In all of the examples listed, 3DP was used to address the shortfalls ((Salmi et al., 2020), (Cox & Koepsell, 2020), and (Bishop & Leigh, 2020)). Makers from across the globe have utilized 3D printers to meet the PPE challenges in a survey by Novak and Loy (2020), from February to March 2020 62% of PPE projects were focused on the production of face shields. Of all the PPE project surveyed, over 60% utilized FDM printers. In many cases, maker production represented volunteer efforts to create PPE that was in short supply. The quick production (throughput) of PPE was critical to alleviate short falls but because of the strain on unpaid volunteers utilizing their own resources, it was critical to minimize the need for materials (print stock) and cost on the maker community. A maker community of public Universities in Tennessee was one of many maker groups producing face shields.

5.2 — COVID-19 3DP IN TENNESSEE

In early March 2020, Tennessee Higher Education Commission (THEC) put out a call to various public Universities across the state of Tennessee to identify the possibility of harnessing 3DP to produce PPE for the Tennessee Emergency Management Agency (TEMA). TEMA would collect and distribute any PPE that was produced. Within 24 hours of the initial THEC call, a team at Austin Peay State University produced a prototype face shield using the Prusa Research RC 1 headband (Figure 23).

TEMA quickly approved the prototype face shield as the model for THEC project to produce. THEC proceeded to mobilize Universities across the state of Tennessee to produce face shields. Universities that participated include Technical and Community Colleges, the University of Tennessee, and Austin Peay State University.

In a project that lasted from March to June 2020, almost 20,000 face shields were delivered to TEMA. TEMA then distributed the PPE to communities, responders, and hospitals facing supply shortfalls.

A face shield (Figure 24) is composed of a FDM printed frame, a piece of elastic, and a cut sheet of clear acetate.

The most time consume component of production is the 3D printed frame.

5.3 — TN PROJECT STATISTICS

As noted previously, a face shield is composed of 3 components a 3D printed headband, a piece of elastic, and an acetate shield. In the TN project, almost 20,000 face shields were produced. Each headband and elastic were matched with 10

Figure 23: Initial APSU Face Shield based on the Prusa RC 1 Headband

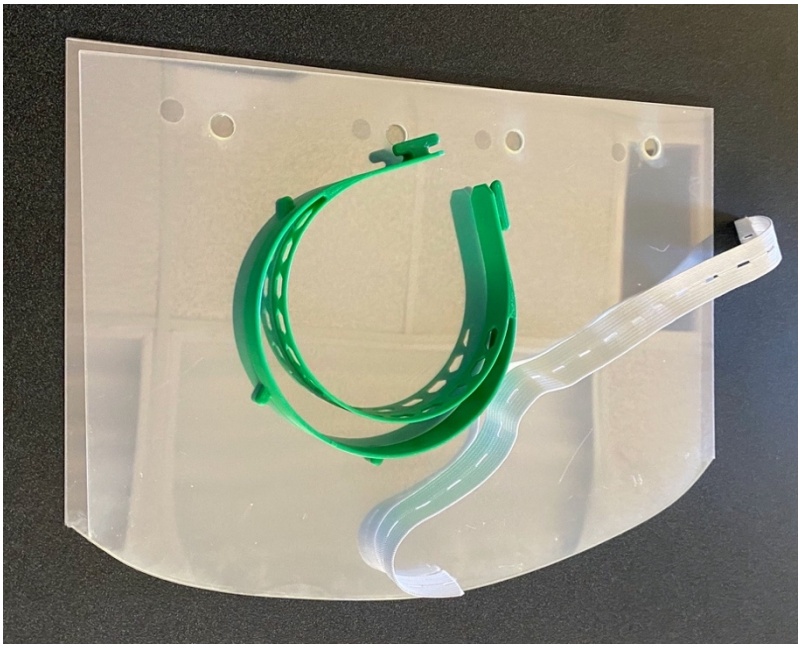

Figure 24: Face Shield Components

replaceable acetate shields. Therefore, a face shield set included 1 headband, 1 piece of elastic, and 10 pieces of acetate. Each set was boxed for deliver and a box contained 36 sets of face shields (Figure 25).

In the case of the team at Austin Peay State University, the printing process for a headband averaged 3.5 hours. It can be extrapolated that the 20,000 headbands made by the consortium of TN Universities represented approximately 70,000 printer hours. The 70,000 hours represented production with little or no optimization. In the pandemic, speed is of the essence. By utilizing optimization, the THEC team could have produced more units in a cheaper manner without sacrificing quality.

5.4 — Case Study Experiment

In Tranter et al. (2017), an optimization technique was described to optimize for energy consumption and quality in injection molding. This methodology describes a straightforward method to optimize the injection molding process and can be adapted to optimizing for throughput, cost, and quality in FDM printing. Based on previous research, the process parameters most likely to have a positive impact on speed, cost, and quality include:

- Layer Thickness (LH)
- Print Speed (PS)
- Infill Density (ID)
- Raster Width (RW) - Infill Line Width in Cura
- Wall Thickness (WT)

Figure 25: TEMA Picking Up a Shipment of Face Shields

Based on the experimental schedule outlined in Table 6 and the lower and upper limits in Table 5, the value of the process parameters for each experimental run are as follows in Table 7

The experiments were conducted on the Creality CR-6 SE and the Artillery Sidewinder X1 over several weeks in December 2020 - April 2021. The original DOE schedule as outlined by Tranter et al. (2017) called for 16 runs (Rows 2-17 in Table 7). An additional run (Row 1 Table 7) was included in this case study to create a baseline headband with all the lower limit parameter values to be a comparator for the inspection process.

During the initial print, it was noted that models did not adhere to the Sidewinder X1 build plate consistently. To correct for this issue, all models on both printers were sliced and printed with a brim (Figure 26). A brim is a single-layer feature added by the slicing software to increase the bed contact area. The brim improves bed adhesion and reduces warping (Johnson & French, 2018).

Utilizing Octoprint and the Print Job History plugin, a sample of the captured results are in Table 8 and Table 9.

As noted previously, all print data was collected via the Octoprint plugin, Print Job History. This plugin collects the time for each print as well as the cost of each print. The data collected by the plunging was exported to a CSV file.

Table 7: Use Case Experimental Schedule

Trial Number	LH	PS	ID	RW	WT
1	.16	50 (60)*	25	0.4	1.2
2	.28	50 (60)*	25	0.4	1.2
3	.16	50 (60)*	25	0.4	.8
4	.16	60 (72)*	25	0.4	1.2
5	.28	60 (72)*	25	0.4	.8
6	.16	50 (60)*	15	0.4	1.2
7	.28	50 (60)*	15	0.4	.8
8	.16	60 (72)*	15	0.4	.8
9	.28	60 (72)*	15	0.4	1.2
10	.16	50 (60)*	25	.8	1.2
11	.28	50 (60)*	25	.8	.8
12	.16	60 (72)*	25	.8	.8
13	.28	60 (72)*	25	.8	1.2
14	.16	50 (60)*	15	.8	.8
15	.28	50 (60)*	15	.8	1.2
16	.16	60 (72)*	15	.8	1.2
17	.28	60 (72)*	15	.8	.8

* 50 (60) and 60 (72) - The print speed lows for CR6 is 50 and Sidewinder X1 is 60 and highs for CR6 is 60 and Sidewinder X1 is 72.

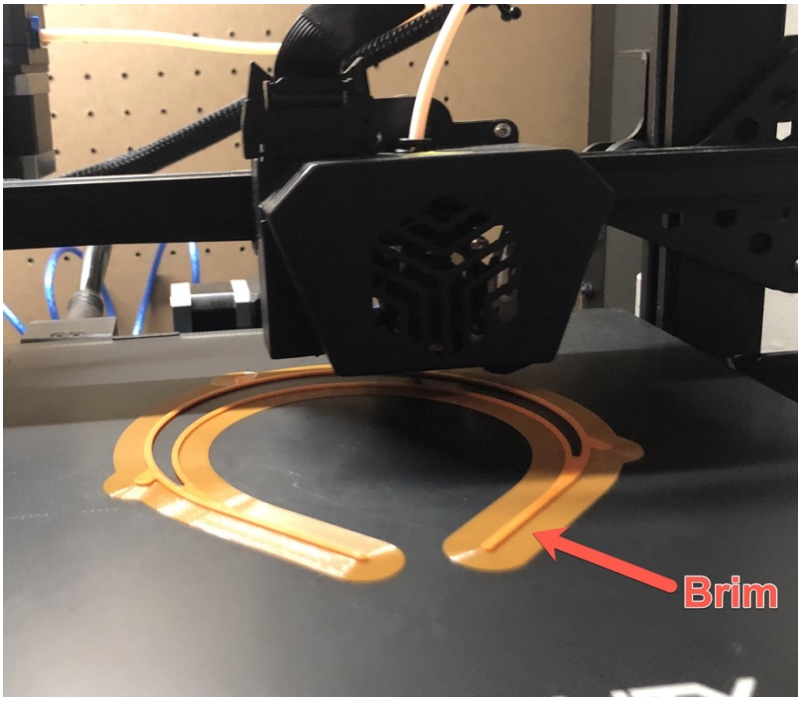

Figure 26: Print with Brim

Table 8: Sample Results from CR-6 SE

Duration	File Name	File Size [bytes]	Used Length [mm]	Used Weight [g]	Used Filament Cost
4h11m25s	CCR6SE_Run10.gcode	12960660	9040	27.19	0.54$
4h11m51s	CCR6SE_Run10.gcode	12960660	9040	27.19	0.54$
4h11m48s	CCR6SE_Run10.gcode	12960660	9040	27.19	0.54$
4h11m55s	CCR6SE_Run10.gcode	12960660	9040	27.19	0.54$
4h12m2s	CCR6SE_Run10.gcode	12960660	9040	27.19	0.54$
2h57m4s	CCR6SE_Run11.gcode	6373067	9330	28.05	0.56$
2h57m4s	CCR6SE_Run11.gcode	6373067	9330	28.05	0.56$
2h57m24s	CCR6SE_Run11.gcode	6373067	9330	28.05	0.56$
2h57m26s	CCR6SE_Run11.gcode	6373067	9330	28.05	0.56$
2h56m19s	CCR6SE_Run11.gcode	6373067	9330	28.05	0.56$
4h40m40s	CCR6SE_Run12.gcode	10926032	9330	28.05	0.56$
4h40m37s	CCR6SE_Run12.gcode	10926032	9330	28.05	0.56$
4h41m4s	CCR6SE_Run12.gcode	10926032	9330	28.05	0.56$
13h28m56s	CCR6SE_Run12.gcode	10926032	9330	28.05	0.56$
4h40m6s	CCR6SE_Run12.gcode	10926032	9330	28.05	0.56$

Table 9: Sample Results from Sidewinder X1

Duration	File Name	File Size [bytes]	Used Length [mm]	Used Weight [g]	Used Filament Cost
4h7m16s	SWX1-Default.gcode	13325390	9950	29.91	0.60$
4h18m5s	SWX1-Default.gcode	13325390	9950	29.91	0.60$
4h6m48s	SWX1-Default.gcode	13325390	9950	29.91	0.60$
4h6m38s	SWX1-Default.gcode	13325390	9950	29.91	0.60$
3h58m2s	SWX1-Default.gcode	13016272	9500	28.56	0.57$
4h2m56s	SWX1-Run10.gcode	13270408	10010	30.09	0.60$
4h3m49s	SWX1-Run10.gcode	13270408	10010	30.09	0.60$
4h2m59s	SWX1-Run10.gcode	13270408	10010	30.09	0.60$

Table 9 Continued

Duration	File Name	File Size [bytes]	Used Length [mm]	Used Weight [g]	Used Filament Cost
4h3m43s	SWX1-Run10.gcode	13270408	10010	30.09	0.60$
2h38m2s	SWX1-Run11.gcode	6385350	10300	30.97	0.62$
2h39m8s	SWX1-Run11.gcode	6385350	10300	30.97	0.62$
2h37m37s	SWX1-Run11.gcode	6385350	10300	30.97	0.62$
2h37m39s	SWX1-Run11.gcode	6385350	10300	30.97	0.62$
2h37m27s	SWX1-Run11.gcode	6385350	10300	30.97	0.62$
3h45m50s	SWX1-Run12.gcode	10657292	10150	30.53	0.61$
3h45m54s	SWX1-Run12.gcode	10657292	10150	30.53	0.61$
3h45m1s	SWX1-Run12.gcode	10657292	10150	30.53	0.61$

Table 9 Continued

Duration	File Name	File Size [bytes]	Used Length [mm]	Used Weight [g]	Used Filament Cost
3h45m50s	SWX1-Run12.gcode	10657292	10150	30.53	0.61$
3h46m22s	SWX1-Run12.gcode	10657292	10150	30.53	0.61$

Upon completion of all the experimental runs, an inspection was conducted based on the process outlined in Chapter 4. The possible range of scores is 0 - 450. Experimental Run 1 (baseline headband) was given a top score of 450 and the sets from each printer was put aside for reference during the inspection process. A sample inspection score card is shown in Figure 27.

Utilizing modeling clay, a mold was created of the index print from each printer (Figure 28). The molds provided a quick and convenient method to measure the dimensional accuracy of the various prints. During the quality assessment, the molds will be used to assess the functionality of a given print. Prints that do not match the index mold will be considered non-functional. Non-functional prints were noted in the quality score card.

CR-6 SE Inspection Score Card

Run	Criteria	weight	Option 1		Option 2		Option 3		Option 4		Option 5		
			rating	weighted score	rating	weighted score	rating	weighted score	rating	weighted score	rating	weighted score	
1	Tactile Roughness Perception	200	100%	200	100%	200	100%	200	100%	200	100%	200	
	Hedonic Tactile Appreciation	150	100%	150	100%	150	100%	150	100%	150	100%	150	
	Visual Impression of Roughness	100	100%	100	100%	100	100%	100	100%	100	100%	100	
	Totals	450		450		450		450		450		450	
2	Tactile Roughness Perception	200	100%	200	100%	200	0%	0	0%	0	0%	0	
	Hedonic Tactile Appreciation	150	100%	150	100%	150	0%	0	0%	0	0%	0	
	Visual Impression of Roughness	100	100%	100	100%	100	0%	0	0%	0	0%	0	
	Totals	450		450		450		0		0		0	
3	Tactile Roughness Perception	200	100%	200	100%	200	100%	200	100%	200	0%	0	
	Hedonic Tactile Appreciation	150	100%	150	100%	150	100%	150	100%	150	0%	0	
	Visual Impression of Roughness	100	100%	100	100%	100	100%	100	100%	100	0%	0	
	Totals	450		450		450		450		450		0	
4	Tactile Roughness Perception	200	100%	0	100%	200	100%	200	100%	200	0%	0	Slight external pimple
	Hedonic Tactile Appreciation	150	100%	0	100%	150	100%	150	100%	150	0%	0	
	Visual Impression of Roughness	100	100%	0	100%	100	75%	75	100%	100	0%	0	
	Totals	450		0		450		425		450		0	

Figure 27: Sample Inspection Score Card

Figure 28: Index Mold

6 — CHAPTER SIX - RESULTS AND DISCUSSION

6.1 — DATA COMPILATION

Upon completion of the experiments, the various results were compiled. The results data included the following:

- The print statistics including time and cost were captured during printing and saved and exported to a CSV file.
- The quality score was captured via an excel spreadsheet.

Several data transformations were required before the data analysis could be accomplished. The time data captured by the Octoprint - Print Job History was stored in hour-minute-second format (Table 8). For example, a replicant for the CR6 SE run 10 had a print time of 4h11m25s. This value had to be converted to a second's format to allow for mathematical analysis. The 4h11m25s translates to 15085 seconds. Once all the time values were converted to seconds format, the data was reviewed for problems.

A time value for a single replica in Run 12 for the CR6 was found to be an anomaly. The captured print time was recorded to be over 13 hours. All other Run 12 replicants were approximately 4.5 hours. The problematic results were reprinted. The Run 12 replicant did not take 13 hours, the recorded data was due to an Octoprint error.

To further simplify analysis, the actual values of the print parameters was added to the DOE schedule for each printer. An example is listed in Table 10.

- Actual Layer Height (alh)

Table 10: Combined Results for the CR-6 SE

trial	lh	ps	id	rw	wt	alh	aps	aid	arw	awt	rep	time
1	-1	-1	-1	-1	1	0.16	50	0.25	0.4	0.8	1	18098
2	1	-1	-1	-1	-1	0.28	50	0.25	0.4	1.2	1	8741
3	-1	1	-1	-1	-1	0.16	60	0.25	0.4	1.2	1	14493
4	1	1	-1	-1	1	0.28	60	0.25	0.4	0.8	1	10191
5	-1	-1	1	-1	-1	0.16	50	0.15	0.4	1.2	1	14914
6	1	-1	1	-1	1	0.28	50	0.15	0.4	0.8	1	10423
7	-1	1	1	-1	1	0.16	60	0.15	0.4	0.8	1	16648
8	1	1	1	-1	-1	0.28	60	0.15	0.4	1.2	1	8534
9	-1	-1	-1	1	-1	0.16	50	0.25	0.8	1.2	1	15085
10	1	-1	-1	1	1	0.28	50	0.25	0.8	0.8	1	10624
11	-1	1	-1	1	1	0.16	60	0.25	0.8	0.8	1	16840
12	1	1	-1	1	-1	0.28	60	0.25	0.8	1.2	1	8645
13	-1	-1	1	1	1	0.16	50	0.15	0.8	0.8	1	17046
14	1	-1	1	1	-1	0.28	50	0.15	0.8	1.2	1	9012
15	-1	1	1	1	-1	0.16	60	0.15	0.8	1.2	1	13488
16	1	1	1	1	1	0.28	60	0.15	0.8	0.8	1	9574
17	-1	-1	-1	-1	1	0.16	50	0.25	0.4	0.8	2	18042
18	1	-1	-1	-1	-1	0.28	50	0.25	0.4	1.2	2	8743

- Actual Print Speed (aps)
- Actual Infill Density (aid)
- Actual Raster Width (arw)
- Actual Wall Thickness (awt)

It was determined during the data review that the energy cost was not captured by the Octoprint plugins. A BN-LINK WIFI Heavy Duty Smart Plug Outlets was connected to each printer, the CR6 and the SWX1. Based on a test print on each printer, the cost of printing per second was calculated to be:

- CR6 - $0.00002972408570537 66 per second
- SWX1 - $0.00000197585775290826 per second

These costs were then added to the collected cost on each respective printer. As can be seen in the calculations, the SWX1 is significantly cheaper to run that the CR6. The corrected data is in Appendix A.

As noted previously, the quality score component of cost and time needed to be factored into the cost and time dependent variables. After a review of the rework time, it was determined that following time values would be utilized based on quality score:

- 450 - Zero (0) rework time
- 450 > and > 399 - Thirty (30) seconds rework time
- 400 > and > 337 - Sixty (60) seconds rework time
- 337 > and > 249 - Ninety (90) second rework time
- 250 > - One Hundred twenty (120) second rework time
- 0 - model unusable

Therefore:

$Time_t = Time_e + Time_r$

where:

- $Time_t$ is Total Time
- $Time_e$ is Time from Experiment
- $Time_r$ is the rework time

The time values listed were added to the time values collected during the experimental process.

To calculate a cost factor, the time values needed to be converted to a cost. To accomplish this, it was estimated that an unskilled laborers cost would be $15 per hour salary and $7.50 per hour benefits for a total of $22.50 per hour. This translates to $0.00625 per second. The cost values to be used based on quality score were as follows:

- 450 - $0.0
- 450 > and > 399 - $.1875
- 400 > and > 337 - $.375
- 337 > and > 249 - $.5625
- 250 > - $.75
- 0 - model unusable

Therefore:

$Cost_t = Cost_e + Cost_r$

where:

- $Cost_t$ is Total Cost
- $Cost_e$ is Cost from Experiment (Filament Cost)
- $Cost_r$ is the rework cost

The data with the quality factors is listed in Appendix A.

Once all transformations were completed, a value was calculated for the response variables of cost, time, and quality for each experimental run. The experimental schedule for each of the printers was combined with the experimental results. The raw results and various stages of transformation are listed in Appendix A.

The CR6 DOE Schedule and SWX1 DOE Schedule results were saved as CSV files to be utilized via Jupyter notebooks.

QUALITY SCORES

As outlined in previous sections, the quality scores were compiled in the score card. The score cards for the CR6 in Appendix A. The scores were used to create the rework tables. Examples are listed in Figure 29 and Figure 30. The complete tables can be found in Appendix A.

6.2 — DATA ANALYSIS

Based upon the research questions and various transformations conducted on the experimental data, the following datasets will be analyzed:

trial	lh	ps	id	rw	wt	alh	aps	aid	arw	awt	rep	cost	time	Quality	rework time	rework cost	rework+cost	rework+time
1	-1	-1	-1	-1	1	0.16	50	0.25	0.4	0.8	1	0.564	18098	450	0	0	0.564	18098
2	1	-1	-1	-1	-1	0.28	50	0.25	0.4	1.2	1	0.536	8741	450	0	0	0.536	8741
3	-1	1	-1	-1	-1	0.16	60	0.25	0.4	1.2	1	0.583	14493	450	0	0	0.583	14493
4	1	1	-1	-1	1	0.28	60	0.25	0.4	0.8	1	0.540	10191	250	90	0.5625	1.103	10281
5	-1	-1	1	-1	-1	0.16	50	0.15	0.4	1.2	1	0.584	14914	450	0	0	0.584	14914
6	1	-1	1	-1	1	0.28	50	0.15	0.4	0.8	1	0.531	10423	450	0	0	0.531	10423
7	-1	1	1	-1	1	0.16	60	0.15	0.4	0.8	1	0.549	16648	450	0	0	0.549	16648
8	1	1	1	-1	-1	0.28	60	0.15	0.4	1.2	1	0.565	8534	450	0	0	0.565	8534
9	-1	-1	-1	1	-1	0.16	50	0.25	0.8	1.2	1	0.585	15085	450	0	0	0.585	15085
10	1	-1	-1	1	1	0.28	50	0.25	0.8	0.8	1	0.592	10624	**450**	0	0	0.592	10624
11	-1	1	-1	1	1	0.16	60	0.25	0.8	0.8	1	0.610	16840	400	30	0.1875	0.798	16870
12	1	1	-1	1	-1	0.28	60	0.25	0.8	1.2	1	0.566	8645	450	0	0	0.566	8645
13	-1	-1	1	1	1	0.16	50	0.15	0.8	0.8	1	0.591	17046	450	0	0	0.591	17046
14	1	-1	1	1	-1	0.28	50	0.15	0.8	1.2	1	0.567	9012	450	0	0	0.567	9012
15	-1	1	1	1	-1	0.16	60	0.15	0.8	1.2	1	0.570	13488	**450**	0	0	0.570	13488
16	1	1	1	1	1	0.28	60	0.15	0.8	0.8	1	0.568	9574	450	0	0	0.568	9574
17	-1	-1	-1	-1	1	0.16	50	0.25	0.4	0.8	2	0.564	18042	450	0	0	0.564	18042
18	1	-1	-1	-1	-1	0.28	50	0.25	0.4	1.2	2	0.536	8743	450	0	0	0.536	8743
19	-1	1	-1	-1	-1	0.16	60	0.25	0.4	1.2	2	0.583	14469	450	0	0	0.583	14469
20	1	1	-1	-1	1	0.28	60	0.25	0.4	0.8	2	0.540	10185	400	30	0.1875	0.728	10215
21	-1	-1	1	-1	-1	0.16	50	0.15	0.4	1.2	2	0.584	14873	400	30	0.1875	0.772	14903
22	1	-1	1	-1	1	0.28	50	0.15	0.4	0.8	2	0.530	10199	450	0	0	0.530	10199
23	-1	1	1	-1	1	0.16	60	0.15	0.4	0.8	2	0.549	16652	450	0	0	0.549	16652
24	1	1	1	-1	-1	0.28	60	0.15	0.4	1.2	2	0.570	10149	450	0	0	0.570	10149
25	-1	-1	-1	1	-1	0.16	50	0.25	0.8	1.2	2	0.585	15111	400	30	0.1875	0.772	15141
26	1	-1	-1	1	1	0.28	50	0.25	0.8	0.8	2	0.592	10624	**450**	0	0	0.592	10624
27	-1	1	-1	1	1	0.16	60	0.25	0.8	0.8	2	0.610	16837	450	0	0	0.610	16837
28	1	1	-1	1	-1	0.28	60	0.25	0.8	1.2	2	0.566	8597	450	0	0	0.566	8597

Figure 29: Highlighted Rows Demonstrate Differences in Raw Cost And Time Vs Those Including Rework Factors for the CR6

trial	lh	ps	id	rw	wt	alh	aps	aid	arw	awt	rep	cost	time	Quality		rework cost	rework+cost	rework+time
1	-1	-1	-1	-1	1	0.16	60	0.25	0.4	0.8	1	0.593	16916	400	30	0.1875	0.781	16946
2	1	-1	-1	-1	-1	0.28	60	0.25	0.4	1.2	1	0.618	9016	112.5	120	0.75	1.368	9136
3	-1	1	-1	-1	-1	0.16	72	0.25	0.4	1.2	1	0.626	12906	450	0	0	0.626	12906
4	1	1	-1	-1	1	0.28	72	0.25	0.4	0.8	1	0.589	9711	112.5	120	0.75	1.339	9831
5	-1	-1	1	-1	-1	0.16	60	0.15	0.4	1.2	1	0.619	14617	450	0	0	0.619	14617
6	1	-1	1	-1	1	0.28	60	0.15	0.4	0.8	1	0.570	10142	**112.5**	120	0.75	1.320	10262
7	-1	1	1	-1	1	0.16	72	0.15	0.4	0.8	1	0.569	14495	112.5	120	0.75	1.319	14615
8	1	1	1	-1	-1	0.28	72	0.15	0.4	1.2	1	0.605	7772	337.5	60	0.375	0.980	7832
9	-1	-1	-1	1	-1	0.16	60	0.25	0.8	1.2	1	0.636	18254	450	0	0	0.636	18254
10	1	-1	-1	1	1	0.28	60	0.25	0.8	0.8	1	0.639	9482	287.5	90	0.5625	1.201	9572
11	-1	1	-1	1	1	0.16	72	0.25	0.8	0.8	1	0.637	13550	**450**	0	0	0.637	13550
12	1	1	-1	1	-1	0.28	72	0.25	0.8	1.2	1	0.619	9646	350	60	0.375	0.994	9706
13	-1	-1	1	1	1	0.16	60	0.15	0.8	0.8	1	0.619	14675	225	120	0.75	1.369	14795
14	1	-1	1	1	-1	0.28	60	0.15	0.8	1.2	1	0.607	8822	450	0	0	0.607	8822
15	-1	1	1	1	-1	0.16	72	0.15	0.8	1.2	1	0.615	12575	400	30	0.1875	0.802	12605
16	1	1	1	1	1	0.28	72	0.15	0.8	0.8	1	0.616	8046	**112.5**	120	0.75	1.366	8166

Figure 30: Highlighted rows demonstrate differences in raw cost and time vs those including rework factors for the SWX1

- Analysis A - Optimization of cost (w/o power) and time and review the results for quality
- Analysis B - Optimization of cost+power and time and review the results for quality
- Analysis C - Optimization of cost+power and time factoring in rework

The various analysis listed will be compared. For all analysis an $\alpha = .05$ was utilized.

The analysis was conducted using the methodologies outlined in Chapter 4 -4.6 — Experimental Process. All data and analysis were conducted in python via Jupyter notebooks. T The steps required to repeat the analysis can be found in Appendix B - Repeatability.

Considering Quality

During this study, it was found that only one (1) headband was unusable. This unusable model was due to the model being moved on the print bed (Figure 31). All models were rated between 100% (excellent quality) and 25% (poor quality). It was found that with slight rework, all headbands could be made usable. The decision was made to factor the effects quality into the dependent variables cost and time rather than treat quality as a separate dependent variable. By factoring quality into cost and time, a more accurate model could be produced.

When compiling the quality scores, it was found that the CR6 demonstrated better quality overall (Table 11). The SWX1 prints were of poorer quality (Table 12). It can be surmised that these differences are due to the overall quality of the printers, The CR6 being of higher quality overall.

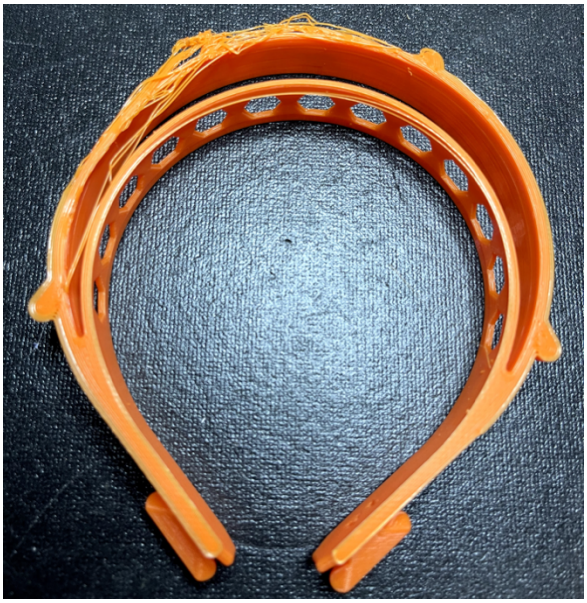

Figure 31: Image of the Unusable Headband

Table 11: Average Quality Scores for the CR6

1	2	3	4	5	TOTALS
weighted score	weighted score	weighted score	weighted score	weighted score	Overall Score
434.375	440.625	445.3125	443.75	446.875	442.1875

Table 12: Average Quality Scores for the SWX1

1	2	3	4	5	TOTALS
weighted score	weighted score	weighted score	weighted score	weighted score	Overall Score
300.78125	294.53125	292.1875	295.3125	295.3125	295.625

In the use of the band molds, it was found not to be valuable. The molds were not a good indication of functionality. The measurements were more valuable.

6.2.1 — Experimental Analysis A

Optimization of cost (w/o power) and time and review the results for quality

In this set of analysis, I will review the ideal print parameters for cost and time without directly factoring in quality. Once the ideal parameters are identified, test prints will be created, and quality will be assessed.

The raw collected results are listed in Appendix A.

6.2.1.1 — Experimental Analysis A - CR6

The initial results (Figure 32) for the CR6 Cost Ordinary Least Squares regression model (OLS) show that several of the primary effects of the experiments are not statistically significant. The variables that are not significant factors in the cost of the model include:

- Layer height (alh) with p-value 0.927017
- Infill density (aid) with p-value 0.0905131

The reduced OLS for the CR6 cost is shown in Figure 33. As can be noted in Figure 33, all the remaining first-order parameters and second-order interactions have a significant impact of the cost of the model.

There parameters include print speed, raster width, and wall thickness. The interactions include all of the interactions of the primary parameters.

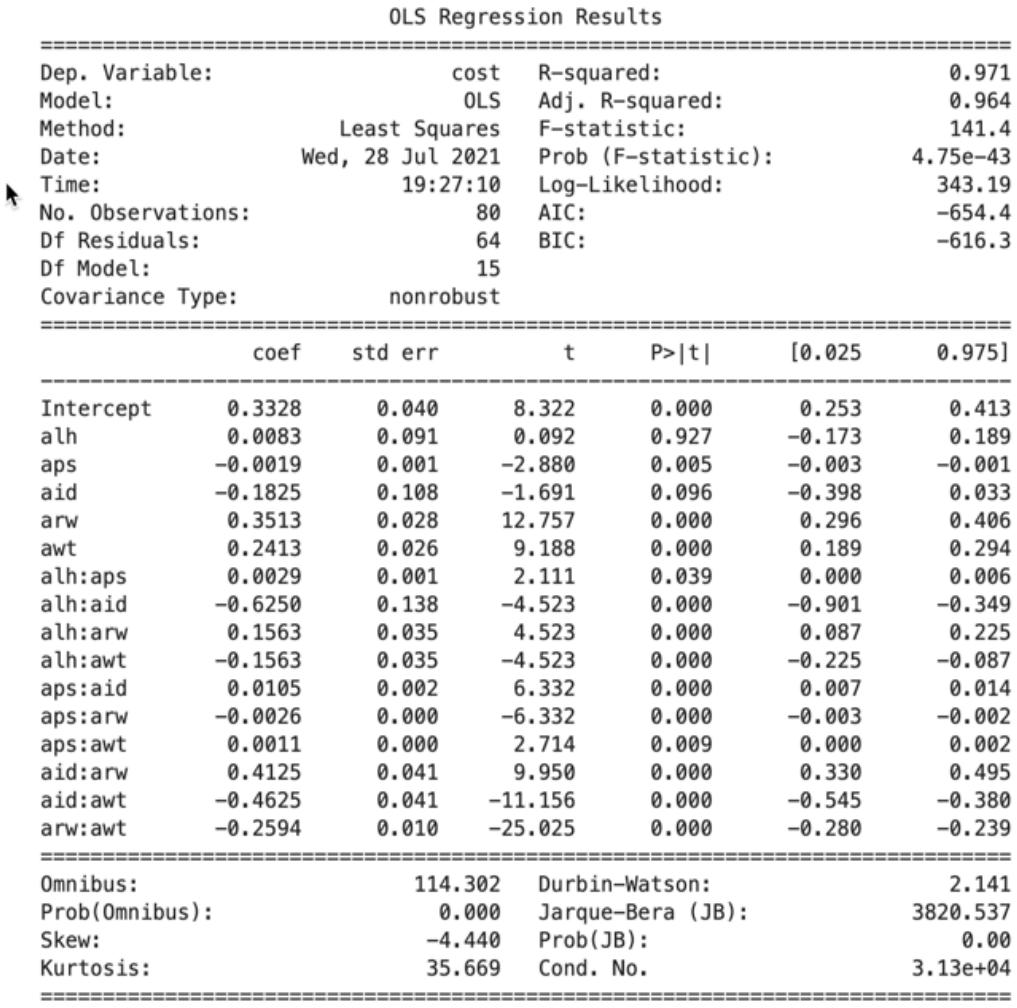

OLS Regression Results

Dep. Variable:	cost	R-squared:	0.971
Model:	OLS	Adj. R-squared:	0.964
Method:	Least Squares	F-statistic:	141.4
Date:	Wed, 28 Jul 2021	Prob (F-statistic):	4.75e-43
Time:	19:27:10	Log-Likelihood:	343.19
No. Observations:	80	AIC:	-654.4
Df Residuals:	64	BIC:	-616.3
Df Model:	15		
Covariance Type:	nonrobust		

	coef	std err	t	P>|t|	[0.025	0.975]
Intercept	0.3328	0.040	8.322	0.000	0.253	0.413
alh	0.0083	0.091	0.092	0.927	-0.173	0.189
aps	-0.0019	0.001	-2.880	0.005	-0.003	-0.001
aid	-0.1825	0.108	-1.691	0.096	-0.398	0.033
arw	0.3513	0.028	12.757	0.000	0.296	0.406
awt	0.2413	0.026	9.188	0.000	0.189	0.294
alh:aps	0.0029	0.001	2.111	0.039	0.000	0.006
alh:aid	-0.6250	0.138	-4.523	0.000	-0.901	-0.349
alh:arw	0.1563	0.035	4.523	0.000	0.087	0.225
alh:awt	-0.1563	0.035	-4.523	0.000	-0.225	-0.087
aps:aid	0.0105	0.002	6.332	0.000	0.007	0.014
aps:arw	-0.0026	0.000	-6.332	0.000	-0.003	-0.002
aps:awt	0.0011	0.000	2.714	0.009	0.000	0.002
aid:arw	0.4125	0.041	9.950	0.000	0.330	0.495
aid:awt	-0.4625	0.041	-11.156	0.000	-0.545	-0.380
arw:awt	-0.2594	0.010	-25.025	0.000	-0.280	-0.239

Omnibus:	114.302	Durbin-Watson:	2.141
Prob(Omnibus):	0.000	Jarque-Bera (JB):	3820.537
Skew:	-4.440	Prob(JB):	0.00
Kurtosis:	35.669	Cond. No.	3.13e+04

Figure 32: Analysis A - CR6 Cost OLS

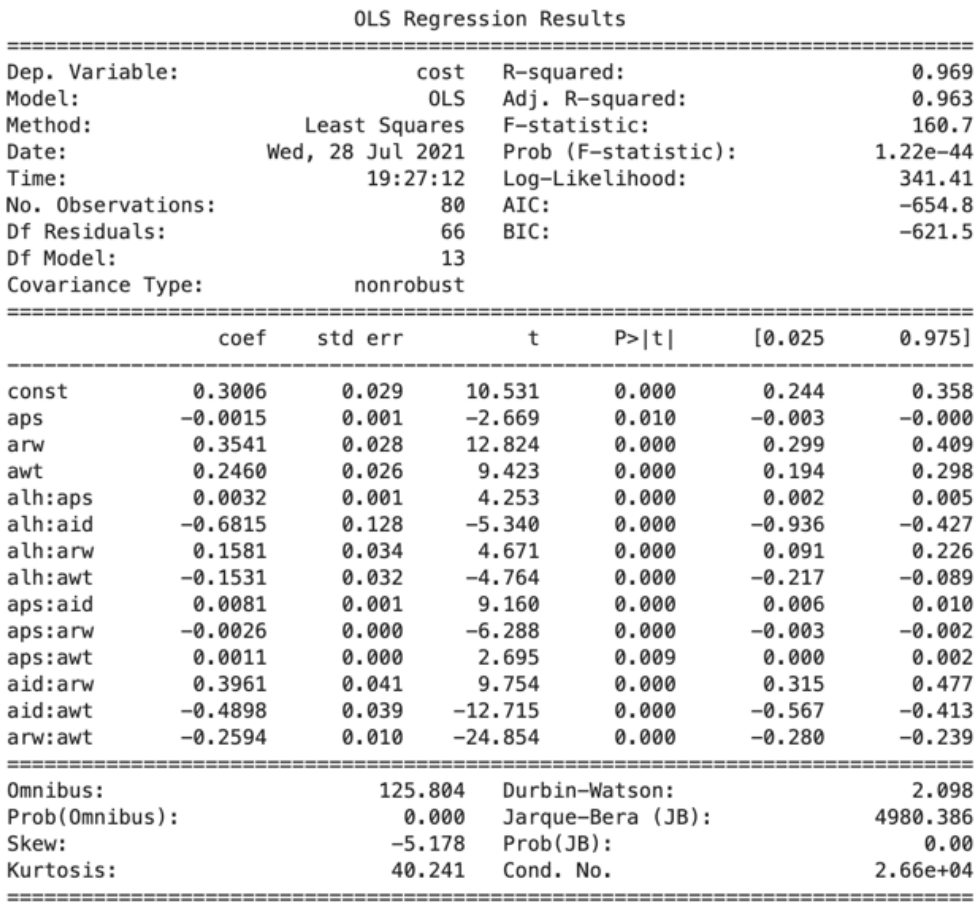

OLS Regression Results

Dep. Variable:	cost	R-squared:	0.969
Model:	OLS	Adj. R-squared:	0.963
Method:	Least Squares	F-statistic:	160.7
Date:	Wed, 28 Jul 2021	Prob (F-statistic):	1.22e-44
Time:	19:27:12	Log-Likelihood:	341.41
No. Observations:	80	AIC:	-654.8
Df Residuals:	66	BIC:	-621.5
Df Model:	13		
Covariance Type:	nonrobust		

	coef	std err	t	P>|t|	[0.025	0.975]
const	0.3006	0.029	10.531	0.000	0.244	0.358
aps	-0.0015	0.001	-2.669	0.010	-0.003	-0.000
arw	0.3541	0.028	12.824	0.000	0.299	0.409
awt	0.2460	0.026	9.423	0.000	0.194	0.298
alh:aps	0.0032	0.001	4.253	0.000	0.002	0.005
alh:aid	-0.6815	0.128	-5.340	0.000	-0.936	-0.427
alh:arw	0.1581	0.034	4.671	0.000	0.091	0.226
alh:awt	-0.1531	0.032	-4.764	0.000	-0.217	-0.089
aps:aid	0.0081	0.001	9.160	0.000	0.006	0.010
aps:arw	-0.0026	0.000	-6.288	0.000	-0.003	-0.002
aps:awt	0.0011	0.000	2.695	0.009	0.000	0.002
aid:arw	0.3961	0.041	9.754	0.000	0.315	0.477
aid:awt	-0.4898	0.039	-12.715	0.000	-0.567	-0.413
arw:awt	-0.2594	0.010	-24.854	0.000	-0.280	-0.239

Omnibus:	125.804	Durbin-Watson:	2.098
Prob(Omnibus):	0.000	Jarque-Bera (JB):	4980.386
Skew:	-5.178	Prob(JB):	0.00
Kurtosis:	40.241	Cond. No.	2.66e+04

Figure 33: Analysis A - CR6 Reduced OLS for Cost

Based on these results (Figure 33), the following linear equation for CR6 cost was developed:

$$Cost$$

$$= 0.30061301677651686 + -0.0014979526099359666 * X2 + 0.3541048685686145$$

$$* X4 + 0.24600811428103486 * X5 + 0.003193676289093103 * X1 * X2$$

$$+ -0.681545835829839 * X1 * X3 + 0.15813870197108404 * X1 * X4$$

$$+ -0.15310216338152616 * X1 * X5 + 0.008101719131677326 * X2 * X3$$

$$+ -0.0026250000000000544 * X2 * X4 + 0.0011250000000000322 * X2 * X5$$

$$+ 0.3961480849887108 * X3 * X4 + -0.4897531916854896 * X3 * X5$$

$$+ -0.2593750000000006 * X4 * X5$$

This function was utilized in the ϵ-constraints calculations.

The analysis for CR6 Time OLS, were obtained (Figure 34).

The variables that are not significant factors in the cost of the model include:

Interaction of actual print speed (aps) and actual wall thickness (awt) with p-value 0.712687

- Actual infill density (aid) with p-value 0.63764
- Actual raster width (arw) with p-value 0.549529
- Interaction of aid and arw with p-value 0.12172
- Interaction of alh and aps with p-value 0.0744513
- Interaction of arw and awt with p-value 0.0725949

The reduce model for CR6 Time is in Figure 35.

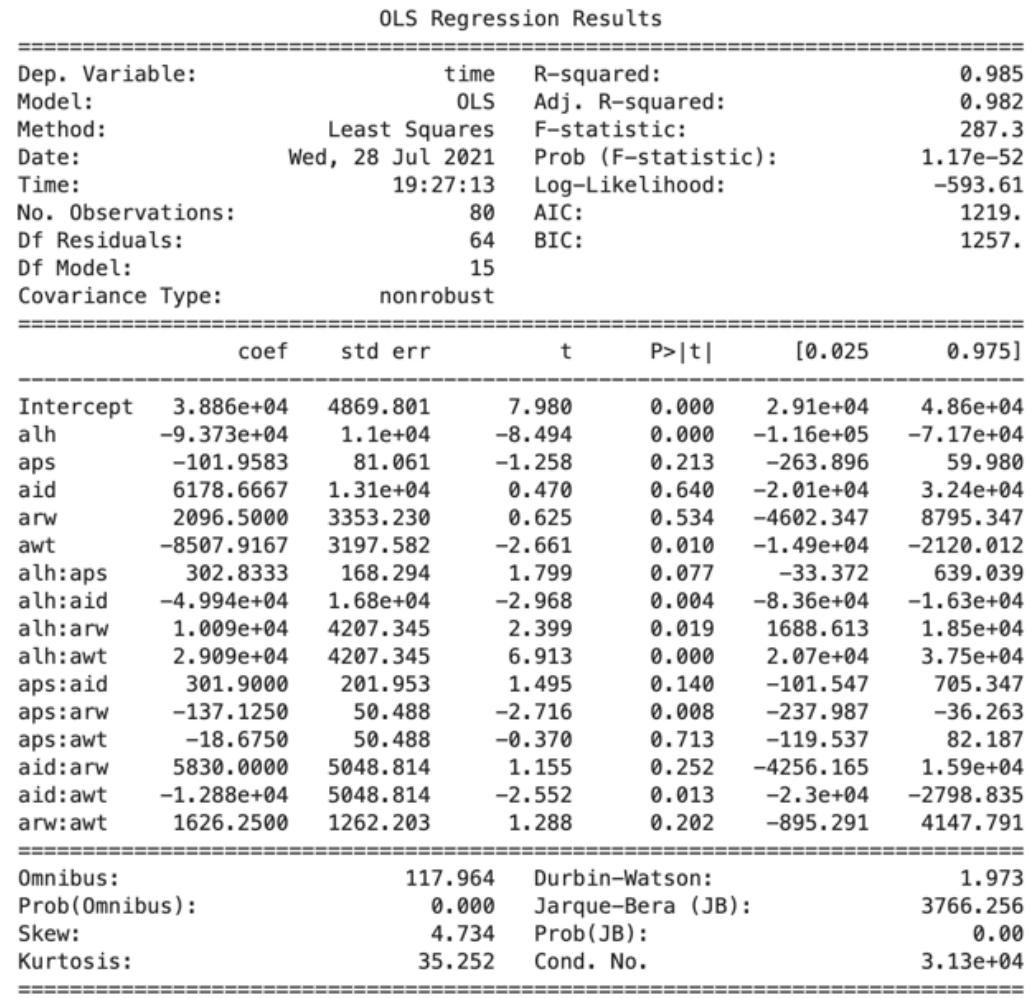

OLS Regression Results

Dep. Variable:	time	R-squared:	0.985
Model:	OLS	Adj. R-squared:	0.982
Method:	Least Squares	F-statistic:	287.3
Date:	Wed, 28 Jul 2021	Prob (F-statistic):	1.17e-52
Time:	19:27:13	Log-Likelihood:	-593.61
No. Observations:	80	AIC:	1219.
Df Residuals:	64	BIC:	1257.
Df Model:	15		
Covariance Type:	nonrobust		

	coef	std err	t	P>|t|	[0.025	0.975]
Intercept	3.886e+04	4869.801	7.980	0.000	2.91e+04	4.86e+04
alh	-9.373e+04	1.1e+04	-8.494	0.000	-1.16e+05	-7.17e+04
aps	-101.9583	81.061	-1.258	0.213	-263.896	59.980
aid	6178.6667	1.31e+04	0.470	0.640	-2.01e+04	3.24e+04
arw	2096.5000	3353.230	0.625	0.534	-4602.347	8795.347
awt	-8507.9167	3197.582	-2.661	0.010	-1.49e+04	-2120.012
alh:aps	302.8333	168.294	1.799	0.077	-33.372	639.039
alh:aid	-4.994e+04	1.68e+04	-2.968	0.004	-8.36e+04	-1.63e+04
alh:arw	1.009e+04	4207.345	2.399	0.019	1688.613	1.85e+04
alh:awt	2.909e+04	4207.345	6.913	0.000	2.07e+04	3.75e+04
aps:aid	301.9000	201.953	1.495	0.140	-101.547	705.347
aps:arw	-137.1250	50.488	-2.716	0.008	-237.987	-36.263
aps:awt	-18.6750	50.488	-0.370	0.713	-119.537	82.187
aid:arw	5830.0000	5048.814	1.155	0.252	-4256.165	1.59e+04
aid:awt	-1.288e+04	5048.814	-2.552	0.013	-2.3e+04	-2798.835
arw:awt	1626.2500	1262.203	1.288	0.202	-895.291	4147.791

Omnibus:	117.964	Durbin-Watson:	1.973
Prob(Omnibus):	0.000	Jarque-Bera (JB):	3766.256
Skew:	4.734	Prob(JB):	0.00
Kurtosis:	35.252	Cond. No.	3.13e+04

Figure 34: Analysis A - CR6 Time OLS

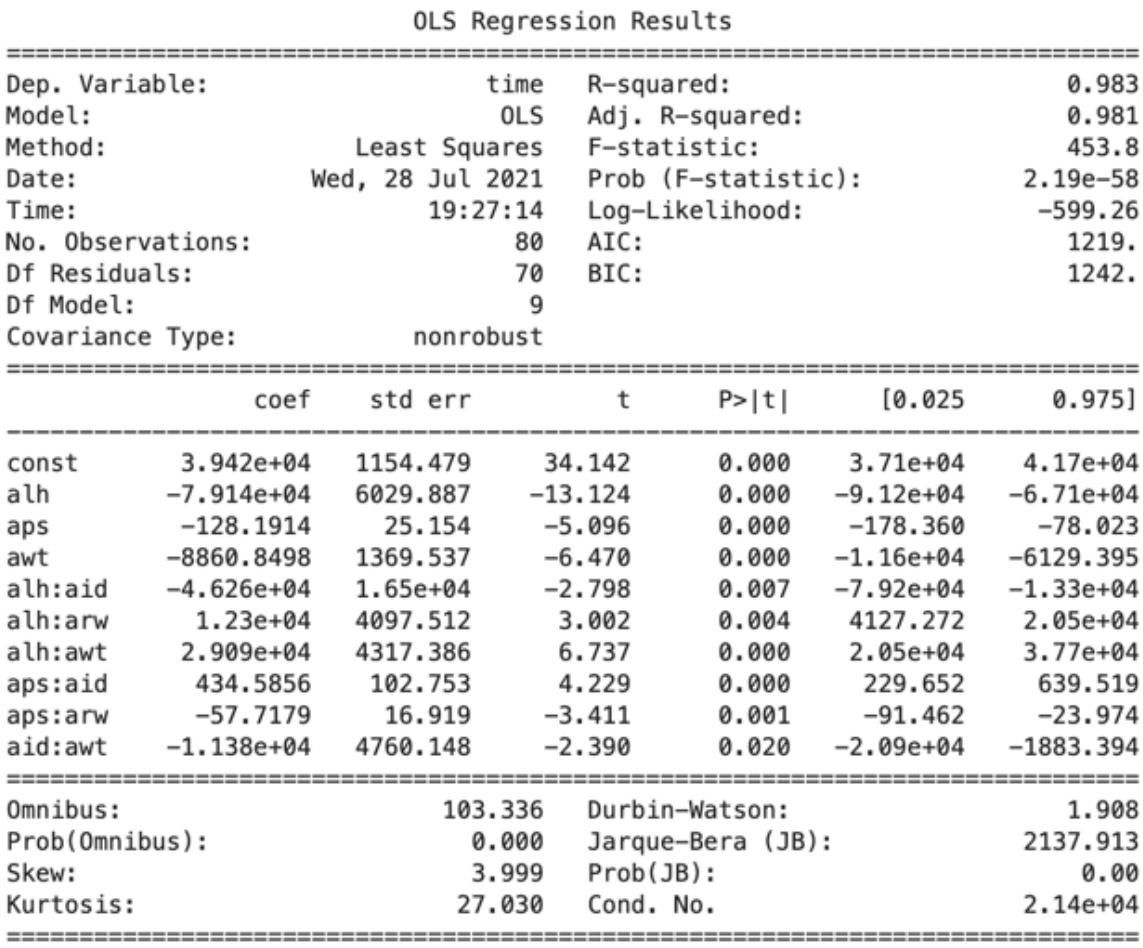

OLS Regression Results

Dep. Variable:	time	R-squared:	0.983
Model:	OLS	Adj. R-squared:	0.981
Method:	Least Squares	F-statistic:	453.8
Date:	Wed, 28 Jul 2021	Prob (F-statistic):	2.19e-58
Time:	19:27:14	Log-Likelihood:	-599.26
No. Observations:	80	AIC:	1219.
Df Residuals:	70	BIC:	1242.
Df Model:	9		
Covariance Type:	nonrobust		

	coef	std err	t	P>|t|	[0.025	0.975]
const	3.942e+04	1154.479	34.142	0.000	3.71e+04	4.17e+04
alh	-7.914e+04	6029.887	-13.124	0.000	-9.12e+04	-6.71e+04
aps	-128.1914	25.154	-5.096	0.000	-178.360	-78.023
awt	-8860.8498	1369.537	-6.470	0.000	-1.16e+04	-6129.395
alh:aid	-4.626e+04	1.65e+04	-2.798	0.007	-7.92e+04	-1.33e+04
alh:arw	1.23e+04	4097.512	3.002	0.004	4127.272	2.05e+04
alh:awt	2.909e+04	4317.386	6.737	0.000	2.05e+04	3.77e+04
aps:aid	434.5856	102.753	4.229	0.000	229.652	639.519
aps:arw	-57.7179	16.919	-3.411	0.001	-91.462	-23.974
aid:awt	-1.138e+04	4760.148	-2.390	0.020	-2.09e+04	-1883.394

Omnibus:	103.336	Durbin-Watson:	1.908
Prob(Omnibus):	0.000	Jarque-Bera (JB):	2137.913
Skew:	3.999	Prob(JB):	0.00
Kurtosis:	27.030	Cond. No.	2.14e+04

Figure 35: Analysis A - CR6 Reduced OLS for Time

The variables and interactions that have a significant impact on time include:

- alh
- aps
- awt
- alh:aid
- alh:arw
- alh:awt
- aps:aid
- aps:arw
- aid:awt

Based on these results (Figure 35), the following linear equation for CR6 time was developed:

$$Time = 39415.87499999855 + -79138.51046393832 * X1 + -128.19137670175314 * X2 + -8860.849838411767 * X5 + -46255.95567867106 * X1 * X3 + 12299.502666120085 * X1 * X4 + 29085.416666666522 * X1 * X5 + 434.58559556786804 * X2 * X3 + -57.717904019688284 * X2 * X4 + -11377.20914127423 * X3 * X5$$

The values utilized for the ϵ-constraint methodology for Analysis A were:

Minimize:

- $f1 = 0.30061301677651686 + -0.0014979526099359666 * X2 + 0.3541048685686145 * X4 + 0.24600811428103486 * X5 +$

$$0.003193676289093103 * X1 * X2 + -0.681545835829839 * X1 * X3 + 0.15813870197108404 * X1 * X4 + -0.15310216338152616 * X1 * X5 + 0.008101719131677326 * X2 * X3 + -0.0026250000000000544 * X2 * X4 + 0.0011250000000000322 * X2 * X5 + 0.3961480849887108 * X3 * X4 + -0.4897531916854896 * X3 * X5 + -0.2593750000000006 * X4 * X5$$

- $f2 = 39415.87499999855 + -79138.51046393832 * X1 + -128.19137670175314 * X2 + -8860.849838411767 * X5 + -46255.95567867106 * X1 * X3 + 12299.502666120085 * X1 * X4 + 29085.416666666522 * X1 * X5 + 434.58559556786804 * X2 * X3 + -57.717904019688284 * X2 * X4 + -11377.20914127423 * X3 * X5$

st:

- $.16 \leq X1 \leq .28$
- $50 \leq X2 \leq 60$
- $.15 \leq X3 \leq .25$
- $.4 \leq X4 \leq .8$
- $.8 \leq X5 \leq 1.2$

When solved, ϵ-contraints methodology produces the following values:

- $(X1, X2, X3, X4, X5) = \begin{pmatrix} 0.28000000999993935, 60.000000599972694, 0.2500000099939384, \\ 0.8000000096771722, 1.2000000119993277 \end{pmatrix}$
- $f1 = 0.53898523398684$
- $f2 = 8557.622612553769$

Where:

- • X1 = layer height = .28 mm
- • X2 = print speed = 60 mm/s
- • X3 = infill density = .25
- • X4 = raster width = .8 mm
- • X5 = wall thickness = 1.2 mm
- • f1 = cost = 0.53898523398684
- • f2 = time = 8557.622612553769 s

In a review of the proposed setting, all the values fit what would be expected for reduced cost and speed. The exception would be infill density at .25. In part, this exception is due to the trade-off necessitated by the optimization of cost and time. Additionally, the model for the headband is composed of very little infill.

As a last step the proposed setting were printed three (3) times. In a review of the of the quality of the print, it was found to be excellent with a score of 450.

6.2.1.2 — Experimental Analysis A - SWX1

The initial results (Figure 36) for the SWX1 Cost OLS model shows that several of the primary effects of the experiments are not statistically significant.

The variables that are not significant factors in the cost of the model include:

- aps:aid with p-value 0.93549
- alh:aid with p-value 0.99566
- aps:arw with p-value 0.970373

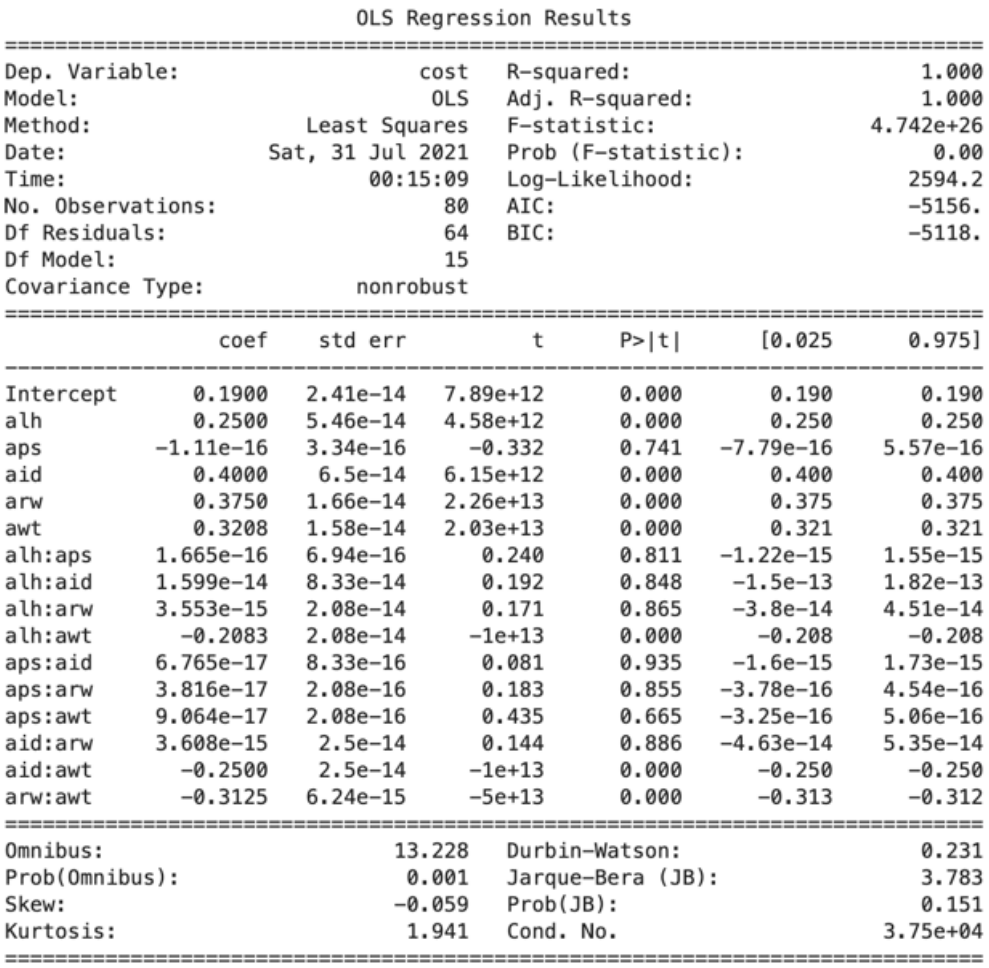

OLS Regression Results

Dep. Variable:	cost	R-squared:	1.000
Model:	OLS	Adj. R-squared:	1.000
Method:	Least Squares	F-statistic:	4.742e+26
Date:	Sat, 31 Jul 2021	Prob (F-statistic):	0.00
Time:	00:15:09	Log-Likelihood:	2594.2
No. Observations:	80	AIC:	-5156.
Df Residuals:	64	BIC:	-5118.
Df Model:	15		
Covariance Type:	nonrobust		

	coef	std err	t	P>|t|	[0.025	0.975]
Intercept	0.1900	2.41e-14	7.89e+12	0.000	0.190	0.190
alh	0.2500	5.46e-14	4.58e+12	0.000	0.250	0.250
aps	-1.11e-16	3.34e-16	-0.332	0.741	-7.79e-16	5.57e-16
aid	0.4000	6.5e-14	6.15e+12	0.000	0.400	0.400
arw	0.3750	1.66e-14	2.26e+13	0.000	0.375	0.375
awt	0.3208	1.58e-14	2.03e+13	0.000	0.321	0.321
alh:aps	1.665e-16	6.94e-16	0.240	0.811	-1.22e-15	1.55e-15
alh:aid	1.599e-14	8.33e-14	0.192	0.848	-1.5e-13	1.82e-13
alh:arw	3.553e-15	2.08e-14	0.171	0.865	-3.8e-14	4.51e-14
alh:awt	-0.2083	2.08e-14	-1e+13	0.000	-0.208	-0.208
aps:aid	6.765e-17	8.33e-16	0.081	0.935	-1.6e-15	1.73e-15
aps:arw	3.816e-17	2.08e-16	0.183	0.855	-3.78e-16	4.54e-16
aps:awt	9.064e-17	2.08e-16	0.435	0.665	-3.25e-16	5.06e-16
aid:arw	3.608e-15	2.5e-14	0.144	0.886	-4.63e-14	5.35e-14
aid:awt	-0.2500	2.5e-14	-1e+13	0.000	-0.250	-0.250
arw:awt	-0.3125	6.24e-15	-5e+13	0.000	-0.313	-0.312

Omnibus:	13.228	Durbin-Watson:	0.231
Prob(Omnibus):	0.001	Jarque-Bera (JB):	3.783
Skew:	-0.059	Prob(JB):	0.151
Kurtosis:	1.941	Cond. No.	3.75e+04

Figure 36: Analysis A - SWX1 Cost OLS

- aps:awt with p-value 0.994181
- alh:arw with p-value 0.949303
- alh:aps with p-value 0.930312
- aid:arw with p-value 0.679975
- aps with p-value 0.787536

The reduced OLS for the SWX1 cost is shown in Figure 37. As can be noted in Figure 37, all the remaining first-order parameters and second-order interactions have a significant impact of the cost of the model.

Based on these results (Figure 37), the following linear equation for SWX1 cost was developed:

$$Cost = 0.1900000000000014 + 0.24999999999999423 * X1 + 0.3999999999999986 * X3 + 0.37499999999999967 * X4 + 0.320833333333332 * X5 + -0.20833333333332477 * X1 * X5 + -0.25000000000000133 * X3 * X5 + -0.3124999999999999 * X4 * X5$$

This function was utilized in the ϵ-constraints calculations.

The analysis for SWX1 Time OLS were obtained (Figure 38).

The variables that are not significant factors in the cost of the model include:

- aps:arw with p-value 0.899404
- alh:awt with p-value 0.760839
- aid:awt with p-value 0.641928
- aid:arw with p-value 0.54847

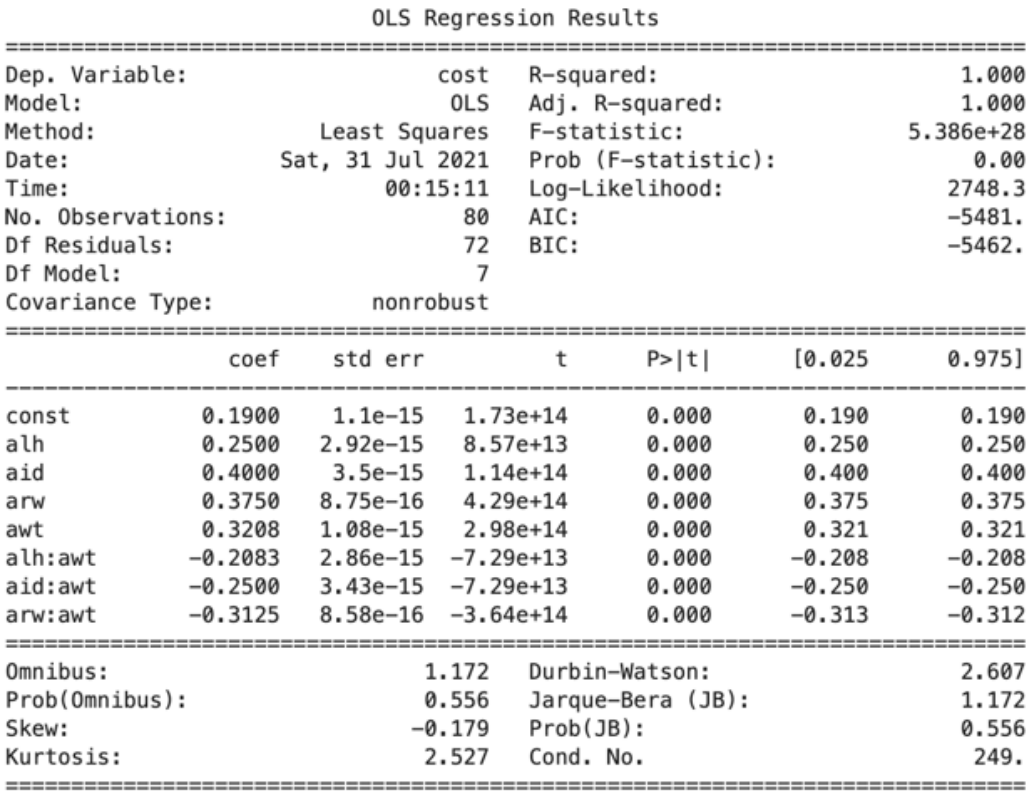

OLS Regression Results

Dep. Variable:	cost	R-squared:	1.000
Model:	OLS	Adj. R-squared:	1.000
Method:	Least Squares	F-statistic:	5.386e+28
Date:	Sat, 31 Jul 2021	Prob (F-statistic):	0.00
Time:	00:15:11	Log-Likelihood:	2748.3
No. Observations:	80	AIC:	-5481.
Df Residuals:	72	BIC:	-5462.
Df Model:	7		
Covariance Type:	nonrobust		

	coef	std err	t	P>|t|	[0.025	0.975]
const	0.1900	1.1e-15	1.73e+14	0.000	0.190	0.190
alh	0.2500	2.92e-15	8.57e+13	0.000	0.250	0.250
aid	0.4000	3.5e-15	1.14e+14	0.000	0.400	0.400
arw	0.3750	8.75e-16	4.29e+14	0.000	0.375	0.375
awt	0.3208	1.08e-15	2.98e+14	0.000	0.321	0.321
alh:awt	-0.2083	2.86e-15	-7.29e+13	0.000	-0.208	-0.208
aid:awt	-0.2500	3.43e-15	-7.29e+13	0.000	-0.250	-0.250
arw:awt	-0.3125	8.58e-16	-3.64e+14	0.000	-0.313	-0.312

Omnibus:	1.172	Durbin-Watson:	2.607
Prob(Omnibus):	0.556	Jarque-Bera (JB):	1.172
Skew:	-0.179	Prob(JB):	0.556
Kurtosis:	2.527	Cond. No.	249.

Figure 37: Analysis A - SWX1 Reduced OLS for Cost

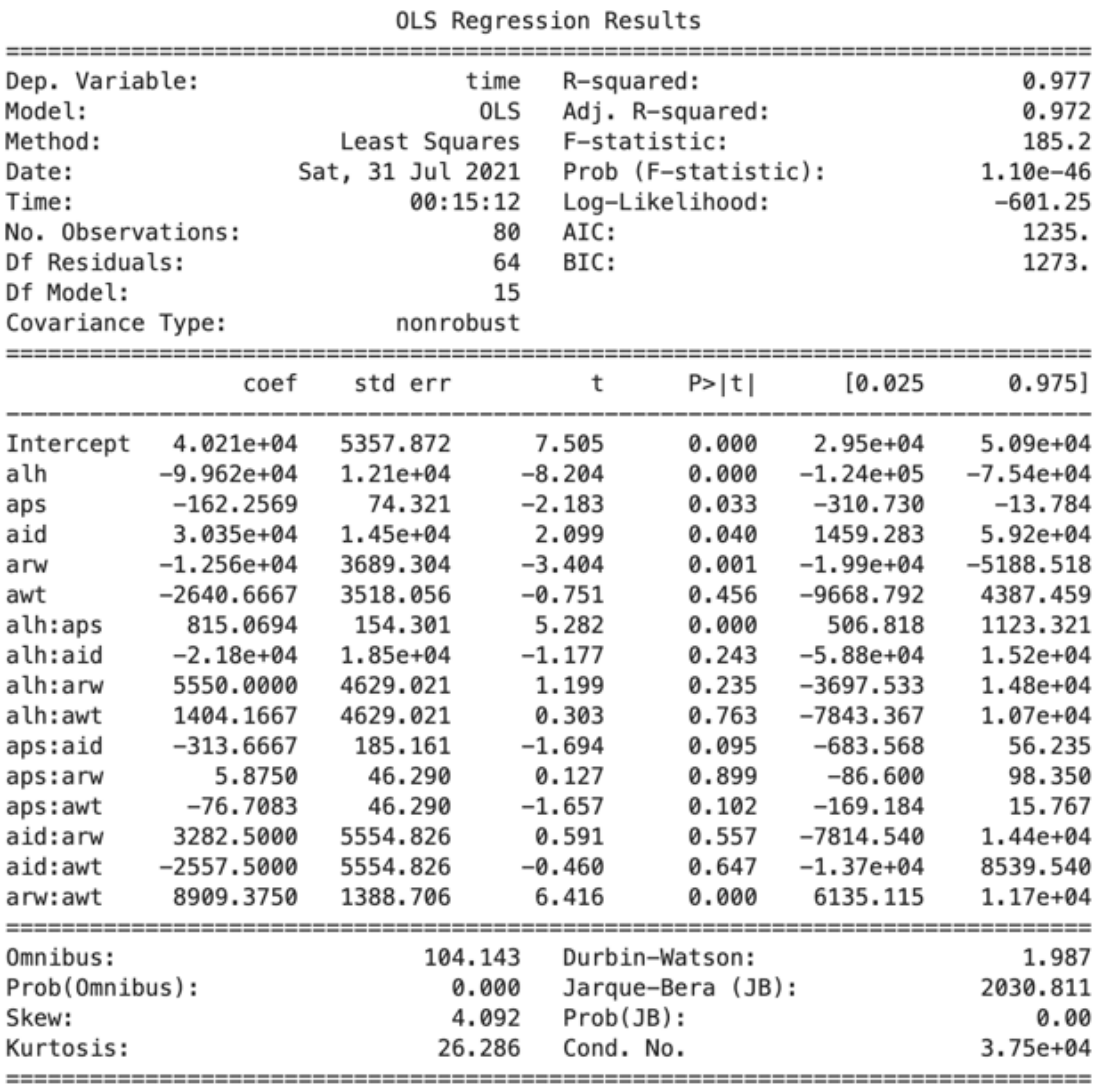

OLS Regression Results

Dep. Variable:	time	R-squared:	0.977
Model:	OLS	Adj. R-squared:	0.972
Method:	Least Squares	F-statistic:	185.2
Date:	Sat, 31 Jul 2021	Prob (F-statistic):	1.10e-46
Time:	00:15:12	Log-Likelihood:	-601.25
No. Observations:	80	AIC:	1235.
Df Residuals:	64	BIC:	1273.
Df Model:	15		
Covariance Type:	nonrobust		

	coef	std err	t	P>|t|	[0.025	0.975]
Intercept	4.021e+04	5357.872	7.505	0.000	2.95e+04	5.09e+04
alh	-9.962e+04	1.21e+04	-8.204	0.000	-1.24e+05	-7.54e+04
aps	-162.2569	74.321	-2.183	0.033	-310.730	-13.784
aid	3.035e+04	1.45e+04	2.099	0.040	1459.283	5.92e+04
arw	-1.256e+04	3689.304	-3.404	0.001	-1.99e+04	-5188.518
awt	-2640.6667	3518.056	-0.751	0.456	-9668.792	4387.459
alh:aps	815.0694	154.301	5.282	0.000	506.818	1123.321
alh:aid	-2.18e+04	1.85e+04	-1.177	0.243	-5.88e+04	1.52e+04
alh:arw	5550.0000	4629.021	1.199	0.235	-3697.533	1.48e+04
alh:awt	1404.1667	4629.021	0.303	0.763	-7843.367	1.07e+04
aps:aid	-313.6667	185.161	-1.694	0.095	-683.568	56.235
aps:arw	5.8750	46.290	0.127	0.899	-86.600	98.350
aps:awt	-76.7083	46.290	-1.657	0.102	-169.184	15.767
aid:arw	3282.5000	5554.826	0.591	0.557	-7814.540	1.44e+04
aid:awt	-2557.5000	5554.826	-0.460	0.647	-1.37e+04	8539.540
arw:awt	8909.3750	1388.706	6.416	0.000	6135.115	1.17e+04

Omnibus:	104.143	Durbin-Watson:	1.987
Prob(Omnibus):	0.000	Jarque-Bera (JB):	2030.811
Skew:	4.092	Prob(JB):	0.00
Kurtosis:	26.286	Cond. No.	3.75e+04

Figure 38: Analysis A - SWX1 Time OLS

- awt with p-value 0.362301
- alh:aid with p-value 0.23091
- alh:arw with p-value 0.223997
- aps:aid with p-value 0.0884672

The reduce model for SWX1 Time is in Figure 39.

Based on these results (Figure 39), the following linear equation for SWX1 time was developed:

$$Time = 41311.84166666333 + -99242.9166666657 * X1 + -181.67424724344346 * X2 + 4263.500000000091 * X3 + -9967.93702290074 * X4 + 815.0694444444525 * X1 * X2 + -116.4993638676806 * X2 * X5 + 8583.812022900747 * X4 * X5$$

The values utilized for the ϵ-constraint methodology for Analysis A were:

Minimize:

- $f1 = 0.1900000000000014 + 0.24999999999999423 * X1 + 0.3999999999999986 * X3 + 0.37499999999999967 * X4 + 0.320833333333332 * X5 + -0.20833333333332477 * X1 * X5 + -0.25000000000000133 * X3 * X5 + -0.3124999999999999 * X4 * X5$
- $f2 = 41311.84166666333 + -99242.9166666657 * X1 + -181.67424724344346 * X2 + 4263.500000000091 * X3 +$

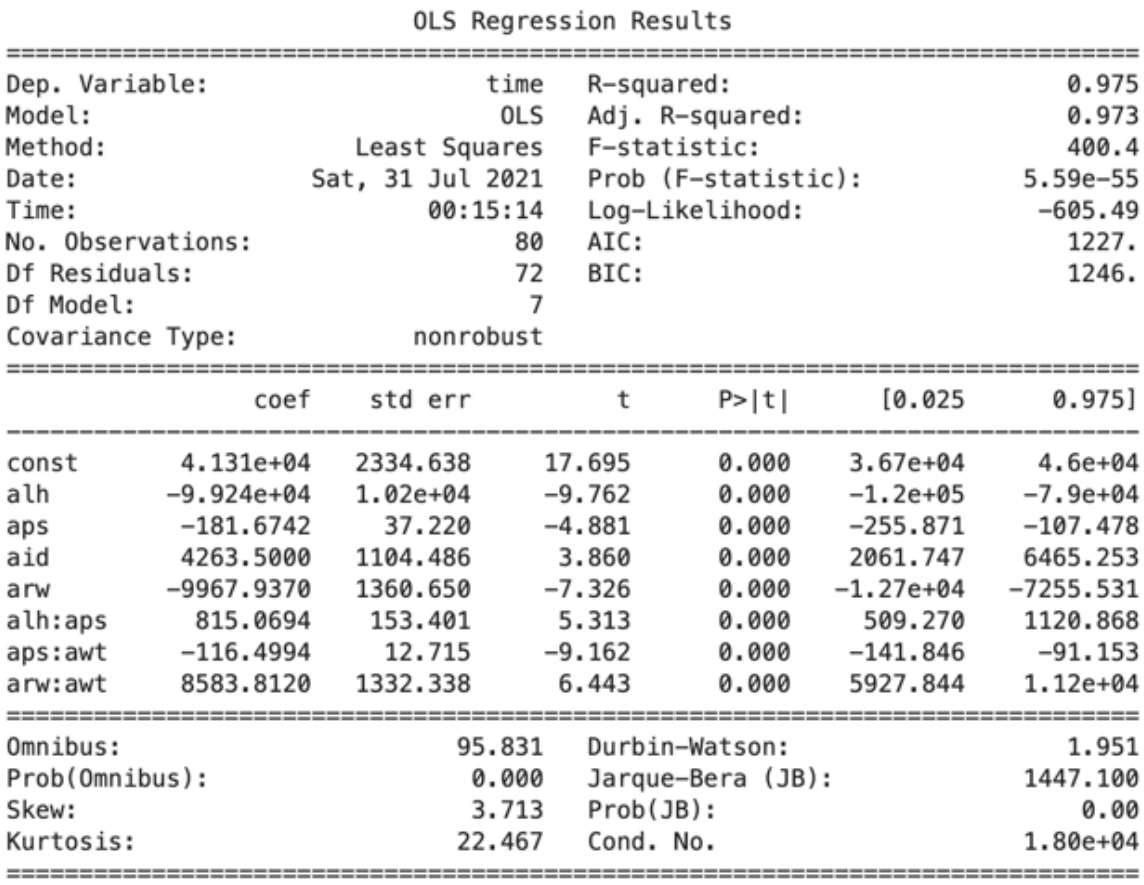

OLS Regression Results

Dep. Variable:	time	R-squared:	0.975
Model:	OLS	Adj. R-squared:	0.973
Method:	Least Squares	F-statistic:	400.4
Date:	Sat, 31 Jul 2021	Prob (F-statistic):	5.59e-55
Time:	00:15:14	Log-Likelihood:	-605.49
No. Observations:	80	AIC:	1227.
Df Residuals:	72	BIC:	1246.
Df Model:	7		
Covariance Type:	nonrobust		

	coef	std err	t	P>|t|	[0.025	0.975]
const	4.131e+04	2334.638	17.695	0.000	3.67e+04	4.6e+04
alh	-9.924e+04	1.02e+04	-9.762	0.000	-1.2e+05	-7.9e+04
aps	-181.6742	37.220	-4.881	0.000	-255.871	-107.478
aid	4263.5000	1104.486	3.860	0.000	2061.747	6465.253
arw	-9967.9370	1360.650	-7.326	0.000	-1.27e+04	-7255.531
alh:aps	815.0694	153.401	5.313	0.000	509.270	1120.868
aps:awt	-116.4994	12.715	-9.162	0.000	-141.846	-91.153
arw:awt	8583.8120	1332.338	6.443	0.000	5927.844	1.12e+04

Omnibus:	95.831	Durbin-Watson:	1.951
Prob(Omnibus):	0.000	Jarque-Bera (JB):	1447.100
Skew:	3.713	Prob(JB):	0.00
Kurtosis:	22.467	Cond. No.	1.80e+04

Figure 39: Analysis A - SWX1 Reduced OLS for Time

$$-9967.93702290074 * X4 + 815.0694444444525 * X1 * X2$$

$$+ -116.4993638676806 * X2 * X5 + 8583.812022900747 * X4 * X5$$

st:

- $.16 \leq X1 \leq .28$
- $50 \leq X2 \leq 60$
- $.15 \leq X3 \leq .25$
- $.4 \leq X4 \leq .8$
- $.8 \leq X5 \leq 1.2$

When solved, ϵ-contraints methodology produces the following values:

- $(X1, X2, X3, X4, X5) =$

$$\begin{pmatrix} 0.28000000999993796, 72.00000071997286, 0.1499999900005892, \\ 0.39999999000704073, 1.2000000119995038 \end{pmatrix}$$

- $f1 = 0.5900000002000078$
- $f2 = 7582.113544009459$

Where:

- • X1 = layer height = .28 mm
- • X2 = print speed = 72 mm/s
- • X3 = infill density = .15
- • X4 = raster width = .4 mm
- • X5 = wall thickness = 1.2 mm
- • f1 = cost = 0.5900000002000078
- • f2 = time = 7582.113544009459 s

In a review of the proposed setting, all the values fit what would be expected for reduced cost and speed.

As a last step the proposed setting were printed three (3) times. In a review of the of the quality of the print, it was found to be excellent with a score of 450.

6.2.2 — EXPERIMENTAL ANALYSIS B

Optimization of cost+power and time and review the results for quality

In this set of analysis, I will review the ideal print parameters for cost and time without factoring in quality (rework). Once the ideal parameters are identified, test prints will be created, and quality will be assessed.

The cost+power collected results are listed in Appendix A.

6.2.2.1 — Experimental Analysis B - CR6

Based on the raw collected results (Table 11 and Table 12). The initial results (Figure 40) for the CR6 Cost OLS model shows that several of the effects are not statistically significant. The variables that are not significant factors in the cost of the model include:

- aid with p-value 0.138052
- alh:awt with p-value 0.089003

The reduced OLS for the CR6 cost is shown in Figure 41. As can be noted in Figure 41, all of the remaining first-order parameters and second-order interactions have a significant impact of the cost of the model.

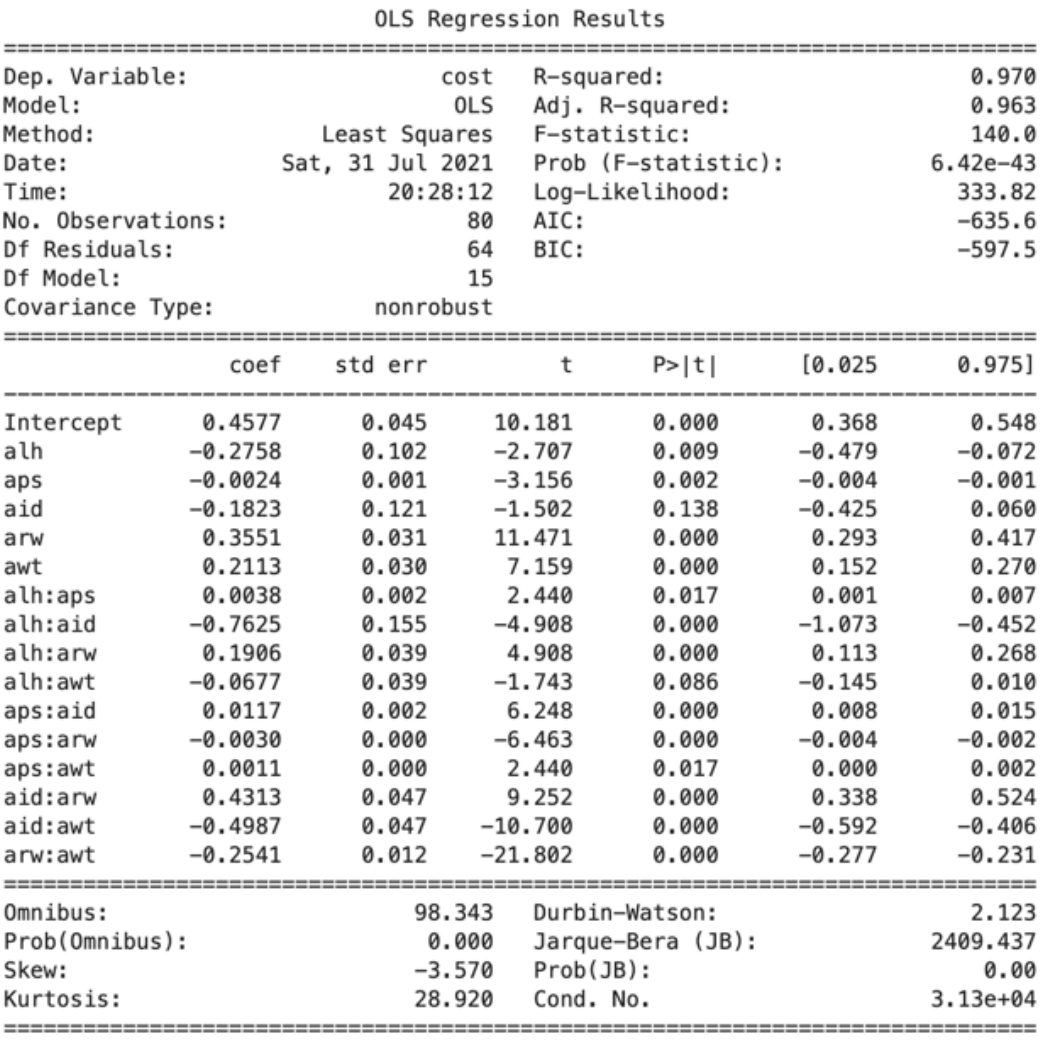

OLS Regression Results

Dep. Variable:	cost	R-squared:	0.970
Model:	OLS	Adj. R-squared:	0.963
Method:	Least Squares	F-statistic:	140.0
Date:	Sat, 31 Jul 2021	Prob (F-statistic):	6.42e-43
Time:	20:28:12	Log-Likelihood:	333.82
No. Observations:	80	AIC:	-635.6
Df Residuals:	64	BIC:	-597.5
Df Model:	15		
Covariance Type:	nonrobust		

	coef	std err	t	P>|t|	[0.025	0.975]
Intercept	0.4577	0.045	10.181	0.000	0.368	0.548
alh	-0.2758	0.102	-2.707	0.009	-0.479	-0.072
aps	-0.0024	0.001	-3.156	0.002	-0.004	-0.001
aid	-0.1823	0.121	-1.502	0.138	-0.425	0.060
arw	0.3551	0.031	11.471	0.000	0.293	0.417
awt	0.2113	0.030	7.159	0.000	0.152	0.270
alh:aps	0.0038	0.002	2.440	0.017	0.001	0.007
alh:aid	-0.7625	0.155	-4.908	0.000	-1.073	-0.452
alh:arw	0.1906	0.039	4.908	0.000	0.113	0.268
alh:awt	-0.0677	0.039	-1.743	0.086	-0.145	0.010
aps:aid	0.0117	0.002	6.248	0.000	0.008	0.015
aps:arw	-0.0030	0.000	-6.463	0.000	-0.004	-0.002
aps:awt	0.0011	0.000	2.440	0.017	0.000	0.002
aid:arw	0.4313	0.047	9.252	0.000	0.338	0.524
aid:awt	-0.4987	0.047	-10.700	0.000	-0.592	-0.406
arw:awt	-0.2541	0.012	-21.802	0.000	-0.277	-0.231

Omnibus:	98.343	Durbin-Watson:	2.123
Prob(Omnibus):	0.000	Jarque-Bera (JB):	2409.437
Skew:	-3.570	Prob(JB):	0.00
Kurtosis:	28.920	Cond. No.	3.13e+04

Figure 40: Analysis B - CR6 Cost OLS

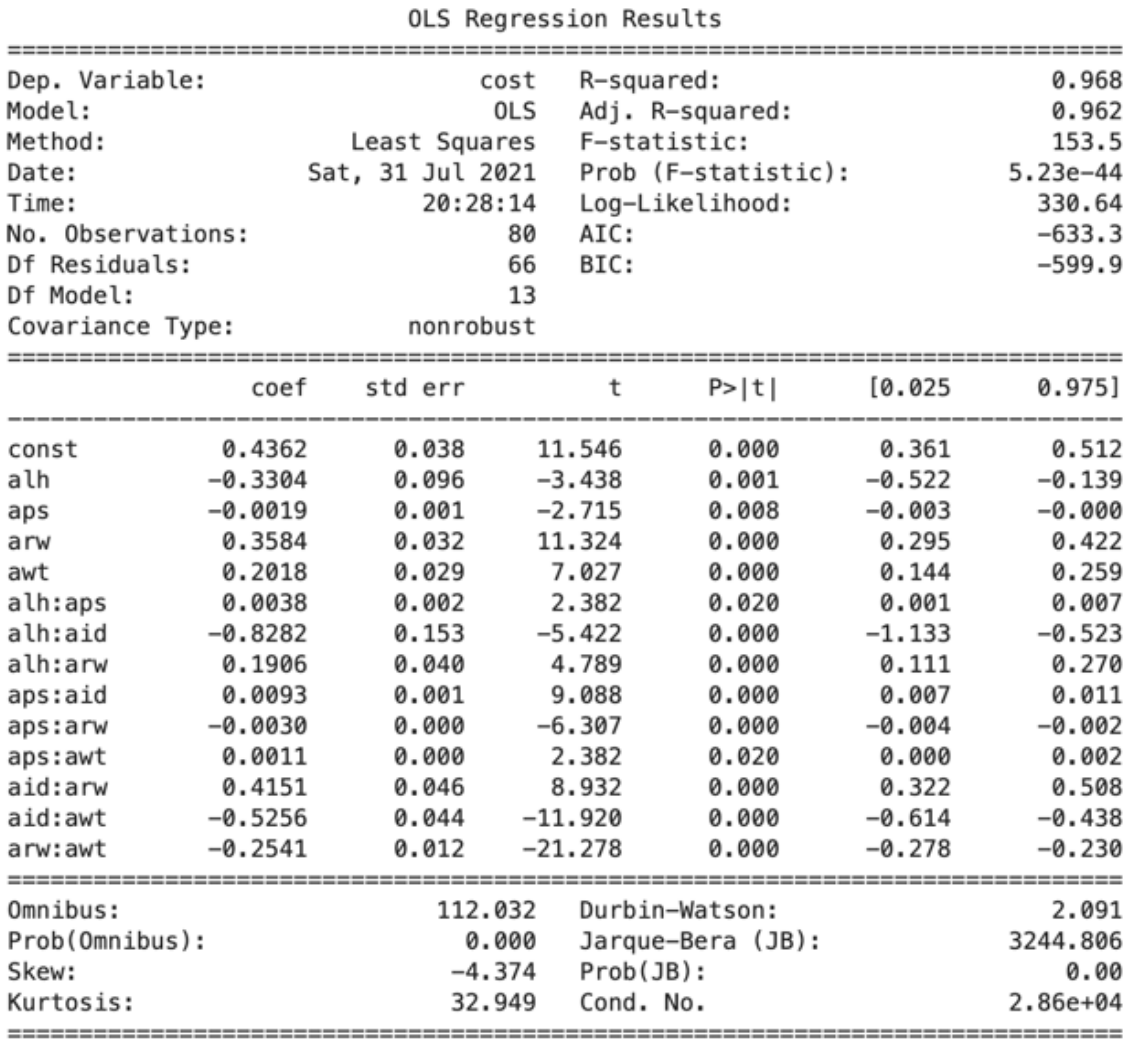

OLS Regression Results

Dep. Variable:	cost	R-squared:	0.968
Model:	OLS	Adj. R-squared:	0.962
Method:	Least Squares	F-statistic:	153.5
Date:	Sat, 31 Jul 2021	Prob (F-statistic):	5.23e-44
Time:	20:28:14	Log-Likelihood:	330.64
No. Observations:	80	AIC:	-633.3
Df Residuals:	66	BIC:	-599.9
Df Model:	13		
Covariance Type:	nonrobust		

	coef	std err	t	P>|t|	[0.025	0.975]
const	0.4362	0.038	11.546	0.000	0.361	0.512
alh	-0.3304	0.096	-3.438	0.001	-0.522	-0.139
aps	-0.0019	0.001	-2.715	0.008	-0.003	-0.000
arw	0.3584	0.032	11.324	0.000	0.295	0.422
awt	0.2018	0.029	7.027	0.000	0.144	0.259
alh:aps	0.0038	0.002	2.382	0.020	0.001	0.007
alh:aid	-0.8282	0.153	-5.422	0.000	-1.133	-0.523
alh:arw	0.1906	0.040	4.789	0.000	0.111	0.270
aps:aid	0.0093	0.001	9.088	0.000	0.007	0.011
aps:arw	-0.0030	0.000	-6.307	0.000	-0.004	-0.002
aps:awt	0.0011	0.000	2.382	0.020	0.000	0.002
aid:arw	0.4151	0.046	8.932	0.000	0.322	0.508
aid:awt	-0.5256	0.044	-11.920	0.000	-0.614	-0.438
arw:awt	-0.2541	0.012	-21.278	0.000	-0.278	-0.230

Omnibus:	112.032	Durbin-Watson:	2.091
Prob(Omnibus):	0.000	Jarque-Bera (JB):	3244.806
Skew:	-4.374	Prob(JB):	0.00
Kurtosis:	32.949	Cond. No.	2.86e+04

Figure 41: Analysis B - CR6 Reduced OLS for Cost

Based on these results (Figure 41), the following linear equation for CR6 cost was developed:

$$Cost$$
$$= 0.43619166666666676 + -0.3303957650272835 * X1 + -0.0018884142076504296$$
$$* X2 + 0.3583517213114778 * X4 + 0.2018153688524602 * X5$$
$$+ 0.00379166666666636 * X1 * X2 + -0.8282295081967748 * X1 * X3$$
$$+ 0.19062500000000449 * X1 * X4 + 0.009283737704918856 * X2 * X3$$
$$+ -0.0030125000000000516 * X2 * X4 + 0.00113750000000004 * X2 * X5$$
$$+ 0.4151163934426205 * X3 * X4 + -0.5256393442622931 * X3 * X5$$
$$+ -0.25406250000000025 * X4 * X5$$

This function was utilized in the ϵ-constraints calculations.

The analysis for CR6 Time OLS were obtained (Figure 42).

The variables that are not significant factors in the time OLS model include:

- aps:awt with p-value 0.712687
- aid with p-value 0.63764
- arw with p-value 0.549529
- aid:arw with p-value 0.12172
- alh:aps with p-value 0.0744513
- arw:awt with p-value 0.0725949

The reduce model for CR6 Time is in Figure 43.

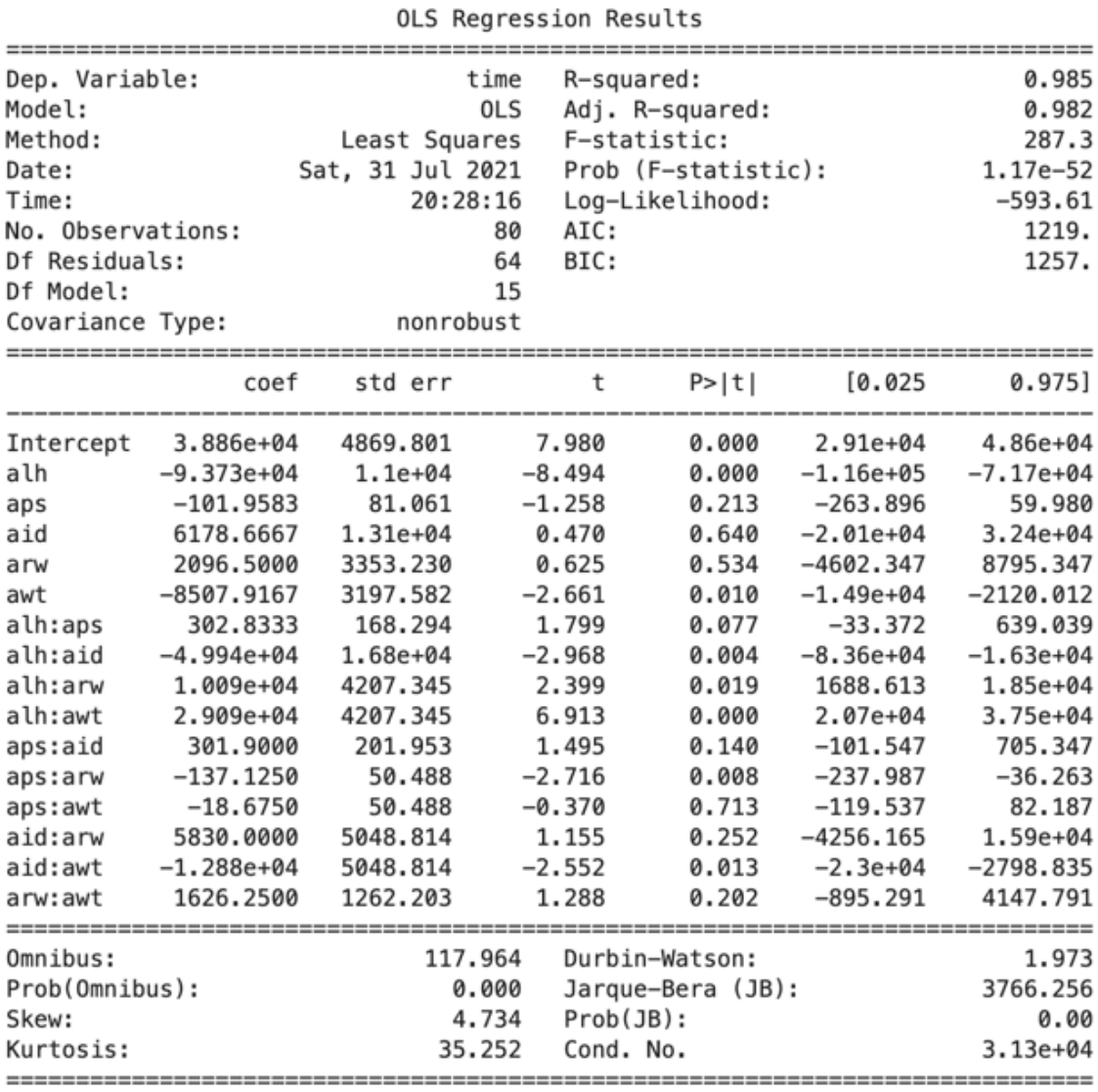

OLS Regression Results

Dep. Variable:	time	R-squared:	0.985
Model:	OLS	Adj. R-squared:	0.982
Method:	Least Squares	F-statistic:	287.3
Date:	Sat, 31 Jul 2021	Prob (F-statistic):	1.17e-52
Time:	20:28:16	Log-Likelihood:	-593.61
No. Observations:	80	AIC:	1219.
Df Residuals:	64	BIC:	1257.
Df Model:	15		
Covariance Type:	nonrobust		

	coef	std err	t	P>|t|	[0.025	0.975]
Intercept	3.886e+04	4869.801	7.980	0.000	2.91e+04	4.86e+04
alh	-9.373e+04	1.1e+04	-8.494	0.000	-1.16e+05	-7.17e+04
aps	-101.9583	81.061	-1.258	0.213	-263.896	59.980
aid	6178.6667	1.31e+04	0.470	0.640	-2.01e+04	3.24e+04
arw	2096.5000	3353.230	0.625	0.534	-4602.347	8795.347
awt	-8507.9167	3197.582	-2.661	0.010	-1.49e+04	-2120.012
alh:aps	302.8333	168.294	1.799	0.077	-33.372	639.039
alh:aid	-4.994e+04	1.68e+04	-2.968	0.004	-8.36e+04	-1.63e+04
alh:arw	1.009e+04	4207.345	2.399	0.019	1688.613	1.85e+04
alh:awt	2.909e+04	4207.345	6.913	0.000	2.07e+04	3.75e+04
aps:aid	301.9000	201.953	1.495	0.140	-101.547	705.347
aps:arw	-137.1250	50.488	-2.716	0.008	-237.987	-36.263
aps:awt	-18.6750	50.488	-0.370	0.713	-119.537	82.187
aid:arw	5830.0000	5048.814	1.155	0.252	-4256.165	1.59e+04
aid:awt	-1.288e+04	5048.814	-2.552	0.013	-2.3e+04	-2798.835
arw:awt	1626.2500	1262.203	1.288	0.202	-895.291	4147.791

Omnibus:	117.964	Durbin-Watson:	1.973
Prob(Omnibus):	0.000	Jarque-Bera (JB):	3766.256
Skew:	4.734	Prob(JB):	0.00
Kurtosis:	35.252	Cond. No.	3.13e+04

Figure 42: Analysis B - CR6 Time OLS

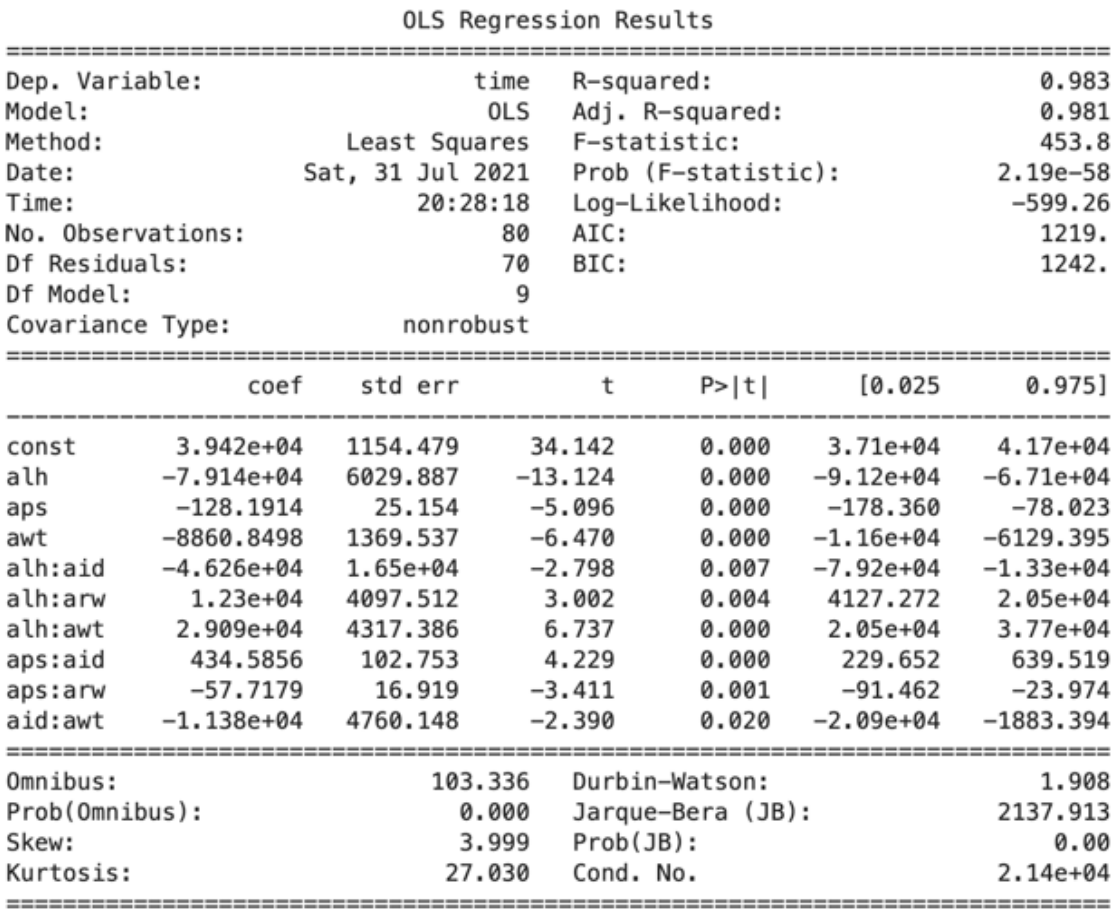

OLS Regression Results

Dep. Variable:	time	R-squared:	0.983
Model:	OLS	Adj. R-squared:	0.981
Method:	Least Squares	F-statistic:	453.8
Date:	Sat, 31 Jul 2021	Prob (F-statistic):	2.19e-58
Time:	20:28:18	Log-Likelihood:	-599.26
No. Observations:	80	AIC:	1219.
Df Residuals:	70	BIC:	1242.
Df Model:	9		
Covariance Type:	nonrobust		

	coef	std err	t	P>|t|	[0.025	0.975]
const	3.942e+04	1154.479	34.142	0.000	3.71e+04	4.17e+04
alh	-7.914e+04	6029.887	-13.124	0.000	-9.12e+04	-6.71e+04
aps	-128.1914	25.154	-5.096	0.000	-178.360	-78.023
awt	-8860.8498	1369.537	-6.470	0.000	-1.16e+04	-6129.395
alh:aid	-4.626e+04	1.65e+04	-2.798	0.007	-7.92e+04	-1.33e+04
alh:arw	1.23e+04	4097.512	3.002	0.004	4127.272	2.05e+04
alh:awt	2.909e+04	4317.386	6.737	0.000	2.05e+04	3.77e+04
aps:aid	434.5856	102.753	4.229	0.000	229.652	639.519
aps:arw	-57.7179	16.919	-3.411	0.001	-91.462	-23.974
aid:awt	-1.138e+04	4760.148	-2.390	0.020	-2.09e+04	-1883.394

Omnibus:	103.336	Durbin-Watson:	1.908
Prob(Omnibus):	0.000	Jarque-Bera (JB):	2137.913
Skew:	3.999	Prob(JB):	0.00
Kurtosis:	27.030	Cond. No.	2.14e+04

Figure 43: Analysis B - CR6 Reduced OLS for Time

Based on these results (Figure 43), the following linear equation for CR6 time was developed:

$$Time = 39415.87499999855 + -79138.51046393832 * X1 + -128.19137670175314 * X2 + -8860.849838411767 * X5 + -46255.95567867106 * X1 * X3 + 12299.502666120085 * X1 * X4 + 29085.416666666522 * X1 * X5 + 434.58559556786804 * X2 * X3 + -57.717904019688284 * X2 * X4 + -11377.20914127423 * X3 * X5$$

The values utilized for the ϵ-constraint methodology for Analysis B were:

Minimize:

- $f1 = 0.43619166666666676 + -0.3303957650272835 * X1 + -0.0018884142076504296 * X2 + 0.3583517213114778 * X4 + 0.2018153688524602 * X5 + 0.00379166666666636 * X1 * X2 + -0.8282295081967748 * X1 * X3 + 0.19062500000000449 * X1 * X4 + 0.009283737704918856 * X2 * X3 + -0.0030125000000000516 * X2 * X4 + 0.00113750000000004 * X2 * X5 + 0.4151163934426205 * X3 * X4 + -0.5256393442622931 * X3 * X5 + -0.25406250000000025 * X4 * X5$
- $f2 = 39415.87499999855 + -79138.51046393832 * X1 + -128.19137670175314 * X2 + -8860.849838411767 * X5 + -46255.95567867106 * X1 * X3 + 12299.502666120085 * X1 * X4 + 29085.416666666522 * X1 * X5 + 434.58559556786804 * X2 * X3 + -57.717904019688284 * X2 * X4 + -11377.20914127423 * X3 * X5$

st:

- $.16 \leq X1 \leq .28$
- $50 \leq X2 \leq 60$
- $.15 \leq X3 \leq .25$
- $.4 \leq X4 \leq .8$
- $.8 \leq X5 \leq 1.2$

When solved, ϵ-contraints methodology produces the following values:

- $(X1, X2, X3, X4, X5) =$

  $\begin{pmatrix} 0.28000000999993935, 60.000000599972694, 0.2500000099939384, \\ 0.8000000096771722, 1.2000000119993277 \end{pmatrix}$

- $f1 = 0.5656472935545355$
- $f2 = 8557.622612553769$

Where:

- • X1 = layer height = .28 mm
- • X2 = print speed = 60 mm/s
- • X3 = infill density = .25
- • X4 = raster width = .8 mm
- • X5 = wall thickness = 1.2 mm
- • f1 = cost = 0.5656472935545355
- • f2 = time = 8557.622612553769 s

The settings in Analysis B match those of Analysis A.

As a last step the proposed setting were printed three (3) times. In a review of the of the quality of the print, it was found to be excellent with a score of 450.

6.2.2.2 — Experimental Analysis B - SWX1

Based on the raw collected results (Table 13 and Table 14). The initial results (Figure 44) for the SWX1 Cost OLS model shows that several of the primary effects of the experiments are not statistically significant.

The variables that are not significant factors in the cost of the model include:

- alh:aid with p-value 0.818098
- aps:arw with p-value 0.643285
- alh:arw with p-value 0.485085
- aps with p-value 0.251449
- aid:arw with p-value 0.164261

The reduced OLS for the SWX1 cost is shown in Figure 45. As can be noted in Figure 45, all of the remaining first-order parameters and second-order interactions have a significant impact of the cost of the model.

Based on these results (Figure 45), the following linear equation for SWX1 cost was developed:

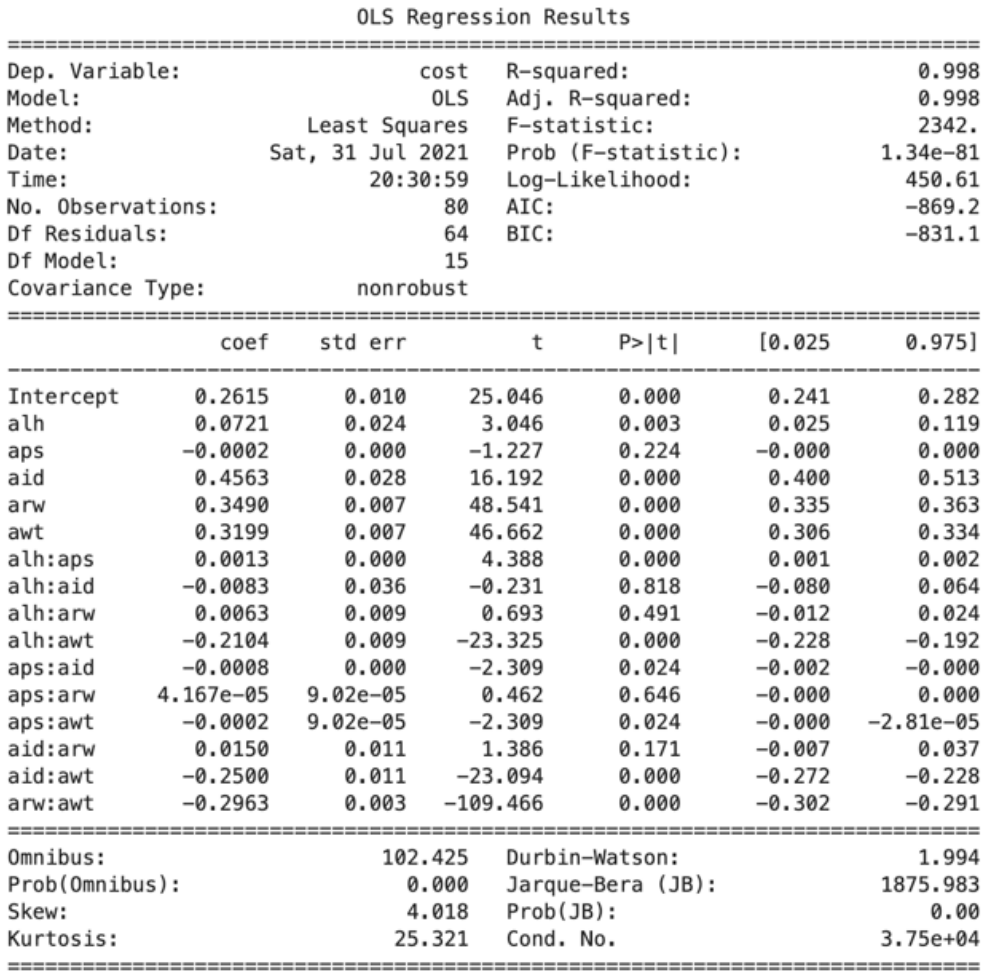

OLS Regression Results

Dep. Variable:	cost	R-squared:	0.998
Model:	OLS	Adj. R-squared:	0.998
Method:	Least Squares	F-statistic:	2342.
Date:	Sat, 31 Jul 2021	Prob (F-statistic):	1.34e-81
Time:	20:30:59	Log-Likelihood:	450.61
No. Observations:	80	AIC:	-869.2
Df Residuals:	64	BIC:	-831.1
Df Model:	15		
Covariance Type:	nonrobust		

	coef	std err	t	P>|t|	[0.025	0.975]
Intercept	0.2615	0.010	25.046	0.000	0.241	0.282
alh	0.0721	0.024	3.046	0.003	0.025	0.119
aps	-0.0002	0.000	-1.227	0.224	-0.000	0.000
aid	0.4563	0.028	16.192	0.000	0.400	0.513
arw	0.3490	0.007	48.541	0.000	0.335	0.363
awt	0.3199	0.007	46.662	0.000	0.306	0.334
alh:aps	0.0013	0.000	4.388	0.000	0.001	0.002
alh:aid	-0.0083	0.036	-0.231	0.818	-0.080	0.064
alh:arw	0.0063	0.009	0.693	0.491	-0.012	0.024
alh:awt	-0.2104	0.009	-23.325	0.000	-0.228	-0.192
aps:aid	-0.0008	0.000	-2.309	0.024	-0.002	-0.000
aps:arw	4.167e-05	9.02e-05	0.462	0.646	-0.000	0.000
aps:awt	-0.0002	9.02e-05	-2.309	0.024	-0.000	-2.81e-05
aid:arw	0.0150	0.011	1.386	0.171	-0.007	0.037
aid:awt	-0.2500	0.011	-23.094	0.000	-0.272	-0.228
arw:awt	-0.2963	0.003	-109.466	0.000	-0.302	-0.291

Omnibus:	102.425	Durbin-Watson:	1.994
Prob(Omnibus):	0.000	Jarque-Bera (JB):	1875.983
Skew:	4.018	Prob(JB):	0.00
Kurtosis:	25.321	Cond. No.	3.75e+04

Figure 44: Analysis B - SWX1 Cost OLS

OLS Regression Results

Dep. Variable:	cost	R-squared:	0.998
Model:	OLS	Adj. R-squared:	0.998
Method:	Least Squares	F-statistic:	3566.
Date:	Sat, 31 Jul 2021	Prob (F-statistic):	1.77e-89
Time:	20:31:01	Log-Likelihood:	448.21
No. Observations:	80	AIC:	-874.4
Df Residuals:	69	BIC:	-848.2
Df Model:	10		
Covariance Type:	nonrobust		

	coef	std err	t	P>|t|	[0.025	0.975]
const	0.2475	0.003	71.944	0.000	0.241	0.254
alh	0.0853	0.019	4.391	0.000	0.047	0.124
aid	0.4780	0.023	21.015	0.000	0.433	0.523
arw	0.3561	0.003	130.018	0.000	0.351	0.362
awt	0.3245	0.006	58.700	0.000	0.313	0.335
alh:aps	0.0012	0.000	4.432	0.000	0.001	0.002
alh:awt	-0.2104	0.009	-23.503	0.000	-0.228	-0.193
aps:aid	-0.0011	0.000	-3.489	0.001	-0.002	-0.000
aps:awt	-0.0003	6.63e-05	-4.179	0.000	-0.000	-0.000
aid:awt	-0.2500	0.011	-23.270	0.000	-0.271	-0.229
arw:awt	-0.2963	0.003	-110.300	0.000	-0.302	-0.291

Omnibus:	99.172	Durbin-Watson:	1.988
Prob(Omnibus):	0.000	Jarque-Bera (JB):	1596.490
Skew:	3.889	Prob(JB):	0.00
Kurtosis:	23.456	Cond. No.	1.62e+04

Figure 45: Analysis B - SWX1 Reduced OLS for Cost

$$Cost$$

$$= 0.24752499999999666 + 0.08528056112224291 * X1 + 0.4780490981963954 * X3$$

$$+ 0.3561250000000017 * X4 + 0.32446325985304236 * X5 + 0.001151052104208572$$

$$* X1 * X2 + -0.21041666666666942 * X1 * X5 + -0.0010537742150968782 * X2 * X3$$

$$+ -0.0002772211088844477 * X2 * X5 + -0.2500000000000011 * X3 * X5$$

$$+ -0.29625000000000157 * X4 * X5$$

This function was utilized in the ϵ-constraints calculations.

The analysis for SWX1 Time OLS were obtained (Figure 46).

The variables that are not significant factors in the throughput of the model include:

- aps:arw with p-value 0.899404
- alh:awt with p-value 0.760839
- aid:awt with p-value 0.641928
- aid:arw with p-value 0.54847
- awt with p-value 0.362301
- alh:aid with p-value 0.23091
- alh:arw with p-value 0.223997
- aps:aid with p-value 0.0884672

The reduce model for SWX1 Time is in Figure 47.

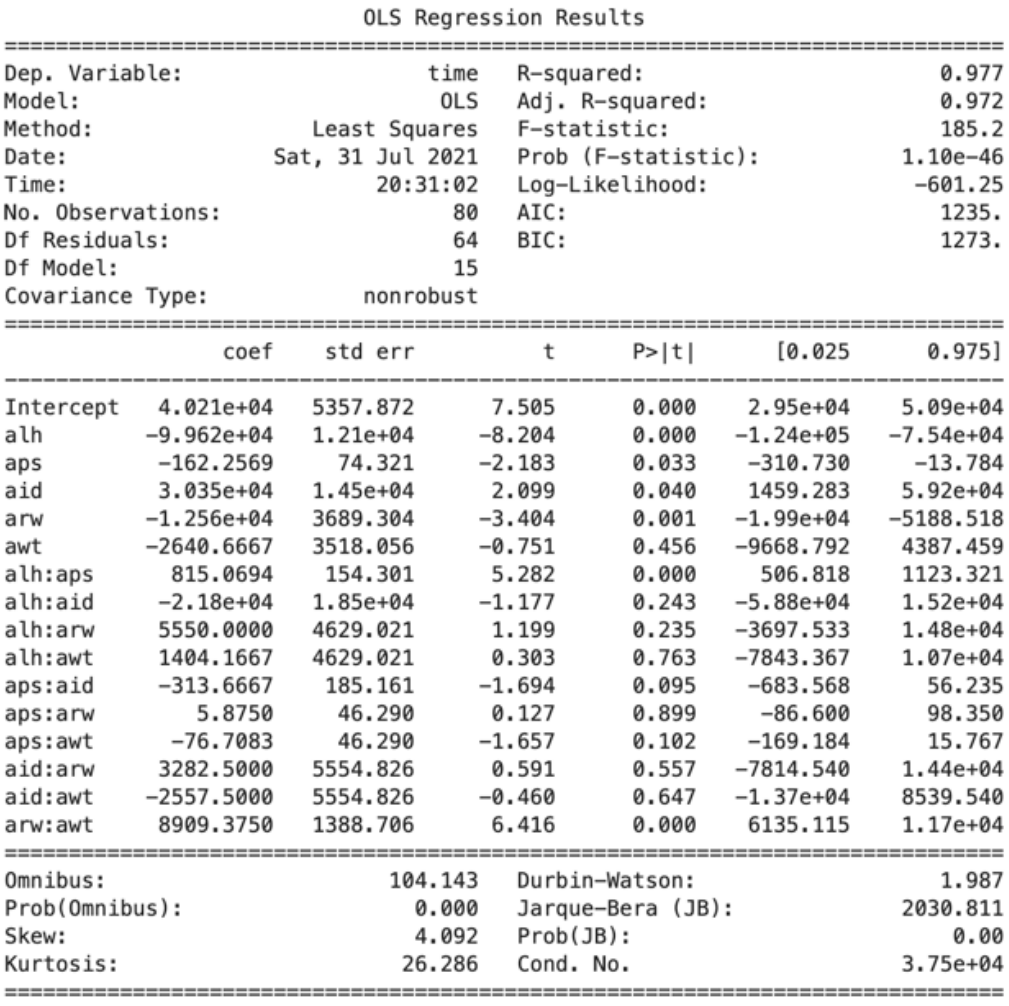

OLS Regression Results

Dep. Variable:	time	R-squared:	0.977
Model:	OLS	Adj. R-squared:	0.972
Method:	Least Squares	F-statistic:	185.2
Date:	Sat, 31 Jul 2021	Prob (F-statistic):	1.10e-46
Time:	20:31:02	Log-Likelihood:	-601.25
No. Observations:	80	AIC:	1235.
Df Residuals:	64	BIC:	1273.
Df Model:	15		
Covariance Type:	nonrobust		

	coef	std err	t	P>|t|	[0.025	0.975]
Intercept	4.021e+04	5357.872	7.505	0.000	2.95e+04	5.09e+04
alh	-9.962e+04	1.21e+04	-8.204	0.000	-1.24e+05	-7.54e+04
aps	-162.2569	74.321	-2.183	0.033	-310.730	-13.784
aid	3.035e+04	1.45e+04	2.099	0.040	1459.283	5.92e+04
arw	-1.256e+04	3689.304	-3.404	0.001	-1.99e+04	-5188.518
awt	-2640.6667	3518.056	-0.751	0.456	-9668.792	4387.459
alh:aps	815.0694	154.301	5.282	0.000	506.818	1123.321
alh:aid	-2.18e+04	1.85e+04	-1.177	0.243	-5.88e+04	1.52e+04
alh:arw	5550.0000	4629.021	1.199	0.235	-3697.533	1.48e+04
alh:awt	1404.1667	4629.021	0.303	0.763	-7843.367	1.07e+04
aps:aid	-313.6667	185.161	-1.694	0.095	-683.568	56.235
aps:arw	5.8750	46.290	0.127	0.899	-86.600	98.350
aps:awt	-76.7083	46.290	-1.657	0.102	-169.184	15.767
aid:arw	3282.5000	5554.826	0.591	0.557	-7814.540	1.44e+04
aid:awt	-2557.5000	5554.826	-0.460	0.647	-1.37e+04	8539.540
arw:awt	8909.3750	1388.706	6.416	0.000	6135.115	1.17e+04

Omnibus:	104.143	Durbin-Watson:	1.987
Prob(Omnibus):	0.000	Jarque-Bera (JB):	2030.811
Skew:	4.092	Prob(JB):	0.00
Kurtosis:	26.286	Cond. No.	3.75e+04

Figure 46: Analysis B - SWX1 Time OLS

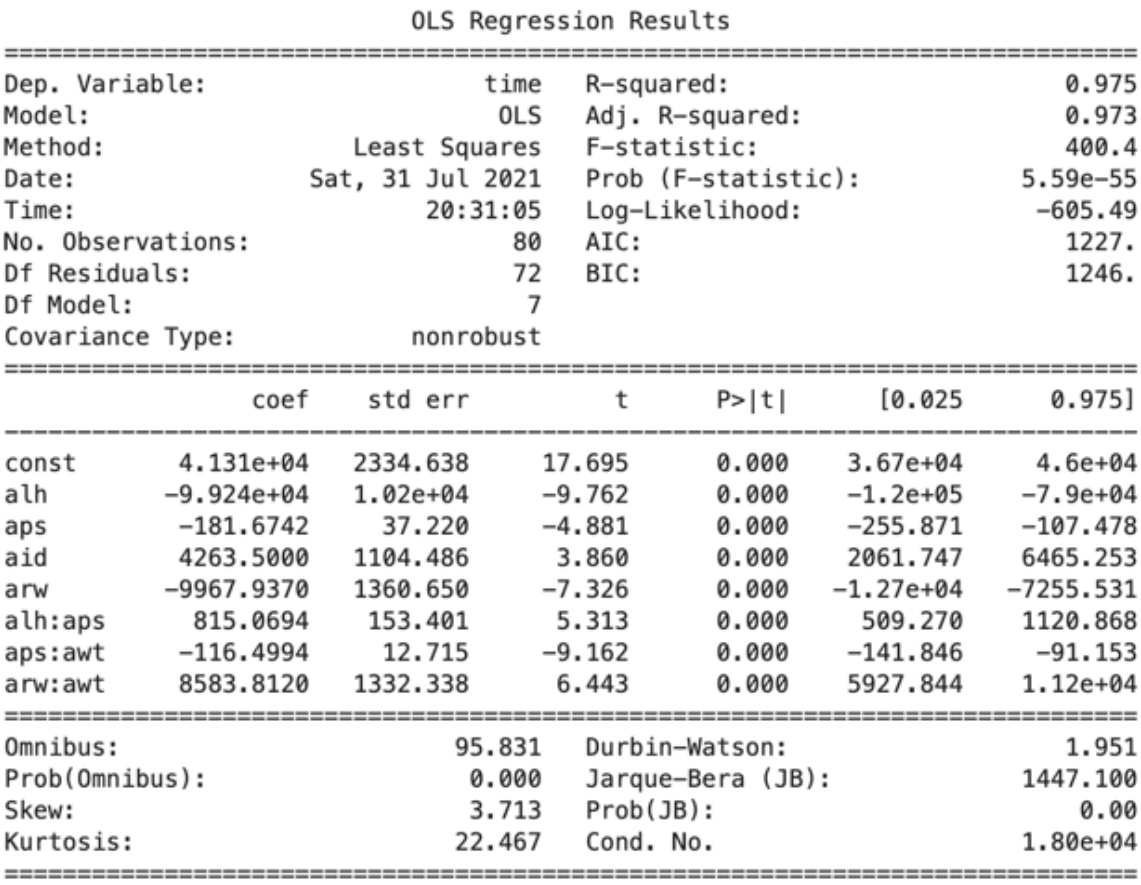

OLS Regression Results

Dep. Variable:	time	R-squared:	0.975
Model:	OLS	Adj. R-squared:	0.973
Method:	Least Squares	F-statistic:	400.4
Date:	Sat, 31 Jul 2021	Prob (F-statistic):	5.59e-55
Time:	20:31:05	Log-Likelihood:	-605.49
No. Observations:	80	AIC:	1227.
Df Residuals:	72	BIC:	1246.
Df Model:	7		
Covariance Type:	nonrobust		

	coef	std err	t	P>|t|	[0.025	0.975]
const	4.131e+04	2334.638	17.695	0.000	3.67e+04	4.6e+04
alh	-9.924e+04	1.02e+04	-9.762	0.000	-1.2e+05	-7.9e+04
aps	-181.6742	37.220	-4.881	0.000	-255.871	-107.478
aid	4263.5000	1104.486	3.860	0.000	2061.747	6465.253
arw	-9967.9370	1360.650	-7.326	0.000	-1.27e+04	-7255.531
alh:aps	815.0694	153.401	5.313	0.000	509.270	1120.868
aps:awt	-116.4994	12.715	-9.162	0.000	-141.846	-91.153
arw:awt	8583.8120	1332.338	6.443	0.000	5927.844	1.12e+04

Omnibus:	95.831	Durbin-Watson:	1.951
Prob(Omnibus):	0.000	Jarque-Bera (JB):	1447.100
Skew:	3.713	Prob(JB):	0.00
Kurtosis:	22.467	Cond. No.	1.80e+04

Figure 47: Analysis B - SWX1 Reduced OLS for Time

Based on these results (Figure 47), the following linear equation for SWX1 time was developed:

$$Time = 41311.84166666333 + -99242.9166666657 * X1 + -181.67424724344346 * X2 + 4263.500000000091 * X3 + -9967.93702290074 * X4 + 815.0694444444525 * X1 * X2 + -116.4993638676806 * X2 * X5 + 8583.812022900747 * X4 * X5$$

The values utilized for the ϵ-constraint methodology for Analysis B were:

Minimize:

- $f1 = 0.24752499999999666 + 0.08528056112224291 * X1 + 0.4780490981963954 * X3 + 0.3561250000000017 * X4 + 0.32446325985304236 * X5 + 0.001151052104208572 * X1 * X2 + -0.21041666666666942 * X1 * X5 + -0.0010537742150968782 * X2 * X3 + -0.0002772211088844477 * X2 * X5 + -0.2500000000000011 * X3 * X5 + -0.29625000000000157 * X4 * X5$
- $f2 = 41311.84166666333 + -99242.9166666657 * X1 + -181.67424724344346 * X2 + 4263.500000000091 * X3 + -9967.93702290074 * X4 + 815.0694444444525 * X1 * X2 + -116.4993638676806 * X2 * X5 + 8583.812022900747 * X4 * X5$

st:

- $.16 \leq X1 \leq .28$
- $50 \leq X2 \leq 60$

- $.15 \leq X3 \leq .25$
- $.4 \leq X4 \leq .8$
- $.8 \leq X5 \leq 1.2$

When solved, ϵ-contraints methodology produces the following values:

- $(X1, X2, X3, X4, X5) =$

$$\begin{pmatrix} 0.28000000999993796, 72.00000071997286, 0.1499999900005892, \\ 0.3999999900070408, 1.2000000119995038 \end{pmatrix}$$

- $f1 = 0.6048893778398489$
- $f2 = 7582.113544009455$

Where:

- • X1 = layer height = .28 mm
- • X2 = print speed = 72 mm/s
- • X3 = infill density = .15
- • X4 = raster width = .4 mm
- • X5 = wall thickness = 1.2 mm
- • f1 = cost = 0.6048893778398489
- • f2 = time = 7582.113544009455 s

The settings in Analysis B match those of Analysis A.

As a last step the proposed setting were printed three (3) times. In a review of the of the quality of the print, it was found to be excellent with a score of 450.

6.2.3 — EXPERIMENTAL ANALYSIS C

Optimization of cost+power and time and review the results for quality

In this set of analysis, I will review the ideal print parameters for cost and time with the addition of rework time and costs to address quality issues. Once the ideal parameters are identified, test prints will be created, and quality will be assessed.

The rework results are listed in Appendix A.

6.2.3.1 — Experimental Analysis C - CR6

The initial results (Figure 48) for the CR6 Cost OLS model shows that several of the effects are not statistically significant. The variables that are not significant factors in the cost of the model include:

- alh:aps with p-value 0.901841
- aid with p-value 0.77787
- alh:aid with p-value 0.475609
- alh:arw with p-value 0.444672
- aps with p-value 0.294638
- aps:awt with p-value 0.351045
- alh with p-value 0.146827
- alh:awt with p-value 0.362181
- aid:arw with p-value 0.11887
- arw:awt with p-value 0.116793

The reduced OLS for the CR6 cost is shown in Figure 49. As can be noted in Figure 49, all the remaining first-order parameters and second-order interactions have a significant impact of the cost of the model.

Based on these results (Figure 49), the following linear equation for CR6 cost was developed:

$$Cost$$
$$= 0.022179997348888314 + 0.9805362539766707 * X4 + 0.4210264448568395 * X5$$
$$+ 0.055398409331918294 * X2 * X3 + -0.016249522799575436 * X2 * X4$$
$$+ -2.5398197242841984 * X3 * X5$$

This function was utilized in the ϵ-constraints calculations.

The analysis for CR6 Time OLS were obtained (Figure 50).

The variables that are not significant factors in the time OLS model include:

- aps:awt with p-value 0.679939
- aid with p-value 0.642097
- arw with p-value 0.529019
- aid:arw with p-value 0.112705
- alh:aps with p-value 0.0748668
- arw:awt with p-value 0.0727373

The reduce model for CR6 Time is in Figure 51.

Based on these results (Figure 51), the following linear equation for CR6 time was developed:

OLS Regression Results

Dep. Variable:	cost	R-squared:	0.373
Model:	OLS	Adj. R-squared:	0.226
Method:	Least Squares	F-statistic:	2.534
Date:	Sat, 31 Jul 2021	Prob (F-statistic):	0.00518
Time:	18:19:29	Log-Likelihood:	93.594
No. Observations:	80	AIC:	-155.2
Df Residuals:	64	BIC:	-117.1
Df Model:	15		
Covariance Type:	nonrobust		

	coef	std err	t	P>|t|	[0.025	0.975]
Intercept	-0.9161	0.906	-1.012	0.316	-2.725	0.893
alh	0.8129	2.052	0.396	0.693	-3.287	4.912
aps	0.0107	0.015	0.713	0.479	-0.019	0.041
aid	-0.6871	2.444	-0.281	0.780	-5.570	4.196
arw	0.9958	0.624	1.597	0.115	-0.250	2.241
awt	1.6889	0.595	2.840	0.006	0.501	2.877
alh:aps	0.0039	0.031	0.124	0.902	-0.059	0.066
alh:aid	2.3708	3.129	0.758	0.451	-3.881	8.623
alh:arw	-0.5906	0.782	-0.755	0.453	-2.154	0.972
alh:awt	-1.2406	0.782	-1.586	0.118	-2.804	0.322
aps:aid	0.0493	0.038	1.311	0.194	-0.026	0.124
aps:arw	-0.0124	0.009	-1.319	0.192	-0.031	0.006
aps:awt	-0.0129	0.009	-1.378	0.173	-0.032	0.006
aid:arw	1.3663	0.939	1.455	0.150	-0.509	3.242
aid:awt	-2.8437	0.939	-3.029	0.004	-4.719	-0.968
arw:awt	-0.3709	0.235	-1.580	0.119	-0.840	0.098

Omnibus:	65.477	Durbin-Watson:	2.187
Prob(Omnibus):	0.000	Jarque-Bera (JB):	524.930
Skew:	2.338	Prob(JB):	1.03e-114
Kurtosis:	14.646	Cond. No.	3.13e+04

Figure 48: Analysis C - CR6 Cost OLS

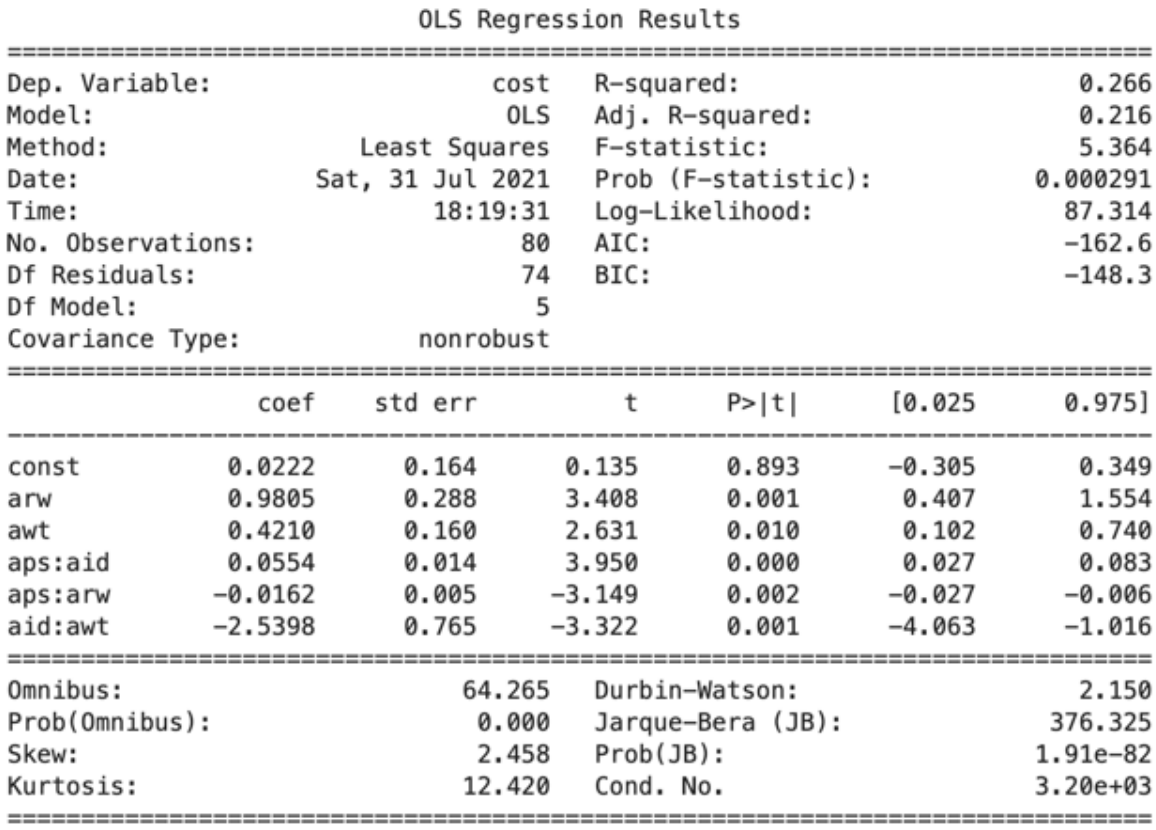

OLS Regression Results

Dep. Variable:	cost	R-squared:	0.266
Model:	OLS	Adj. R-squared:	0.216
Method:	Least Squares	F-statistic:	5.364
Date:	Sat, 31 Jul 2021	Prob (F-statistic):	0.000291
Time:	18:19:31	Log-Likelihood:	87.314
No. Observations:	80	AIC:	-162.6
Df Residuals:	74	BIC:	-148.3
Df Model:	5		
Covariance Type:	nonrobust		

	coef	std err	t	P>|t|	[0.025	0.975]
const	0.0222	0.164	0.135	0.893	-0.305	0.349
arw	0.9805	0.288	3.408	0.001	0.407	1.554
awt	0.4210	0.160	2.631	0.010	0.102	0.740
aps:aid	0.0554	0.014	3.950	0.000	0.027	0.083
aps:arw	-0.0162	0.005	-3.149	0.002	-0.027	-0.006
aid:awt	-2.5398	0.765	-3.322	0.001	-4.063	-1.016

Omnibus:	64.265	Durbin-Watson:	2.150
Prob(Omnibus):	0.000	Jarque-Bera (JB):	376.325
Skew:	2.458	Prob(JB):	1.91e-82
Kurtosis:	12.420	Cond. No.	3.20e+03

Figure 49: Analysis C - CR6 Reduced OLS for Cost

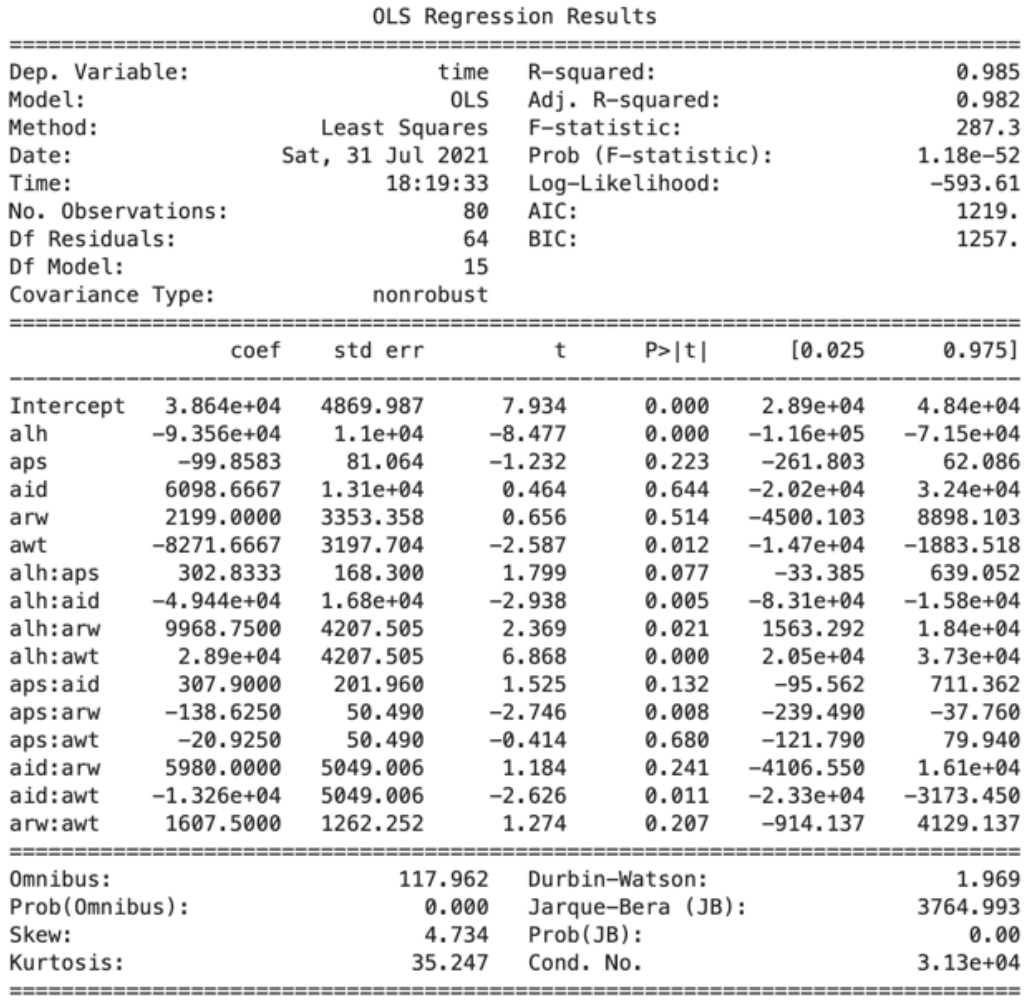

OLS Regression Results

Dep. Variable:	time	R-squared:	0.985
Model:	OLS	Adj. R-squared:	0.982
Method:	Least Squares	F-statistic:	287.3
Date:	Sat, 31 Jul 2021	Prob (F-statistic):	1.18e-52
Time:	18:19:33	Log-Likelihood:	-593.61
No. Observations:	80	AIC:	1219.
Df Residuals:	64	BIC:	1257.
Df Model:	15		
Covariance Type:	nonrobust		

	coef	std err	t	P>|t|	[0.025	0.975]
Intercept	3.864e+04	4869.987	7.934	0.000	2.89e+04	4.84e+04
alh	-9.356e+04	1.1e+04	-8.477	0.000	-1.16e+05	-7.15e+04
aps	-99.8583	81.064	-1.232	0.223	-261.803	62.086
aid	6098.6667	1.31e+04	0.464	0.644	-2.02e+04	3.24e+04
arw	2199.0000	3353.358	0.656	0.514	-4500.103	8898.103
awt	-8271.6667	3197.704	-2.587	0.012	-1.47e+04	-1883.518
alh:aps	302.8333	168.300	1.799	0.077	-33.385	639.052
alh:aid	-4.944e+04	1.68e+04	-2.938	0.005	-8.31e+04	-1.58e+04
alh:arw	9968.7500	4207.505	2.369	0.021	1563.292	1.84e+04
alh:awt	2.89e+04	4207.505	6.868	0.000	2.05e+04	3.73e+04
aps:aid	307.9000	201.960	1.525	0.132	-95.562	711.362
aps:arw	-138.6250	50.490	-2.746	0.008	-239.490	-37.760
aps:awt	-20.9250	50.490	-0.414	0.680	-121.790	79.940
aid:arw	5980.0000	5049.006	1.184	0.241	-4106.550	1.61e+04
aid:awt	-1.326e+04	5049.006	-2.626	0.011	-2.33e+04	-3173.450
arw:awt	1607.5000	1262.252	1.274	0.207	-914.137	4129.137

Omnibus:	117.962	Durbin-Watson:	1.969
Prob(Omnibus):	0.000	Jarque-Bera (JB):	3764.993
Skew:	4.734	Prob(JB):	0.00
Kurtosis:	35.247	Cond. No.	3.13e+04

Figure 50: Analysis C - CR6 Time OLS

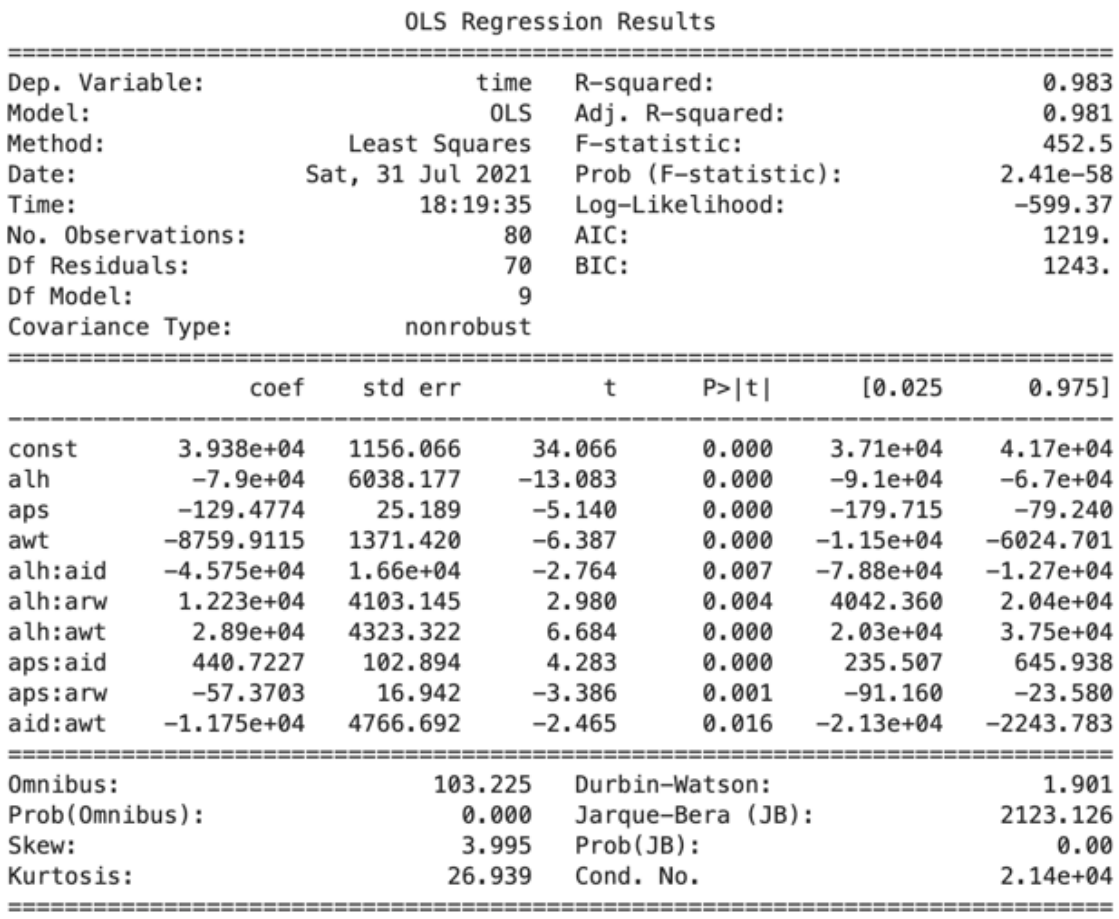

OLS Regression Results

Dep. Variable:	time	R-squared:	0.983
Model:	OLS	Adj. R-squared:	0.981
Method:	Least Squares	F-statistic:	452.5
Date:	Sat, 31 Jul 2021	Prob (F-statistic):	2.41e-58
Time:	18:19:35	Log-Likelihood:	-599.37
No. Observations:	80	AIC:	1219.
Df Residuals:	70	BIC:	1243.
Df Model:	9		
Covariance Type:	nonrobust		

	coef	std err	t	P>|t|	[0.025	0.975]
const	3.938e+04	1156.066	34.066	0.000	3.71e+04	4.17e+04
alh	-7.9e+04	6038.177	-13.083	0.000	-9.1e+04	-6.7e+04
aps	-129.4774	25.189	-5.140	0.000	-179.715	-79.240
awt	-8759.9115	1371.420	-6.387	0.000	-1.15e+04	-6024.701
alh:aid	-4.575e+04	1.66e+04	-2.764	0.007	-7.88e+04	-1.27e+04
alh:arw	1.223e+04	4103.145	2.980	0.004	4042.360	2.04e+04
alh:awt	2.89e+04	4323.322	6.684	0.000	2.03e+04	3.75e+04
aps:aid	440.7227	102.894	4.283	0.000	235.507	645.938
aps:arw	-57.3703	16.942	-3.386	0.001	-91.160	-23.580
aid:awt	-1.175e+04	4766.692	-2.465	0.016	-2.13e+04	-2243.783

Omnibus:	103.225	Durbin-Watson:	1.901
Prob(Omnibus):	0.000	Jarque-Bera (JB):	2123.126
Skew:	3.995	Prob(JB):	0.00
Kurtosis:	26.939	Cond. No.	2.14e+04

Figure 51: Analysis C - CR6 Reduced OLS for Time

$$Time$$

$$= 39383.12499999856 + -78995.06592013844 * X1 + -129.4773731249602 * X2$$

$$+ -8759.911472760796 * X5 + -45752.146814405125 * X1 * X3$$

$$+ 12225.825471698428 * X1 * X4 + 28897.916666666522 * X1 * X5$$

$$+ 440.7227146814413 * X2 * X3 + -57.37028301886791 * X2 * X4$$

$$+ -11750.650969529073 * X3 * X5$$

The values utilized for the ϵ-constraint methodology for Analysis B were:

Minimize:

- $f1 = 0.022179997348888314 + 0.9805362539766707 * X4 +$
  $0.4210264448568395 * X5 + 0.055398409331918294 * X2 * X3 +$
  $-0.016249522799575436 * X2 * X4 + -2.5398197242841984 * X3 * X5$
- $f2 = 39383.12499999856 + -78995.06592013844 * X1 +$
  $-129.4773731249602 * X2 + -8759.911472760796 * X5 +$
  $-45752.146814405125 * X1 * X3 + 12225.825471698428 * X1 * X4 +$
  $28897.916666666522 * X1 * X5 + 440.7227146814413 * X2 * X3 +$
  $-57.37028301886791 * X2 * X4 + -11750.650969529073 * X3 * X5$

st:

- $.16 \leq X1 \leq .28$
- $50 \leq X2 \leq 60$
- $.15 \leq X3 \leq .25$
- $.4 \leq X4 \leq .8$

- $.8 \leq X5 \leq 1.2$

When solved, ϵ-contraints methodology produces the following values:

- $(X1, X2, X3, X4, X5) =$

$$\begin{pmatrix} 0.2800000099999455, 60.00000059996157, 0.25000000999464544, \\ 0.800000009867982, 1.200000011999305 \end{pmatrix}$$

- $f1 = 0.6008938634299353$
- $f2 = 8557.622612553769$

Where:

- • X1 = layer height = .28 mm
- • X2 = print speed = 60 mm/s
- • X3 = infill density = .25
- • X4 = raster width = .8 mm
- • X5 = wall thickness = 1.2 mm
- • f1 = cost = 0.6008938634299353
- • f2 = time = 8557.622612553769 s

The settings in Analysis C match those of Analysis A.

As a last step the proposed setting were printed three (3) times. In a review of the of the quality of the print, it was found to be excellent with a score of 450.

6.2.3.2 — Experimental Analysis C - SWX1

The initial results (Figure 52) for the SWX1 Cost OLS model shows that several of the primary effects of the experiments are not statistically significant.

The variables that are not significant factors in the cost of the model include:

- arw with p-value 0.834584
- alh:awt with p-value 0.723342
- aid with p-value 0.253413

The reduced OLS for the SWX1 cost is shown in Figure 53. As can be noted in Figure 53, all the remaining first-order parameters and second-order interactions have a significant impact of the cost of the model.

Based on these results (Figure 53), the following linear equation for SWX1 cost was developed:

$$Cost$$

$$= -7.512756311165274 + 15.594282277667375 * X1 + 0.1501013849966114 * X2$$

$$+ 3.3568541135900944 * X5 + -0.1873958333333725 * X1 * X2 + 14.97406461978116$$

$$* X1 * X3 + -6.3471031138125085 * X1 * X4 + -0.17544472807322514 * X2 * X3$$

$$+ 0.02025357325229224 * X2 * X4 + -0.07640624999999765 * X2 * X5$$

$$+ 3.2956081485919615 * X3 * X4 + 6.441435526274299 * X3 * X5$$

$$+ -0.6702353647414601 * X4 * X5$$

This function was utilized in the ϵ-constraints calculations.

The analysis for SWX1 Time OLS were obtained (Figure 54).

OLS Regression Results

Dep. Variable:	cost	R-squared:	0.879
Model:	OLS	Adj. R-squared:	0.851
Method:	Least Squares	F-statistic:	31.04
Date:	Sat, 31 Jul 2021	Prob (F-statistic):	1.26e-23
Time:	18:50:16	Log-Likelihood:	66.692
No. Observations:	80	AIC:	-101.4
Df Residuals:	64	BIC:	-63.27
Df Model:	15		
Covariance Type:	nonrobust		

	coef	std err	t	P>|t|	[0.025	0.975]
Intercept	-6.7997	1.267	-5.365	0.000	-9.332	-4.268
alh	14.9792	2.872	5.215	0.000	9.241	20.717
aps	0.1432	0.018	8.147	0.000	0.108	0.178
aid	-3.8274	3.421	-1.119	0.267	-10.662	3.007
arw	0.1830	0.873	0.210	0.835	-1.561	1.927
awt	3.1783	0.832	3.819	0.000	1.516	4.841
alh:aps	-0.1874	0.037	-5.134	0.000	-0.260	-0.114
alh:aid	16.3792	4.380	3.739	0.000	7.629	25.130
alh:arw	-6.4344	1.095	-5.876	0.000	-8.622	-4.247
alh:awt	0.3865	1.095	0.353	0.725	-1.801	2.574
aps:aid	-0.1333	0.044	-3.043	0.003	-0.221	-0.046
aps:arw	0.0176	0.011	1.610	0.112	-0.004	0.040
aps:awt	-0.0764	0.011	-6.977	0.000	-0.098	-0.055
aid:arw	3.5262	1.314	2.683	0.009	0.901	6.151
aid:awt	7.0162	1.314	5.339	0.000	4.391	9.641
arw:awt	-0.7059	0.329	-2.149	0.035	-1.362	-0.050

Omnibus:	51.730	Durbin-Watson:	2.230
Prob(Omnibus):	0.000	Jarque-Bera (JB):	778.361
Skew:	-1.374	Prob(JB):	9.57e-170
Kurtosis:	18.032	Cond. No.	3.75e+04

Figure 52: Analysis C - SWX1 Cost OLS

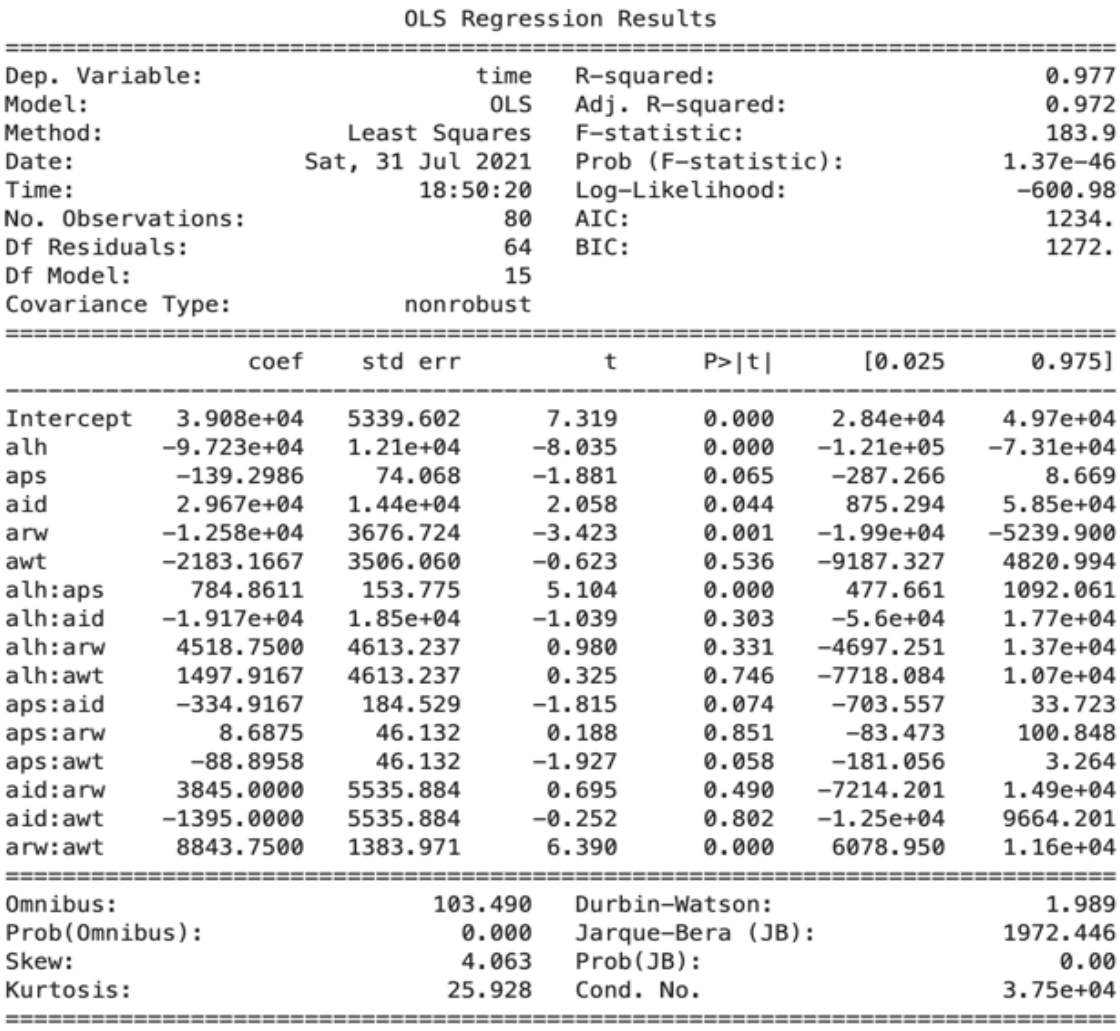

OLS Regression Results

Dep. Variable:	time	R-squared:	0.977
Model:	OLS	Adj. R-squared:	0.972
Method:	Least Squares	F-statistic:	183.9
Date:	Sat, 31 Jul 2021	Prob (F-statistic):	1.37e-46
Time:	18:50:20	Log-Likelihood:	-600.98
No. Observations:	80	AIC:	1234.
Df Residuals:	64	BIC:	1272.
Df Model:	15		
Covariance Type:	nonrobust		

	coef	std err	t	P>|t|	[0.025	0.975]
Intercept	3.908e+04	5339.602	7.319	0.000	2.84e+04	4.97e+04
alh	-9.723e+04	1.21e+04	-8.035	0.000	-1.21e+05	-7.31e+04
aps	-139.2986	74.068	-1.881	0.065	-287.266	8.669
aid	2.967e+04	1.44e+04	2.058	0.044	875.294	5.85e+04
arw	-1.258e+04	3676.724	-3.423	0.001	-1.99e+04	-5239.900
awt	-2183.1667	3506.060	-0.623	0.536	-9187.327	4820.994
alh:aps	784.8611	153.775	5.104	0.000	477.661	1092.061
alh:aid	-1.917e+04	1.85e+04	-1.039	0.303	-5.6e+04	1.77e+04
alh:arw	4518.7500	4613.237	0.980	0.331	-4697.251	1.37e+04
alh:awt	1497.9167	4613.237	0.325	0.746	-7718.084	1.07e+04
aps:aid	-334.9167	184.529	-1.815	0.074	-703.557	33.723
aps:arw	8.6875	46.132	0.188	0.851	-83.473	100.848
aps:awt	-88.8958	46.132	-1.927	0.058	-181.056	3.264
aid:arw	3845.0000	5535.884	0.695	0.490	-7214.201	1.49e+04
aid:awt	-1395.0000	5535.884	-0.252	0.802	-1.25e+04	9664.201
arw:awt	8843.7500	1383.971	6.390	0.000	6078.950	1.16e+04

Omnibus:	103.490	Durbin-Watson:	1.989
Prob(Omnibus):	0.000	Jarque-Bera (JB):	1972.446
Skew:	4.063	Prob(JB):	0.00
Kurtosis:	25.928	Cond. No.	3.75e+04

Figure 53: Analysis C - SWX1 Reduced OLS for Cost

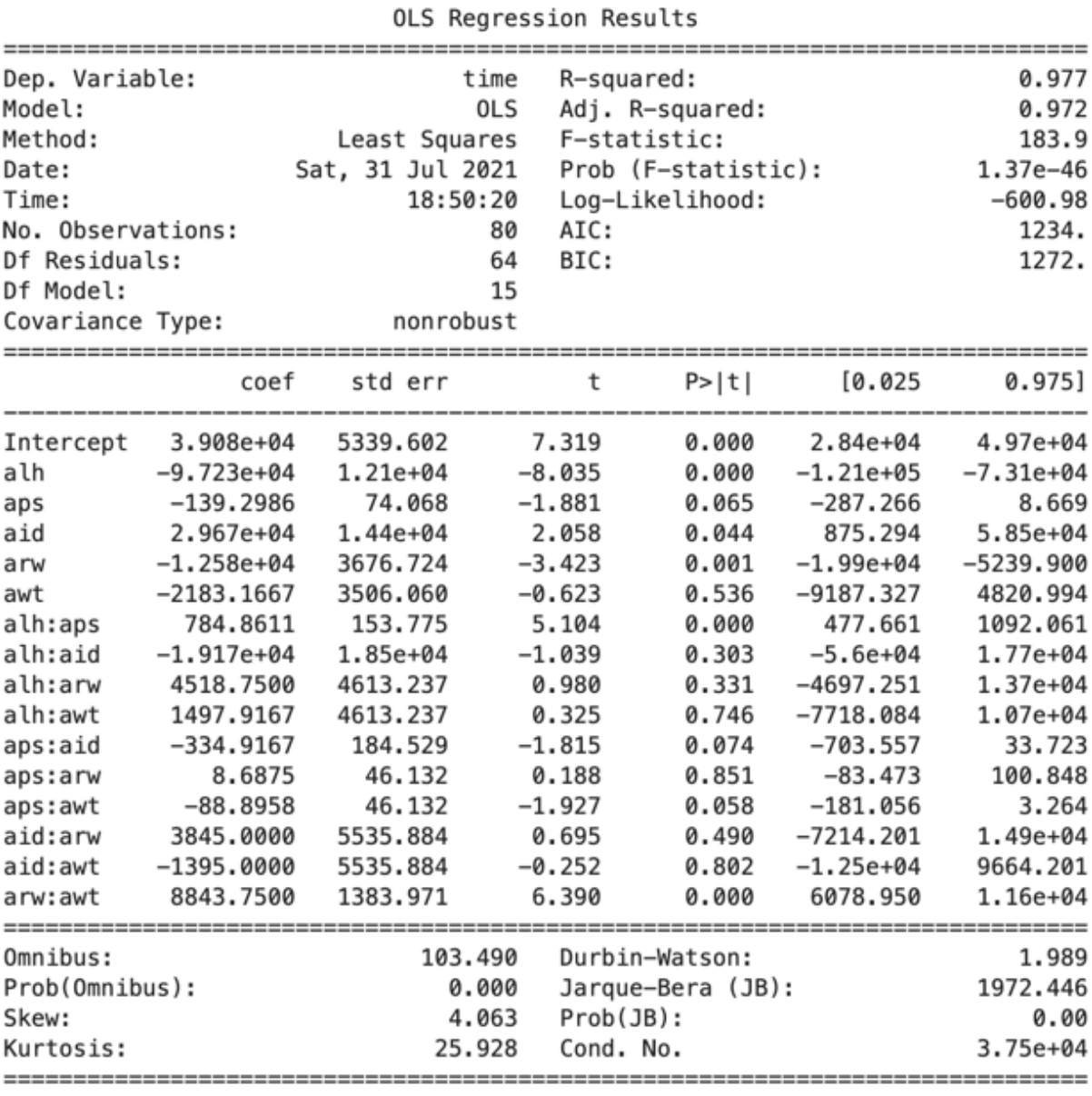

OLS Regression Results

Dep. Variable:	time	R-squared:	0.977
Model:	OLS	Adj. R-squared:	0.972
Method:	Least Squares	F-statistic:	183.9
Date:	Sat, 31 Jul 2021	Prob (F-statistic):	1.37e-46
Time:	18:50:20	Log-Likelihood:	-600.98
No. Observations:	80	AIC:	1234.
Df Residuals:	64	BIC:	1272.
Df Model:	15		
Covariance Type:	nonrobust		

	coef	std err	t	P>|t|	[0.025	0.975]
Intercept	3.908e+04	5339.602	7.319	0.000	2.84e+04	4.97e+04
alh	-9.723e+04	1.21e+04	-8.035	0.000	-1.21e+05	-7.31e+04
aps	-139.2986	74.068	-1.881	0.065	-287.266	8.669
aid	2.967e+04	1.44e+04	2.058	0.044	875.294	5.85e+04
arw	-1.258e+04	3676.724	-3.423	0.001	-1.99e+04	-5239.900
awt	-2183.1667	3506.060	-0.623	0.536	-9187.327	4820.994
alh:aps	784.8611	153.775	5.104	0.000	477.661	1092.061
alh:aid	-1.917e+04	1.85e+04	-1.039	0.303	-5.6e+04	1.77e+04
alh:arw	4518.7500	4613.237	0.980	0.331	-4697.251	1.37e+04
alh:awt	1497.9167	4613.237	0.325	0.746	-7718.084	1.07e+04
aps:aid	-334.9167	184.529	-1.815	0.074	-703.557	33.723
aps:arw	8.6875	46.132	0.188	0.851	-83.473	100.848
aps:awt	-88.8958	46.132	-1.927	0.058	-181.056	3.264
aid:arw	3845.0000	5535.884	0.695	0.490	-7214.201	1.49e+04
aid:awt	-1395.0000	5535.884	-0.252	0.802	-1.25e+04	9664.201
arw:awt	8843.7500	1383.971	6.390	0.000	6078.950	1.16e+04

Omnibus:	103.490	Durbin-Watson:	1.989
Prob(Omnibus):	0.000	Jarque-Bera (JB):	1972.446
Skew:	4.063	Prob(JB):	0.00
Kurtosis:	25.928	Cond. No.	3.75e+04

Figure 54: Analysis C - SWX1 Time OLS

The variables that are not significant factors in the cost of the model include:

- aps:arw with p-value 0.851224
- aid:awt with p-value 0.800387
- alh:awt with p-value 0.742837
- awt with p-value 0.494038
- aid:arw with p-value 0.478725
- alh:arw with p-value 0.316918
- alh:aid with p-value 0.288586
- aps:aid with p-value 0.0661897

The reduce model for SWX1 Time is in Figure 55.

Based on these results (Figure 55), the following linear equation for SWX1 time was developed:

$$Time = 40760.716666663415 + -96855.41666666564 * X1 + -171.22354749789565 * X2 + 4256.00000000009 * X3 + -10004.306297709902 * X4 + 784.8611111111159 * X1 * X2 + -118.74173027989448 * X2 * X5 + 8599.556297709905 * X4 * X5$$

The values utilized for the ϵ-constraint methodology for Analysis B were:

Minimize:

- $f1 = -7.512756311165274 + 15.594282277667375 * X1 + 0.1501013849966114 * X2 + 3.3568541135900944 * X5 + -0.1873958333333725 * X1 * X2 + 14.97406461978116 * X1 * X3 +$

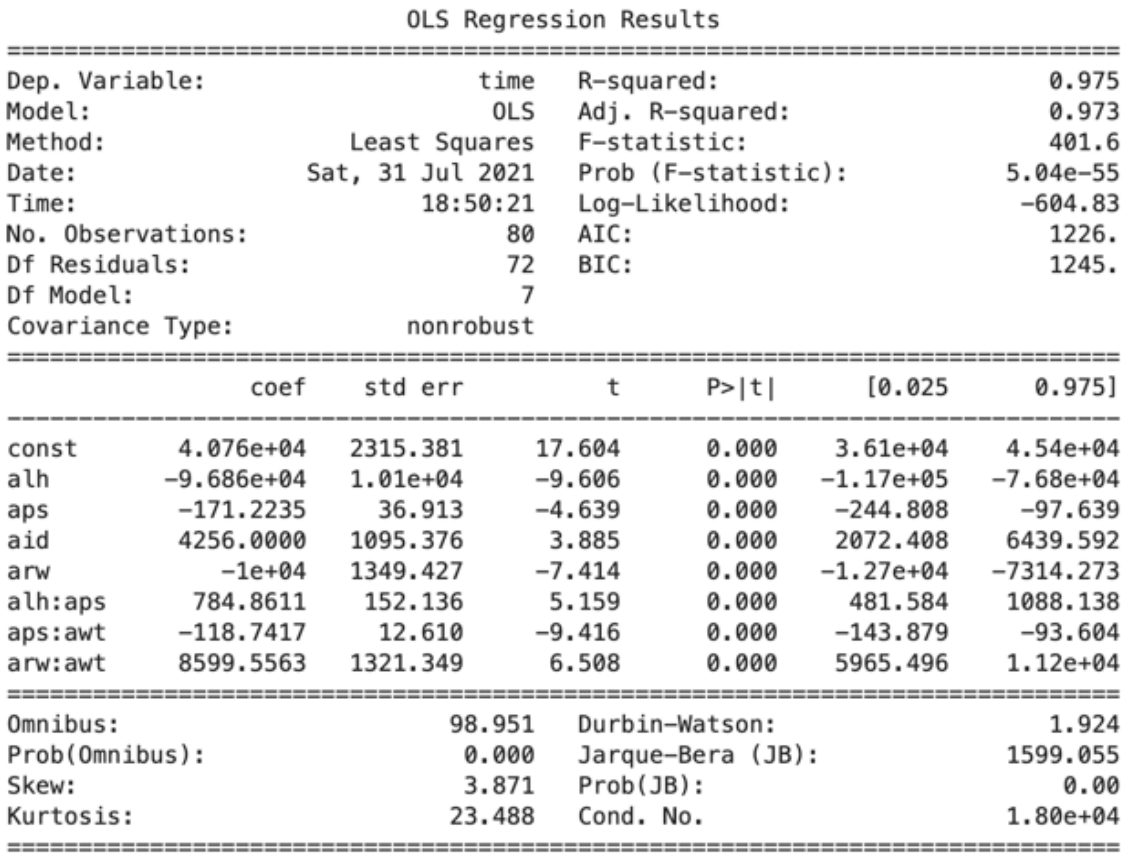

OLS Regression Results

Dep. Variable:	time	R-squared:	0.975
Model:	OLS	Adj. R-squared:	0.973
Method:	Least Squares	F-statistic:	401.6
Date:	Sat, 31 Jul 2021	Prob (F-statistic):	5.04e-55
Time:	18:50:21	Log-Likelihood:	-604.83
No. Observations:	80	AIC:	1226.
Df Residuals:	72	BIC:	1245.
Df Model:	7		
Covariance Type:	nonrobust		

	coef	std err	t	P>|t|	[0.025	0.975]
const	4.076e+04	2315.381	17.604	0.000	3.61e+04	4.54e+04
alh	-9.686e+04	1.01e+04	-9.606	0.000	-1.17e+05	-7.68e+04
aps	-171.2235	36.913	-4.639	0.000	-244.808	-97.639
aid	4256.0000	1095.376	3.885	0.000	2072.408	6439.592
arw	-1e+04	1349.427	-7.414	0.000	-1.27e+04	-7314.273
alh:aps	784.8611	152.136	5.159	0.000	481.584	1088.138
aps:awt	-118.7417	12.610	-9.416	0.000	-143.879	-93.604
arw:awt	8599.5563	1321.349	6.508	0.000	5965.496	1.12e+04

Omnibus:	98.951	Durbin-Watson:	1.924
Prob(Omnibus):	0.000	Jarque-Bera (JB):	1599.055
Skew:	3.871	Prob(JB):	0.00
Kurtosis:	23.488	Cond. No.	1.80e+04

Figure 55: Analysis C - SWX1 Reduced OLS for Time

$$-6.3471031138125085 * X1 * X4 + -0.17544472807322514 * X2 * X3$$
$$+ 0.02025357325229224 * X2 * X4 + -0.07640624999999765 * X2 * X5$$
$$+ 3.2956081485919615 * X3 * X4 + 6.441435526274299 * X3 * X5$$
$$+ -0.6702353647414601 * X4 * X5$$

- $f2 = 40760.716666663415 + -96855.41666666564 * X1 +$
  $-171.22354749789565 * X2 + 4256.00000000009 * X3 +$
  $-10004.306297709902 * X4 + 784.8611111111159 * X1 * X2 +$
  $-118.74173027989448 * X2 * X5 + 8599.556297709905 * X4 * X5$

st:

- $.16 \leq X1 \leq .28$
- $50 \leq X2 \leq 60$
- $.15 \leq X3 \leq .25$
- $.4 \leq X4 \leq .8$
- $.8 \leq X5 \leq 1.2$

When solved, ϵ-contraints methodology produces the following values:

- $(X1, X2, X3, X4, X5) =$
  $\begin{pmatrix} 0.2800000099999376, 72.00000071997307, 0.14999999000059022, \\ 0.39999999000739667, 1.2000000119995191 \end{pmatrix}$
- $f1 = 0.9517842950707984$
- $f2 = 7641.0830096684$

Where:

- • X1 = layer height = .28 mm

- • X2 = print speed = 72 mm/s
- • X3 = infill density = .15
- • X4 = raster width = .4 mm
- • X5 = wall thickness = 1.2 mm
- • f1 = cost = 0.9517842950707984
- • f2 = time = 7641.0830096684 s

The settings in Analysis C match those of Analysis A.

As a last step the proposed setting were printed three (3) times. In a review of the of the quality of the print, it was found to be excellent with a score of 450.

6.3 — Addressing the Research Questions

6.3.1 — Primary Problems Addressed

What parameters should be optimized to increase speed, reduce costs, and achieve satisfactory quality?

In the case of the CR6, the optimized parameters were:

- $(X1, X2, X3, X4, X5) =$

$$\begin{pmatrix} 0.28000000999993935, 60.000000599972694, 0.2500000099939384, \\ 0.8000000096771722, 1.2000000119993277 \end{pmatrix}$$

Where:

- • X1 = layer height = .28 mm
- • X2 = print speed = 60 mm/s
- • X3 = infill density = .25

- • X4 = raster width = .8 mm
- • X5 = wall thickness = 1.2 mm

Both the infill density and wall thickness did not use the expected values. Both were the opposite of the expected. In the case of infill density, this result is more surprising. It is believed that this result is due to the minimal amount of infill in the model. Using Cura, a preview was generated of the optimized print (Figure 56). This figure shows the model at layer 35 of 71. The infill density, represented in orange, is extremely minimal. Additionally, the Cura generated rough estimate of print time shows the infill as 1% of overall print time (Figure 57).

In the case of models with significantly more infill, it is expected that the result would meet expectations.

The optimized parameters for the SWX1 were:

- $(X1, X2, X3, X4, X5) =$

$$\begin{pmatrix} 0.28000000999993796, 72.00000071997286, 0.1499999900005892, \\ 0.39999999000704073, 1.2000000119995038 \end{pmatrix}$$

Where:

- • X1 = layer height = .28 mm
- • X2 = print speed = 72 mm/s
- • X3 = infill density = .15
- • X4 = raster width = .4 mm
- • X5 = wall thickness = 1.2 mm

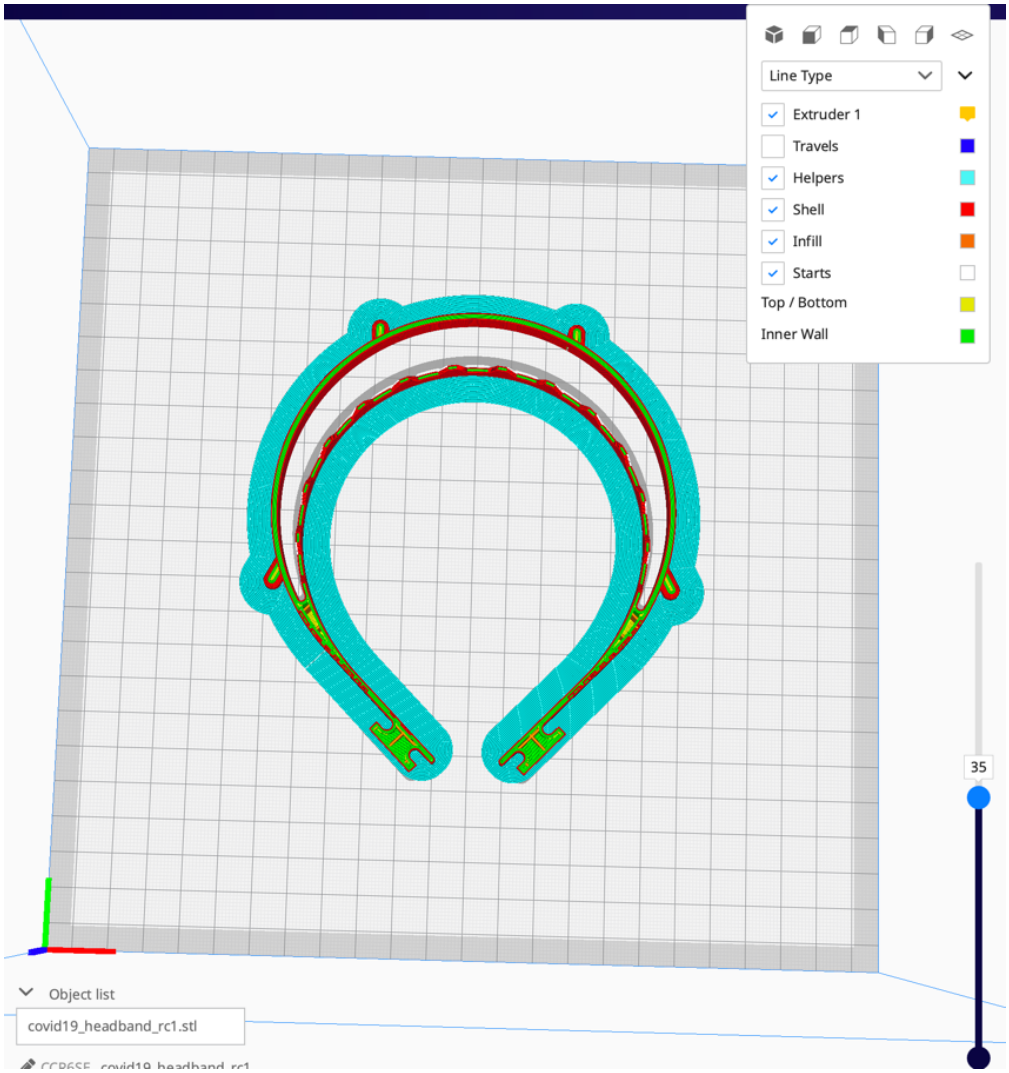

Figure 56: CR6 Cura Preview at 35 of 71 Layers

Figure 57: CR6 Cura Time Estimate

In the case of the SWX1, both the raster width and wall thickness were not as expected. It is believed that these unexpected values can be explained as compromises due to the optimization of cost and time.

What is the contribution of each parameter to the increase speed, reduce costs, and achieve satisfactory quality?

In the case of both printers, layer height and print speed are shown to have an impact on cost and time. The linear equation for each printer in each analysis, gives an indication of the contribution of each variable for cost and time.

CR6 Analysis A

$$Cost$$

$$= 0.30061301677651686 + -0.0014979526099359666 * X2 + 0.3541048685686145 * X4 + 0.24600811428103486 * X5 + 0.003193676289093103 * X1 * X2 + -0.681545835829839 * X1 * X3 + 0.15813870197108404 * X1 * X4 + -0.15310216338152616 * X1 * X5 + 0.008101719131677326 * X2 * X3 + -0.0026250000000000544 * X2 * X4 + 0.0011250000000000322 * X2 * X5 + 0.3961480849887108 * X3 * X4 + -0.4897531916854896 * X3 * X5 + -0.2593750000000006 * X4 * X5$$

$$Time$$

$$= 39415.87499999855 + -79138.51046393832 * X1 + -128.19137670175314 * X2 + -8860.849838411767 * X5 + -46255.95567867106 * X1 * X3 + 12299.502666120085 * X1 * X4 + 29085.416666666522 * X1 * X5 + 434.58559556786804 * X2 * X3 + -57.717904019688284 * X2 * X4 + -11377.20914127423 * X3 * X5$$

SWX1 Analysis A

$$Cost$$

$$= 0.1900000000000014 + 0.24999999999999423 * X1 + 0.3999999999999986 * X3$$

$$+ 0.37499999999999967 * X4 + 0.320833333333332 * X5 + -0.20833333333332477$$

$$* X1 * X5 + -0.25000000000000133 * X3 * X5 + -0.3124999999999999 * X4 * X5$$

$$Time$$

$$= 41311.84166666333 + -99242.9166666657 * X1 + -181.67424724344346 * X2$$

$$+ 4263.500000000091 * X3 + -9967.93702290074 * X4 + 815.0694444444525 * X1$$

$$* X2 + -116.4993638676806 * X2 * X5 + 8583.812022900747 * X4 * X5$$

CR6 Analysis B

$$Cost$$

$$= 0.43619166666666676 + -0.3303957650272835 * X1 + -0.0018884142076504296$$

$$* X2 + 0.3583517213114778 * X4 + 0.2018153688524602 * X5$$

$$+ 0.00379166666666636 * X1 * X2 + -0.8282295081967748 * X1 * X3$$

$$+ 0.19062500000000449 * X1 * X4 + 0.009283737704918856 * X2 * X3$$

$$+ -0.0030125000000000516 * X2 * X4 + 0.00113750000000004 * X2 * X5$$

$$+ 0.4151163934426205 * X3 * X4 + -0.5256393442622931 * X3 * X5$$

$$+ -0.25406250000000025 * X4 * X5$$

$$Time$$

$$= 39415.87499999855 + -79138.51046393832 * X1 + -128.19137670175314 * X2$$

$$+ -8860.849838411767 * X5 + -46255.95567867106 * X1 * X3 + 12299.502666120085$$

$$* X1 * X4 + 29085.416666666522 * X1 * X5 + 434.58559556786804 * X2 * X3$$

$$+ -57.717904019688284 * X2 * X4 + -11377.20914127423 * X3 * X5$$

SWX1 Analysis B

$$Cost$$

$$= 0.24752499999999666 + 0.08528056112224291 * X1 + 0.4780490981963954 * X3$$

$$+ 0.3561250000000017 * X4 + 0.32446325985304236 * X5 + 0.001151052104208572$$

$$* X1 * X2 + -0.21041666666666942 * X1 * X5 + -0.0010537742150968782 * X2 * X3$$

$$+ -0.0002772211088844477 * X2 * X5 + -0.2500000000000011 * X3 * X5$$

$$+ -0.29625000000000157 * X4 * X5$$

$$Time$$

$$= 41311.84166666333 + -99242.9166666657 * X1 + -181.67424724344346 * X2$$

$$+ 4263.500000000091 * X3 + -9967.93702290074 * X4 + 815.0694444444525 * X1$$

$$* X2 + -116.4993638676806 * X2 * X5 + 8583.812022900747 * X4 * X5$$

CR6 Analysis C

$$Cost$$

$$= 0.022179997348888314 + 0.9805362539766707 * X4 + 0.4210264448568395 * X5$$

$$+ 0.055398409331918294 * X2 * X3 + -0.016249522799575436 * X2 * X4$$

$$+ -2.5398197242841984 * X3 * X5$$

$$Time$$

$$= 39383.12499999856 + -78995.06592013844 * X1 + -129.4773731249602 * X2$$

$$+ -8759.911472760796 * X5 + -45752.146814405125 * X1 * X3$$

$$+ 12225.825471698428 * X1 * X4 + 28897.916666666522 * X1 * X5$$

$$+ 440.7227146814413 * X2 * X3 + -57.37028301886791 * X2 * X4$$

$$+ -11750.650969529073 * X3 * X5$$

SWX1 Analysis C

$$Cost$$

$$= -7.512756311165274 + 15.594282277667375 * X1 + 0.1501013849966114 * X2$$

$$+ 3.3568541135900944 * X5 + -0.1873958333333725 * X1 * X2 + 14.97406461978116$$

$$* X1 * X3 + -6.3471031138125085 * X1 * X4 + -0.17544472807322514 * X2 * X3$$

$$+ 0.02025357325229224 * X2 * X4 + -0.07640624999999765 * X2 * X5$$

$$+ 3.2956081485919615 * X3 * X4 + 6.441435526274299 * X3 * X5$$

$$+ -0.6702353647414601 * X4 * X5$$

$$Time$$

$$= 40760.716666663415 + -96855.41666666564 * X1 + -171.22354749789565 * X2$$

$$+ 4256.00000000009 * X3 + -10004.306297709902 * X4 + 784.8611111111159 * X1$$

$$* X2 + -118.74173027989448 * X2 * X5 + 8599.556297709905 * X4 * X5$$

Where, in all cases:

- • X1 = layer height
- • X2 = print speed
- • X3 = infill density

- • X4 = raster width
- • X5 = wall thickness

6.3.2 — Secondary Problems Addressed

Because of the subjective nature of quality inspection, what is an acceptable methodology to quantify the quality of a 3D printed model?

Using the quality assessment methodology outlined in 4.3 — The Inspection Score and 4.4 — Inspection Measurements sections, a quick and easy quality scoring method was obtained.

Accessibility of the optimization methodologies remains the domain of engineers. Can the optimization method utilized in this study be made accessible to makers?

Utilizing open-source tools such as python and jupyter notebooks, it is possible to create a set of tools to allow for makers to run additional experiments. This study demonstrates two (2) areas that could be improved. These areas are:

- Automation of the addition of the linear equation to the ϵ-constraints function Figure 58.
- Reduction of the number of experimental runs

In the case of automation, in each case, the linear equation for cost and time developed must be manually cut and paste into the ϵ-constraints function in the jupyter notebook Figure 58. In the initial analysis, I made the mistake of not updating the equations. By automating this process, it can eliminate future mistakes.

Figure 58: Section Requiring Cut and Paste to add Linear equation to python function

The experiments needed to complete this analysis are resource intensive in the case of both the time and filament needed to complete these experiments and analysis. Work needs to be done to reduce the resource usage.

Does the additive nature of FDM allow for the quick elimination of print parameters?

Based on the quality results, the quality of the models varied greater than expected. There does not seem to be a correlation with a particular print parameter and the quality score.

It was found that there was a difference between the printers. The SWX1 was found to have a greater difference in the various quality scores.

7 — CHAPTER SEVEN - CONCLUSIONS AND RECOMMENDATIONS

7.1 — CONCLUSIONS

This research demonstrates the use of design of experiments (DOE) and ϵ-constraints methodology to optimize multiple parameters in 3DP. The methods utilized in this research use open-source technologies to accomplish the optimization. The methods are straight forward and offer a blueprint for future optimization experiments and research for makers.

The quality scoring identified in this study offer a standardized method to assess the quality of 3DP models. This method is particularly important for use in settings outside of the laboratory. It follows the methodologies currently employed by the maker community.

As outlined in the 4.4 — Inspection Measurements section, a mold was used to assist with the assessment of functionality. It was found during this investigation that the mold was not particularly informative. A better indicator of quality was the three (3) measurements utilized.

An interesting observation of this research is the fact that Analysis A, B, and C all identify the same settings as optimal. When reviewing the various value changes due to the inclusion of power usage and rework cost/time, the results are particularly surprising.

In the case of the CR6, the optimized parameters were:

- $(X1, X2, X3, X4, X5) =$

$$\begin{pmatrix} 0.28000000999993935, 60.000000599972694, 0.2500000099939384, \\ 0.8000000096771722, 1.2000000119993277 \end{pmatrix}$$

Where:

- • X1 = layer height = .28 mm
- • X2 = print speed = 60 mm/s
- • X3 = infill density = .25
- • X4 = raster width = .8 mm
- • X5 = wall thickness = 1.2 mm

he optimized parameters for the SWX1 were:

- $(X1, X2, X3, X4, X5) =$

$$\begin{pmatrix} 0.28000000999993796, 72.00000071997286, 0.1499999900005892, \\ 0.39999999000704073, 1.2000000119995038 \end{pmatrix}$$

Where:

- • X1 = layer height = .28 mm
- • X2 = print speed = 72 mm/s
- • X3 = infill density = .15
- • X4 = raster width = .4 mm
- • X5 = wall thickness = 1.2 mm

In the case of the CR6, infill density did not impact cost and time. This contrasts with the SWX1 where infill density was optimized. It would be expected that both printers would optimize the same parameters.

7.2 — RECOMMENDATIONS

Future research should review the following items:

- Future research should utilize a variety of model geometries. In the case of infill density, models should be selected with greater infill percentages.
- The quality scoring methodology should be tested by other researchers. Effort should be made to use the method in other settings.
- In future studies, various inexpensive 3DP printers should be tested.
- With the use of varied printers, the make and model should be included as a variable.

LIST OF REFERENCES

Akçay, H., & Anagün, A. S. (2013). Multi response optimization application on a manufacturing factory. *Mathematical and Computational Applications*, *18*(3), 531-538.

Baldwin, R., & Mauro, B. W. D. (2020). Economics in the Time of COVID-19.

Baumann, F. W., Schuermann, M., Odefey, U., & Pfeil, M. (2017). *From gcode to stl: Reconstruct models from 3d printing as a service*.

Bhushan, B., & Caspers, M. (2017). An overview of additive manufacturing (3D printing) for microfabrication. *Microsystem Technologies*, *23*(4), 1117-1124.

Bishop, E. G., & Leigh, S. J. (2020). Using large-scale additive manufacturing as a bridge manufacturing process in response to shortages in personal protective equipment during the COVID-19 outbreak. *International journal of bioprinting*, *6*(4).

BLS. (2020). State Employment and Unemployment Summary.

Bose, S., Ke, D., Sahasrabudhe, H., & Bandyopadhyay, A. (2018). Additive manufacturing of biomaterials. *Progress in materials science*, *93*, 45-111.

Bose, S., Vahabzadeh, S., & Bandyopadhyay, A. (2013). Bone tissue engineering using 3D printing. *Materials today*, *16*(12), 496-504.

Bown, C. P. (2020). COVID-19: China's exports of medical supplies provide a ray of hope. *PIIE Trade and Investment Policy Watch, March*, *26*.

Bradshaw, S., Bowyer, A., & Haufe, P. (2010b). The intellectual property implications of low-cost 3D printing. *ScriptEd*, *7*, 5.

Bradshaw, S., Bowyer, A., & Haufe, P. (2010b). The intellectual property implications of low-cost 3D printing. *ScriptEd*, *7*, 5.

Browder, R. E., Aldrich, H. E., & Bradley, S. W. (2019). The emergence of the maker movement: Implications for entrepreneurship research. *Journal of Business Venturing*.

Cascella, M., Rajnik, M., Cuomo, A., & Dulebohn…, S. C. (2020). Features, evaluation and treatment coronavirus (COVID-19). *Statpearls …*.

CDC. (2020). Symptoms of Coronavirus. https://www.cdc.gov/coronavirus/2019-nCoV/index.html.

Chang, D., Xu, H., Rebaza, A., Sharma, L., & Cruz, C. S. D. (2020). Protecting health-care workers from subclinical coronavirus infection. *The Lancet Respiratory Medicine*, *8*(3), e13.

Christensen, R. (1996). *Analysis of variance, design, and regression: applied statistical methods*. CRC Press.

Clark, P. A. (2020). 'This Is Truly a Last Resort.' Makers Are 3D Printing Ventilator Parts and Sewing Masks Amid a Critical Shortage in Medical Supplies. https://time.com/5811091/makers-3d-printing-coronavirus/.

Cox, J. L., & Koepsell, S. A. (2020). 3D-printing to address COVID-19 testing supply shortages. *Laboratory medicine*, *51*(4), e45-e46.

Dey, A., & Yodo, N. (2019). A systematic survey of FDM process parameter optimization and their influence on part characteristics. *Journal of Manufacturing and Materials Processing*, *3*, 64.

Dordlofva, C., Lindwall, A., T\"orlind, P., & others. (2016). Opportunities and challenges for additive manufacturing in space applications. *DS 85-1: Proceedings of*

NordDesign 2016, Volume 1, Trondheim, Norway, 10th-12th August 2016, 401-410.

Drury, C. G., & Watson, J. (2002). Good practices in visual inspection. *Human factors in aviation maintenance-phase nine, progress report, FAA/Human Factors in Aviation Maintenance.@ URL: http://hfskyway. faa. gov*.

Durakovic, B. (2018). Design for additive manufacturing: Benefits, trends and challenges. *Periodicals of Engineering and Natural Sciences*, *6*(2), 179-191.

Emanuel, E. J., Persad, G., Upshur, R., Thome, B., Parker, M., Glickman, A. et al. (2020). Fair allocation of scarce medical resources in the time of Covid-19.

FAA. (1997). VISUAL INSPECTION FOR AIRCRAFT. *FAA AC 43-204*.

Feldman, A. (2020). Inside A Silicon Valley Unicorn's Urgent Dash To 3D-Print Face Shields And Test Swabs To Battle COVID-19. https://www.forbes.com/sites/amyfeldman/2020/03/25/inside-a-silicon-valley-unicorns-urgent-dash-to-3d-print-face-shields-and-test-swabs-to-battle-covid-19/#5f68b19c4370.

Fisher, R. A. (1992). Statistical methods for research workers Breakthroughs in statistics. In (pp. 66-70). Springer.

Forest, C. R., Moore, R. A., Jariwala, A. S., & Fasse…, B. B. (2014). The Invention Studio: A University Maker Space and Culture. *Advances in Engineering …*.

Gibson, I., Rosen, D., & Stucker, B. (2010). *Additive Manufacturing Technologies – Rapid Prototyping to Direct Digital Manufacturing* (5).

Gibson, I., Rosen, D. W., & Stucker, B. (2014). *Additive manufacturing technologies* (17). Springer.

Gu, P., Zhang, X., Zeng, Y., & Ferguson, B. (2001). Quality analysis and optimization of solid ground curing process. *Journal of manufacturing systems*, *20*(4), 250.

Gurrala, P. K., & Regalla, S. P. (2012). *Optimization of support material and build time in fused deposition modeling (FDM)*.

Halassi, S., Semeijn, J., & Kiratli, N. (2019). From consumer to prosumer: a supply chain revolution in 3D printing. *International Journal of Physical Distribution & Logistics Management*.

Holm, E. J. V. (2015). Makerspaces and contributions to entrepreneurship. *Procedia-Social and Behavioral Sciences*.

Holman, W. (2015). Makerspace: Towards a new civic infrastructure. *Places Journal*.

Ingole, D. S., Deshmukh, T. R., Kuthe, A. M., & Ashtankar, K. M. (2011). Build orientation analysis for minimum cost determination in FDM. *Proceedings of the Institution of Mechanical Engineers, Part B: Journal of Engineering Manufacture*, *225*(10), 1925-1938.

Johnson, G. A., & French, J. J. (2018). Evaluation of infill effect on mechanical properties of consumer 3D printing materials. *Advances in Technology Innovation*, *3*(4), 179.

Kačergis, L., Mitkus, R., & Sinapius, M. (2019). Influence of fused deposition modeling process parameters on the transformation of 4D printed morphing structures. *Smart Materials and Structures*, *28*(10), 105042.

Klotz, L. E., Horman, M., & Bodenschatz, M. (2007). A lean modeling protocol for evaluating green project delivery. *Lean Construction Journal*, *3*(1).

Kluytmans-van den Bergh, M. F. Q., Buiting, A. G. M., Pas, S. D., Bentvelsen, R. G., van den Bijllaardt, W., van Oudheusden, A. J. G. et al. (2020). Prevalence and clinical presentation of health care workers with symptoms of coronavirus disease 2019 in 2 Dutch hospitals during an early phase of the pandemic. *JAMA network open*, *3*(5), e209673-e209673.

Kluyver, T., Ragan-Kelley, B., Pérez, F., Granger, B. E., Bussonnier, M., Frederic, J. et al. (2016). *Jupyter Notebooks-a publishing format for reproducible computational workflows.*

Kruth, J.-P., Mercelis, P., Van Vaerenbergh, J., Froyen, L., & Rombouts, M. (2005). Binding mechanisms in selective laser sintering and selective laser melting. *Rapid prototyping journal*.

Kumar, L. J., & Nair, C. G. K. (2017). Current trends of additive manufacturing in the aerospace industry Advances in 3d printing \& additive manufacturing technologies. In (pp. 39-54). Springer.

Lai, X., Wang, M., Qin, C., Tan, L., Ran, L., Chen, D. et al. (2020). Coronavirus disease 2019 (COVID-2019) infection among health care workers and implications for prevention measures in a tertiary hospital in Wuhan, China. *JAMA Network Open*, *3*(5), e209666-e209666.

Larson, M. G. (2008). Analysis of variance. *Circulation*, *117*(1), 115-121.

Li, Y., Linke, B. S., Voet, H., Falk, B., Schmitt, R., & Lam, M. (2017). Cost, sustainability and surface roughness quality–A comprehensive analysis of products made with personal 3D printers. *CIRP Journal of Manufacturing Science and Technology*, *16*, 1-11.

LIANG, Q. I. N. G.-J. I. E., & LI, X. I. A. O.-D. O. N. G. (2017). Application of FDM additive manufacturing technology in making medical surgical model. *DEStech Transactions on Engineering and Technology Research*, ecame).

Livingston, E., Desai, A., & Berkwits, M. (2020). Sourcing personal protective equipment during the COVID-19 pandemic. *Jama*, *323*(19), 1912-1914.

Ludwig, T., Stickel, O., Boden, A., & Pipek, V. (2014). *Towards sociable technologies: an empirical study on designing appropriation infrastructures for 3D printing*.

McCue, T. J. (2020). 3D Printer Groups Continue Working Round The Clock To Help 2020 PPE Shortage. https://www.forbes.com/sites/tjmccue/2020/03/30/protect-healthcare-workers-3d-printer-groups-race-to-help-2020-ppe-shortage-coronavirus-covid19/#76ccdb494ee2.

Mehta, P. S., Ocampo, J. S., Tovar, A., & Chaudhari, P. (2016). Bio-inspired design of lightweight and protective structures.

Melchore, J. A. (2011). Sound practices for consistent human visual inspection. *Aaps Pharmscitech*, *12*(1), 215-221.

Merriam-Webster. (n.d.). Optimization. In Merriam-Webster.com dictionary. Retrieved 12/5/2020, https://www.merriam-webster.com/dictionary/optimization.

Mohamed, O. A., Masood, S. H., & Bhowmik, J. L. (2016a). Mathematical modeling and FDM process parameters optimization using response surface methodology based on Q-optimal design. *Applied Mathematical Modelling*.

Mohamed, O. A., Masood, S. H., & Bhowmik, J. L. (2016b). Parametric analysis of the build cost for FDM additive processed parts using response surface methodology. *Ref. Modul. Mater. Sci. Mater. Eng*.

Mohamed, O. A., Masood, S. H., & Bhowmik, J. L. (2018). Analysis of wear behavior of additively manufactured PC-ABS parts. *Materials Letters*.

Montgomery, D. C. (2017). *Design and analysis of experiments*. John wiley & sons.

MP, G., Shinde, Y., Madaki, R., & Nadaf, S. (2019). IoT based 3D Printer.

Mwema, F. M., Akinlabi, E. T., & Fatoba, O. S. (2020). Visual assessment of 3D printed elements: A practical quality assessment for home-made FDM products. *Materials Today: Proceedings*.

Nasir, H., Ahmed, H., Haas, C., & Goodrum, P. M. (2014). An analysis of construction productivity differences between Canada and the United States. *Construction Management and Economics*, *32*(6), 595-607.

Natrella, M. (2010). NIST/SEMATECH e-Handbook of Statistical Methods{Natrella, 2010, #87438}. *Nist/Sematech*, *49*.

Ngo, T. D., Kashani, A., Imbalzano, G., Nguyen, K. T. Q., & Hui, D. (2018). Additive manufacturing (3D printing): A review of materials, methods, applications and challenges. *Composites Part B: Engineering*, *143*, 172-196.

Nitti, D. F. (2019). 3D printing, challenges for the future of intellectual property rights. *tesi.luiss.it*.

Novak, J. I., & Loy, J. (2020a). A critical review of initial 3D printed products responding to COVID-19 health and supply chain challenges. *Emerald Open Research*, *2*, 24.

Novak, J. I., & Loy, J. (2020b). A quantitative analysis of 3D printed face shields and masks during COVID-19. *Emerald Open Research*, *2*, 42.

Novakova-Marcincinova, L., & Kuric, I. (2012). Basic and advanced materials for fused deposition modeling rapid prototyping technology. *Manuf. and Ind. Eng*, *11*(1), 24-27.

Papavlasopoulou, S., Giannakos, M. N., & Jaccheri, L. (2017). Empirical studies on the Maker Movement, a promising approach to learning: A literature review. *Entertainment Computing*, *18*, 57-78.

Patil, P., Singh, D., Raykar, S. J., & Bhamu, J. (2021). Multi-objective optimization of process parameters of Fused Deposition Modeling (FDM) for printing Polylactic Acid (PLA) polymer components. *Materials Today: Proceedings*.

Paul, S. K., & Chowdhury, P. (2020). A production recovery plan in manufacturing supply chains for a high-demand item during COVID-19. *International Journal of Physical Distribution & Logistics Management*.

Pohlman, J. T., & Leitner, D. W. (2003). A comparison of ordinary least squares and logistic regression.

Popescu, D., Zapciu, A., Amza, C., Baciu, F., & Marinescu, R. (2018). FDM process parameters influence over the mechanical properties of polymer specimens: A review. *Polymer Testing*.

Research, P. (2020). Prusa Face Shield. https://www.prusaprinters.org/prints/25857-prusa-face-shield.

Qureshi, A. J., Mahmood, S., & Wong…, W. L. E. (2015). Design for Scalability and Strength Optimisation for components created through FDM process. *DS 80-6 Proceedings …*.

Ramananantoandro, T., Larricq, P., & Eterradossi, O. (2014). Relationships between 3D roughness parameters and visuotactile perception of surfaces of maritime pinewood and MDF. *Holzforschung*, *68*(1), 93-101.

Rayna, T., Striukova, L., & Darlington, J. (2015). Co-creation and user innovation: The role of online 3D printing platforms. *Journal of Engineering and Technology Management*, *37*, 90-102.

Rio-Chanona, R. M. D., Mealy, P., & Pichler…, A. (2020). Supply and demand shocks in the COVID-19 pandemic: An industry and occupation perspective. *arXiv preprint arXiv …*.

Romero, L., Guerrero, A., Espinosa, M. M., Jimenez, M., Dominguez, I. A., & Dominguez, M. (2014). *Additive manufacturing with RepRap methodology: current situation and future prospects*.

Salmi, M., Akmal, J. S., Pei, E., Wolff, J., Jaribion, A., & Khajavi, S. H. (2020). 3D printing in COVID-19: productivity estimation of the most promising open source solutions in emergency situations. *Applied Sciences*, *10*(11), 4004.

Salvendy, G. (2001). *Handbook of Industrial Engineering*. John Wiley \& Sons.

Shi, Y., Yu, X., Zhao, H., Wang, H., Zhao, R., & Sheng, J. (2020). Host susceptibility to severe COVID-19 and establishment of a host risk score: findings of 487 cases outside Wuhan. *Critical Care*, *24*(1), 1-4.

Singhal, T. (2020). A review of coronavirus disease-2019 (COVID-19). *The Indian Journal of Pediatrics*, 1-6.

Šljivic, M., Pavlovic, A., Kraišnik, M., & Ilić, J. (2019). *Comparing the accuracy of 3D slicer software in printed enduse parts*.

Šljivic, M., Pavlovic, A., & Kraišnik…, M. (2019). Comparing the accuracy of 3D slicer software in printed enduse parts. *IOP Conference Series …*.

Sohrabi, C., Alsafi, Z., O'Neill, N., Khan, M., Kerwan, A., Al-Jabir, A. et al. (2020). World Health Organization declares global emergency: A review of the 2019 novel coronavirus (COVID-19). *International Journal of Surgery*.

Solomon, I. J., Sevvel, P., & Gunasekaran, J. (2020). A review on the various processing parameters in FDM. *Materials Today: Proceedings*.

Stănciulescu, Ş., Schulze, S., & Wąsowski, A. (2015). *Forked and integrated variants in an open-source firmware project*.

Tamburin, A. (2020). Tennessee colleges mass producing face shields to guard against coronavirus using 3D printers. *Tennessean*.

Taylor, W., Melloy, B., Dharwada, P., Gramopadhye, A., & Toler, J. (2004). The effects of static multiple sources of noise on the visual search component of human inspection. *International journal of industrial ergonomics*, *34*(3), 195-207.

theone8480. (2018). required info on professional settings in cura. https://community.ultimaker.com/topic/21507-required-info-on-professional-settings-in-cura/.

Thompson, M. K., Moroni, G., Vaneker, T., Fadel, G., Campbell, R. I., Gibson, I. et al. (2016). Design for Additive Manufacturing: Trends, opportunities, considerations, and constraints. *CIRP annals*, *65*(2), 737-760.

Tino, R., Moore, R., Antoline, S., Ravi, P., Wake, N., Ionita, C. N. et al. (2020). COVID-19 and the role of 3D printing in medicine. *3D Printing in Medicine*, *6*(1).

Tofail, S. A. M., Koumoulos, E. P., Bandyopadhyay, A., Bose, S., O'Donoghue, L., & Charitidis, C. (2018). Additive manufacturing: scientific and technological challenges, market uptake and opportunities. *Materials Today*, *21*(1), 22-37.

Tranter, J. B., Refalo, P., & Rochman, A. (2017). Towards sustainable injection molding of ABS plastic products. *Journal of Manufacturing Processes*, *29*, 399-406.

Valerga, A. P., Batista, M., Salguero, J., & Girot, F. (2018). Influence of PLA filament conditions on characteristics of FDM parts. *Materials*, *11*(8), 1322.

Vecchione, A., & Woltjer, G. (2020). How Library Maker Spaces Can #FlattentheCurve. https://www.libraryjournal.com/?detailStory=how-library-maker-spaces-can-flatten-the-curve-covid-19-coronavirus.

Warm, J. S., Parasuraman, R., & Matthews, G. (2008). Vigilance requires hard mental work and is stressful. *Human factors*, *50*(3), 433-441.

Wattanasaeng, N., & Ransikarbum, K. (2021). Model and Analysis of Economic-and Risk-Based Objective Optimization Problem for Plant Location within Industrial Estates Using Epsilon-Constraint Algorithms. *Computation*, *9*(4), 46.

Wesemann, C., Pieralli, S., Fretwurst, T., Nold, J., & Nelson…, K. (2020). 3-d printed protective equipment during covid-19 pandemic. *Materials*.

Westervelt, E. (2020). Can The U.S. Crowdsource Its Way Out Of A Mask Shortage? No, But It Still Helps. https://www.npr.org/2020/03/25/820795727/can-the-u-s-crowdsource-its-way-out-of-a-mask-shortage-no-but-it-still-helps.

WHO. (2020). WHO Coronavirus Disease (COVID-19) Dashboard. https://covid19.who.int/table.

Wohlers, T., & Gornet, T. (2014). History of additive manufacturing. *Wohlers report*, *24*(2014), 118.

Wu, P., Wang, J., & Wang, X. (2016). A critical review of the use of 3-D printing in the construction industry. *Automation in Construction*, *68*, 21-31.

Yin, D., Liu, Y., Padmanabhan, A., Terstriep, J., Rush, J., & Wang, S. (2017). *A CyberGIS-Jupyter Framework for Geospatial Analytics at Scale*.

Yoon, H.-S., Lee, J.-Y., Kim, H.-S., Kim, M.-S., Kim, E.-S., Shin, Y.-J. et al. (2014). A comparison of energy consumption in bulk forming, subtractive, and additive processes: Review and case study. *International Journal of Precision Engineering and Manufacturing-Green Technology*, *1*(3), 261-279.

Zaharin, H. A., Rani, A. M. A., & Ginta…, T. L. (2018). Additive manufacturing technology for biomedical components: A review. *IOP Conf. Ser. Mater. Sci …*.

APPENDIX

APPENDIX A - EXPERIMENTAL DATA

RAW RESULTS

Table 13: Raw Results for the CR-6 SE

trial	alh	aps	aid	arw	awt	rep	cost	time
1	0.16	50	0.25	0.4	0.8	1	0.51	18098
2	0.28	50	0.25	0.4	1.2	1	0.51	8741
3	0.16	60	0.25	0.4	1.2	1	0.54	14493
4	0.28	60	0.25	0.4	0.8	1	0.51	10191
5	0.16	50	0.15	0.4	1.2	1	0.54	14914
6	0.28	50	0.15	0.4	0.8	1	0.5	10423
7	0.16	60	0.15	0.4	0.8	1	0.5	16648
8	0.28	60	0.15	0.4	1.2	1	0.54	8534
9	0.16	50	0.25	0.8	1.2	1	0.54	15085
10	0.28	50	0.25	0.8	0.8	1	0.56	10624
11	0.16	60	0.25	0.8	0.8	1	0.56	16840
12	0.28	60	0.25	0.8	1.2	1	0.54	8645
13	0.16	50	0.15	0.8	0.8	1	0.54	17046
14	0.28	50	0.15	0.8	1.2	1	0.54	9012
15	0.16	60	0.15	0.8	1.2	1	0.53	13488

Table 13 Continued

trial	alh	aps	aid	arw	awt	rep	cost	time
16	0.28	60	0.15	0.8	0.8	1	0.54	9574
17	0.16	50	0.25	0.4	0.8	2	0.51	18042
18	0.28	50	0.25	0.4	1.2	2	0.51	8743
19	0.16	60	0.25	0.4	1.2	2	0.54	14469
20	0.28	60	0.25	0.4	0.8	2	0.51	10185
21	0.16	50	0.15	0.4	1.2	2	0.54	14873
22	0.28	50	0.15	0.4	0.8	2	0.5	10199
23	0.16	60	0.15	0.4	0.8	2	0.5	16652
24	0.28	60	0.15	0.4	1.2	2	0.54	10149
25	0.16	50	0.25	0.8	1.2	2	0.54	15111
26	0.28	50	0.25	0.8	0.8	2	0.56	10624
27	0.16	60	0.25	0.8	0.8	2	0.56	16837
28	0.28	60	0.25	0.8	1.2	2	0.54	8597
29	0.16	50	0.15	0.8	0.8	2	0.54	16923
30	0.28	50	0.15	0.8	1.2	2	0.53	8932
31	0.16	60	0.15	0.8	1.2	2	0.54	13389
32	0.28	60	0.15	0.8	0.8	2	0.54	9521
33	0.16	50	0.25	0.4	0.8	3	0.51	17930
34	0.28	50	0.25	0.4	1.2	3	0.51	8777

Table 13 Continued

trial	alh	aps	aid	arw	awt	rep	cost	time
35	0.16	60	0.25	0.4	1.2	3	0.54	14478
36	0.28	60	0.25	0.4	0.8	3	0.51	10199
37	0.16	50	0.15	0.4	1.2	3	0.54	15060
38	0.28	50	0.15	0.4	0.8	3	0.5	10345
39	0.16	60	0.15	0.4	0.8	3	0.5	16658
40	0.28	60	0.15	0.4	1.2	3	0.54	8492
41	0.16	50	0.25	0.8	1.2	3	0.54	15108
42	0.28	50	0.25	0.8	0.8	3	0.56	10644
43	0.16	60	0.25	0.8	0.8	3	0.56	16864
44	0.28	60	0.25	0.8	1.2	3	0.54	8587
45	0.16	50	0.15	0.8	0.8	3	0.54	17046
46	0.28	50	0.15	0.8	1.2	3	0.54	12589
47	0.16	60	0.15	0.8	1.2	3	0.53	13465
48	0.28	60	0.15	0.8	0.8	3	0.54	9466
49	0.16	50	0.25	0.4	0.8	4	0.51	18026
50	0.28	50	0.25	0.4	1.2	4	0.51	8733
51	0.16	60	0.25	0.4	1.2	4	0.54	14448
52	0.28	60	0.25	0.4	0.8	4	0.51	10118
53	0.16	50	0.15	0.4	1.2	4	0.54	15063

Table 13 Continued

trial	alh	aps	aid	arw	awt	rep	cost	time
54	0.28	50	0.15	0.4	0.8	4	0.5	10421
55	0.16	60	0.15	0.4	0.8	4	0.5	16653
56	0.28	60	0.15	0.4	1.2	4	0.54	8480
57	0.16	50	0.25	0.8	1.2	4	0.54	15115
58	0.28	50	0.25	0.8	0.8	4	0.56	10646
59	0.16	60	0.25	0.8	0.8	4	0.56	16477
60	0.28	60	0.25	0.8	1.2	4	0.54	8580
61	0.16	50	0.15	0.8	0.8	4	0.54	17065
62	0.28	50	0.15	0.8	1.2	4	0.54	8944
63	0.16	60	0.15	0.8	1.2	4	0.53	13478
64	0.28	60	0.15	0.8	0.8	4	0.54	9448
65	0.16	50	0.25	0.4	0.8	5	0.48	17634
66	0.28	50	0.25	0.4	1.2	5	0.51	8736
67	0.16	60	0.25	0.4	1.2	5	0.54	14360
68	0.28	60	0.25	0.4	0.8	5	0.51	10200
69	0.16	50	0.15	0.4	1.2	5	0.54	15026
70	0.28	50	0.15	0.4	0.8	5	0.5	10422
71	0.16	60	0.15	0.4	0.8	5	0.5	16565
72	0.28	60	0.15	0.4	1.2	5	0.54	8538

Table 13 Continued

trial	alh	aps	aid	arw	awt	rep	cost	time
73	0.16	50	0.25	0.8	1.2	5	0.54	15122
74	0.28	50	0.25	0.8	0.8	5	0.56	10579
75	0.16	60	0.25	0.8	0.8	5	0.56	16806
76	0.28	60	0.25	0.8	1.2	5	0.54	8582
77	0.16	50	0.15	0.8	0.8	5	0.54	17058
78	0.28	50	0.15	0.8	1.2	5	0.54	8958
79	0.16	60	0.15	0.8	1.2	5	0.53	13462
80	0.28	60	0.15	0.8	0.8	5	0.54	9459

Table 14: Raw Results for the SWX1

trial	alh	aps	aid	arw	awt	rep	cost	time
1	0.16	60	0.25	0.4	0.8	1	$ 0.560	16916
2	0.28	60	0.25	0.4	1.2	1	$ 0.600	9016
3	0.16	72	0.25	0.4	1.2	1	$ 0.600	12906
4	0.28	72	0.25	0.4	0.8	1	$ 0.570	9711
5	0.16	60	0.15	0.4	1.2	1	$ 0.590	14617
6	0.28	60	0.15	0.4	0.8	1	$ 0.550	10142
7	0.16	72	0.15	0.4	0.8	1	$ 0.540	14495
8	0.28	72	0.15	0.4	1.2	1	$ 0.590	7772
9	0.16	60	0.25	0.8	1.2	1	$ 0.600	18254
10	0.28	60	0.25	0.8	0.8	1	$ 0.620	9482
11	0.16	72	0.25	0.8	0.8	1	$ 0.610	13550
12	0.28	72	0.25	0.8	1.2	1	$ 0.600	9646
13	0.16	60	0.15	0.8	0.8	1	$ 0.590	14675
14	0.28	60	0.15	0.8	1.2	1	$ 0.590	8822
15	0.16	72	0.15	0.8	1.2	1	$ 0.590	12575
16	0.28	72	0.15	0.8	0.8	1	$ 0.600	8046
17	0.16	60	0.25	0.4	0.8	2	$ 0.560	16882
18	0.28	60	0.25	0.4	1.2	2	$ 0.600	8981
19	0.16	72	0.25	0.4	1.2	2	$ 0.600	12872

Table 14 Continued

trial	alh	aps	aid	arw	awt	rep	cost	time
20	0.28	72	0.25	0.4	0.8	2	$ 0.570	9707
21	0.16	60	0.15	0.4	1.2	2	$ 0.590	14566
22	0.28	60	0.15	0.4	0.8	2	$ 0.550	10064
23	0.16	72	0.15	0.4	0.8	2	$ 0.540	14576
24	0.28	72	0.15	0.4	1.2	2	$ 0.590	7783
25	0.16	60	0.25	0.8	1.2	2	$ 0.600	14654
26	0.28	60	0.25	0.8	0.8	2	$ 0.620	9548
27	0.16	72	0.25	0.8	0.8	2	$ 0.610	13554
28	0.28	72	0.25	0.8	1.2	2	$ 0.600	7774
29	0.16	60	0.15	0.8	0.8	2	$ 0.590	14672
30	0.28	60	0.15	0.8	1.2	2	$ 0.590	8833
31	0.16	72	0.15	0.8	1.2	2	$ 0.590	12602
32	0.28	72	0.15	0.8	0.8	2	$ 0.600	8114
33	0.16	60	0.25	0.4	0.8	3	$ 0.560	16897
34	0.28	60	0.25	0.4	1.2	3	$ 0.600	8997
35	0.16	72	0.25	0.4	1.2	3	$ 0.600	12872
36	0.28	72	0.25	0.4	0.8	3	$ 0.570	9705
37	0.16	60	0.15	0.4	1.2	3	$ 0.590	14660
38	0.28	60	0.15	0.4	0.8	3	$ 0.550	10094

Table 14 Continued

trial	alh	aps	aid	arw	awt	rep	cost	time
39	0.16	72	0.15	0.4	0.8	3	$ 0.540	14474
40	0.28	72	0.15	0.4	1.2	3	$ 0.590	7775
41	0.16	60	0.25	0.8	1.2	3	$ 0.600	14576
42	0.28	60	0.25	0.8	0.8	3	$ 0.620	9457
43	0.16	72	0.25	0.8	0.8	3	$ 0.610	13501
44	0.28	72	0.25	0.8	1.2	3	$ 0.600	7747
45	0.16	60	0.15	0.8	0.8	3	$ 0.590	14682
46	0.28	60	0.15	0.8	1.2	3	$ 0.590	8841
47	0.16	72	0.15	0.8	1.2	3	$ 0.590	12605
48	0.28	72	0.15	0.8	0.8	3	$ 0.600	9770
49	0.16	60	0.25	0.4	0.8	4	$ 0.560	16913
50	0.28	60	0.25	0.4	1.2	4	$ 0.600	8975
51	0.16	72	0.25	0.4	1.2	4	$ 0.600	12869
52	0.28	72	0.25	0.4	0.8	4	$ 0.570	9682
53	0.16	60	0.15	0.4	1.2	4	$ 0.590	14664
54	0.28	60	0.15	0.4	0.8	4	$ 0.550	10132
55	0.16	72	0.15	0.4	0.8	4	$ 0.540	14470
56	0.28	72	0.15	0.4	1.2	4	$ 0.590	7778
57	0.16	60	0.25	0.8	1.2	4	$ 0.600	14629

Table 14 Continued

trial	alh	aps	aid	arw	awt	rep	cost	time
58	0.28	60	0.25	0.8	0.8	4	$ 0.620	9459
59	0.16	72	0.25	0.8	0.8	4	$ 0.610	13550
60	0.28	72	0.25	0.8	1.2	4	$ 0.600	7737
61	0.16	60	0.15	0.8	0.8	4	$ 0.590	14748
62	0.28	60	0.15	0.8	1.2	4	$ 0.590	8836
63	0.16	72	0.15	0.8	1.2	4	$ 0.590	12545
64	0.28	72	0.15	0.8	0.8	4	$ 0.600	8094
65	0.16	60	0.25	0.4	0.8	5	$ 0.560	16885
66	0.28	60	0.25	0.4	1.2	5	$ 0.600	8981
67	0.16	72	0.25	0.4	1.2	5	$ 0.600	12788
68	0.28	72	0.25	0.4	0.8	5	$ 0.570	9708
69	0.16	60	0.15	0.4	1.2	5	$ 0.590	14655
70	0.28	60	0.15	0.4	0.8	5	$ 0.550	10023
71	0.16	72	0.15	0.4	0.8	5	$ 0.540	14549
72	0.28	72	0.15	0.4	1.2	5	$ 0.590	7760
73	0.16	60	0.25	0.8	1.2	5	$ 0.600	14579
74	0.28	60	0.25	0.8	0.8	5	$ 0.620	9447
75	0.16	72	0.25	0.8	0.8	5	$ 0.610	13582
76	0.28	72	0.25	0.8	1.2	5	$ 0.600	7777

Table 14 Continued

trial	alh	aps	aid	arw	awt	rep	cost	time
77	0.16	60	0.15	0.8	0.8	5	$ 0.590	14665
78	0.28	60	0.15	0.8	1.2	5	$ 0.590	8846
79	0.16	72	0.15	0.8	1.2	5	$ 0.590	12591
80	0.28	72	0.15	0.8	0.8	5	$ 0.600	8101

Table 15: Cost+Power Results for the CR-6 SE

trial	alh	aps	aid	arw	awt	rep	cost
1	0.16	50	0.25	0.4	0.8	1	0.564
2	0.28	50	0.25	0.4	1.2	1	0.536
3	0.16	60	0.25	0.4	1.2	1	0.583
4	0.28	60	0.25	0.4	0.8	1	0.540
5	0.16	50	0.15	0.4	1.2	1	0.584
6	0.28	50	0.15	0.4	0.8	1	0.531
7	0.16	60	0.15	0.4	0.8	1	0.549
8	0.28	60	0.15	0.4	1.2	1	0.565
9	0.16	50	0.25	0.8	1.2	1	0.585
10	0.28	50	0.25	0.8	0.8	1	0.592
11	0.16	60	0.25	0.8	0.8	1	0.610
12	0.28	60	0.25	0.8	1.2	1	0.566
13	0.16	50	0.15	0.8	0.8	1	0.591
14	0.28	50	0.15	0.8	1.2	1	0.567
15	0.16	60	0.15	0.8	1.2	1	0.570
16	0.28	60	0.15	0.8	0.8	1	0.568
17	0.16	50	0.25	0.4	0.8	2	0.564
18	0.28	50	0.25	0.4	1.2	2	0.536
19	0.16	60	0.25	0.4	1.2	2	0.583

Table 15 Continued

trial	alh	aps	aid	arw	awt	rep	cost
20	0.28	60	0.25	0.4	0.8	2	0.540
21	0.16	50	0.15	0.4	1.2	2	0.584
22	0.28	50	0.15	0.4	0.8	2	0.530
23	0.16	60	0.15	0.4	0.8	2	0.549
24	0.28	60	0.15	0.4	1.2	2	0.570
25	0.16	50	0.25	0.8	1.2	2	0.585
26	0.28	50	0.25	0.8	0.8	2	0.592
27	0.16	60	0.25	0.8	0.8	2	0.610
28	0.28	60	0.25	0.8	1.2	2	0.566
29	0.16	50	0.15	0.8	0.8	2	0.590
30	0.28	50	0.15	0.8	1.2	2	0.557
31	0.16	60	0.15	0.8	1.2	2	0.580
32	0.28	60	0.15	0.8	0.8	2	0.568
33	0.16	50	0.25	0.4	0.8	3	0.563
34	0.28	50	0.25	0.4	1.2	3	0.536
35	0.16	60	0.25	0.4	1.2	3	0.583
36	0.28	60	0.25	0.4	0.8	3	0.540
37	0.16	50	0.15	0.4	1.2	3	0.585
38	0.28	50	0.15	0.4	0.8	3	0.531

Table 15 Continued

trial	alh	aps	aid	arw	awt	rep	cost
39	0.16	60	0.15	0.4	0.8	3	0.550
40	0.28	60	0.15	0.4	1.2	3	0.565
41	0.16	50	0.25	0.8	1.2	3	0.585
42	0.28	50	0.25	0.8	0.8	3	0.592
43	0.16	60	0.25	0.8	0.8	3	0.610
44	0.28	60	0.25	0.8	1.2	3	0.566
45	0.16	50	0.15	0.8	0.8	3	0.591
46	0.28	50	0.15	0.8	1.2	3	0.577
47	0.16	60	0.15	0.8	1.2	3	0.570
48	0.28	60	0.15	0.8	0.8	3	0.568
49	0.16	50	0.25	0.4	0.8	4	0.564
50	0.28	50	0.25	0.4	1.2	4	0.536
51	0.16	60	0.25	0.4	1.2	4	0.583
52	0.28	60	0.25	0.4	0.8	4	0.540
53	0.16	50	0.15	0.4	1.2	4	0.585
54	0.28	50	0.15	0.4	0.8	4	0.531
55	0.16	60	0.15	0.4	0.8	4	0.549
56	0.28	60	0.15	0.4	1.2	4	0.565
57	0.16	50	0.25	0.8	1.2	4	0.585

Table 15 Continued

trial	alh	aps	aid	arw	awt	rep	cost
58	0.28	50	0.25	0.8	0.8	4	0.592
59	0.16	60	0.25	0.8	0.8	4	0.609
60	0.28	60	0.25	0.8	1.2	4	0.566
61	0.16	50	0.15	0.8	0.8	4	0.591
62	0.28	50	0.15	0.8	1.2	4	0.567
63	0.16	60	0.15	0.8	1.2	4	0.570
64	0.28	60	0.15	0.8	0.8	4	0.568
65	0.16	50	0.25	0.4	0.8	5	0.532
66	0.28	50	0.25	0.4	1.2	5	0.536
67	0.16	60	0.25	0.4	1.2	5	0.583
68	0.28	60	0.25	0.4	0.8	5	0.540
69	0.16	50	0.15	0.4	1.2	5	0.585
70	0.28	50	0.15	0.4	0.8	5	0.531
71	0.16	60	0.15	0.4	0.8	5	0.549
72	0.28	60	0.15	0.4	1.2	5	0.565
73	0.16	50	0.25	0.8	1.2	5	0.585
74	0.28	50	0.25	0.8	0.8	5	0.591
75	0.16	60	0.25	0.8	0.8	5	0.610
76	0.28	60	0.25	0.8	1.2	5	0.566

Table 15 Continued

trial	alh	aps	aid	arw	awt	rep	cost
77	0.16	50	0.15	0.8	0.8	5	0.591
78	0.28	50	0.15	0.8	1.2	5	0.567
79	0.16	60	0.15	0.8	1.2	5	0.570
80	0.28	60	0.15	0.8	0.8	5	0.568

Table 16: Cost+Power Results for the SWX1

trial	alh	aps	aid	arw	awt	rep	cost
1	0.16	60	0.25	0.4	0.8	1	0.593
2	0.28	60	0.25	0.4	1.2	1	0.618
3	0.16	72	0.25	0.4	1.2	1	0.626
4	0.28	72	0.25	0.4	0.8	1	0.589
5	0.16	60	0.15	0.4	1.2	1	0.619
6	0.28	60	0.15	0.4	0.8	1	0.570
7	0.16	72	0.15	0.4	0.8	1	0.569
8	0.28	72	0.15	0.4	1.2	1	0.605
9	0.16	60	0.25	0.8	1.2	1	0.636
10	0.28	60	0.25	0.8	0.8	1	0.639
11	0.16	72	0.25	0.8	0.8	1	0.637
12	0.28	72	0.25	0.8	1.2	1	0.619
13	0.16	60	0.15	0.8	0.8	1	0.619
14	0.28	60	0.15	0.8	1.2	1	0.607
15	0.16	72	0.15	0.8	1.2	1	0.615
16	0.28	72	0.15	0.8	0.8	1	0.616
17	0.16	60	0.25	0.4	0.8	2	0.593
18	0.28	60	0.25	0.4	1.2	2	0.618
19	0.16	72	0.25	0.4	1.2	2	0.625

Table 16 Continued

trial	alh	aps	aid	arw	awt	rep	cost
20	0.28	72	0.25	0.4	0.8	2	0.589
21	0.16	60	0.15	0.4	1.2	2	0.619
22	0.28	60	0.15	0.4	0.8	2	0.570
23	0.16	72	0.15	0.4	0.8	2	0.569
24	0.28	72	0.15	0.4	1.2	2	0.605
25	0.16	60	0.25	0.8	1.2	2	0.629
26	0.28	60	0.25	0.8	0.8	2	0.639
27	0.16	72	0.25	0.8	0.8	2	0.637
28	0.28	72	0.25	0.8	1.2	2	0.615
29	0.16	60	0.15	0.8	0.8	2	0.619
30	0.28	60	0.15	0.8	1.2	2	0.607
31	0.16	72	0.15	0.8	1.2	2	0.615
32	0.28	72	0.15	0.8	0.8	2	0.616
33	0.16	60	0.25	0.4	0.8	3	0.593
34	0.28	60	0.25	0.4	1.2	3	0.618
35	0.16	72	0.25	0.4	1.2	3	0.625
36	0.28	72	0.25	0.4	0.8	3	0.589
37	0.16	60	0.15	0.4	1.2	3	0.619
38	0.28	60	0.15	0.4	0.8	3	0.570

Table 16 Continued

trial	alh	aps	aid	arw	awt	rep	cost
39	0.16	72	0.15	0.4	0.8	3	0.569
40	0.28	72	0.15	0.4	1.2	3	0.605
41	0.16	60	0.25	0.8	1.2	3	0.629
42	0.28	60	0.25	0.8	0.8	3	0.639
43	0.16	72	0.25	0.8	0.8	3	0.637
44	0.28	72	0.25	0.8	1.2	3	0.615
45	0.16	60	0.15	0.8	0.8	3	0.619
46	0.28	60	0.15	0.8	1.2	3	0.607
47	0.16	72	0.15	0.8	1.2	3	0.615
48	0.28	72	0.15	0.8	0.8	3	0.619
49	0.16	60	0.25	0.4	0.8	4	0.593
50	0.28	60	0.25	0.4	1.2	4	0.618
51	0.16	72	0.25	0.4	1.2	4	0.625
52	0.28	72	0.25	0.4	0.8	4	0.589
53	0.16	60	0.15	0.4	1.2	4	0.619
54	0.28	60	0.15	0.4	0.8	4	0.570
55	0.16	72	0.15	0.4	0.8	4	0.569
56	0.28	72	0.15	0.4	1.2	4	0.605
57	0.16	60	0.25	0.8	1.2	4	0.629

Table 16 Continued

trial	alh	aps	aid	arw	awt	rep	cost
58	0.28	60	0.25	0.8	0.8	4	0.639
59	0.16	72	0.25	0.8	0.8	4	0.637
60	0.28	72	0.25	0.8	1.2	4	0.615
61	0.16	60	0.15	0.8	0.8	4	0.619
62	0.28	60	0.15	0.8	1.2	4	0.607
63	0.16	72	0.15	0.8	1.2	4	0.615
64	0.28	72	0.15	0.8	0.8	4	0.616
65	0.16	60	0.25	0.4	0.8	5	0.593
66	0.28	60	0.25	0.4	1.2	5	0.618
67	0.16	72	0.25	0.4	1.2	5	0.625
68	0.28	72	0.25	0.4	0.8	5	0.589
69	0.16	60	0.15	0.4	1.2	5	0.619
70	0.28	60	0.15	0.4	0.8	5	0.570
71	0.16	72	0.15	0.4	0.8	5	0.569
72	0.28	72	0.15	0.4	1.2	5	0.605
73	0.16	60	0.25	0.8	1.2	5	0.629
74	0.28	60	0.25	0.8	0.8	5	0.639
75	0.16	72	0.25	0.8	0.8	5	0.637
76	0.28	72	0.25	0.8	1.2	5	0.615

Table 16 Continued

trial	alh	aps	aid	arw	awt	rep	cost
77	0.16	60	0.15	0.8	0.8	5	0.619
78	0.28	60	0.15	0.8	1.2	5	0.607
79	0.16	72	0.15	0.8	1.2	5	0.615
80	0.28	72	0.15	0.8	0.8	5	0.616

Table 17: Rework Results for the CR-6 SE

trial	alh	aps	aid	arw	awt	rep	cost	time
1	0.16	50	0.25	0.4	0.8	1	0.564	18098
2	0.28	50	0.25	0.4	1.2	1	0.536	8741
3	0.16	60	0.25	0.4	1.2	1	0.583	14493
4	0.28	60	0.25	0.4	0.8	1	1.103	10281
5	0.16	50	0.15	0.4	1.2	1	0.584	14914
6	0.28	50	0.15	0.4	0.8	1	0.531	10423
7	0.16	60	0.15	0.4	0.8	1	0.549	16648
8	0.28	60	0.15	0.4	1.2	1	0.565	8534
9	0.16	50	0.25	0.8	1.2	1	0.585	15085
10	0.28	50	0.25	0.8	0.8	1	0.592	10624
11	0.16	60	0.25	0.8	0.8	1	0.798	16870
12	0.28	60	0.25	0.8	1.2	1	0.566	8645
13	0.16	50	0.15	0.8	0.8	1	0.591	17046
14	0.28	50	0.15	0.8	1.2	1	0.567	9012
15	0.16	60	0.15	0.8	1.2	1	0.570	13488
16	0.28	60	0.15	0.8	0.8	1	0.568	9574
17	0.16	50	0.25	0.4	0.8	2	0.564	18042
18	0.28	50	0.25	0.4	1.2	2	0.536	8743
19	0.16	60	0.25	0.4	1.2	2	0.583	14469

Table 17 Continued

trial	alh	aps	aid	arw	awt	rep	cost	time
20	0.28	60	0.25	0.4	0.8	2	0.728	10215
21	0.16	50	0.15	0.4	1.2	2	0.772	14903
22	0.28	50	0.15	0.4	0.8	2	0.530	10199
23	0.16	60	0.15	0.4	0.8	2	0.549	16652
24	0.28	60	0.15	0.4	1.2	2	0.570	10149
25	0.16	50	0.25	0.8	1.2	2	0.772	15141
26	0.28	50	0.25	0.8	0.8	2	0.592	10624
27	0.16	60	0.25	0.8	0.8	2	0.610	16837
28	0.28	60	0.25	0.8	1.2	2	0.566	8597
29	0.16	50	0.15	0.8	0.8	2	0.590	16923
30	0.28	50	0.15	0.8	1.2	2	0.557	8932
31	0.16	60	0.15	0.8	1.2	2	0.580	13389
32	0.28	60	0.15	0.8	0.8	2	0.568	9521
33	0.16	50	0.25	0.4	0.8	3	0.563	17930
34	0.28	50	0.25	0.4	1.2	3	0.536	8777
35	0.16	60	0.25	0.4	1.2	3	0.583	14478
36	0.28	60	0.25	0.4	0.8	3	0.540	10199
37	0.16	50	0.15	0.4	1.2	3	0.585	15060
38	0.28	50	0.15	0.4	0.8	3	0.531	10345

Table 17 Continued

trial	alh	aps	aid	arw	awt	rep	cost	time
39	0.16	60	0.15	0.4	0.8	3	0.550	16658
40	0.28	60	0.15	0.4	1.2	3	0.565	8492
41	0.16	50	0.25	0.8	1.2	3	0.585	15108
42	0.28	50	0.25	0.8	0.8	3	0.967	10704
43	0.16	60	0.25	0.8	0.8	3	0.610	16864
44	0.28	60	0.25	0.8	1.2	3	0.566	8587
45	0.16	50	0.15	0.8	0.8	3	0.591	17046
46	0.28	50	0.15	0.8	1.2	3	0.577	12589
47	0.16	60	0.15	0.8	1.2	3	0.570	13465
48	0.28	60	0.15	0.8	0.8	3	0.568	9466
49	0.16	50	0.25	0.4	0.8	4	0.564	18026
50	0.28	50	0.25	0.4	1.2	4	0.536	8733
51	0.16	60	0.25	0.4	1.2	4	0.583	14448
52	0.28	60	0.25	0.4	0.8	4	0.540	10118
53	0.16	50	0.15	0.4	1.2	4	0.585	15063
54	0.28	50	0.15	0.4	0.8	4	0.531	10421
55	0.16	60	0.15	0.4	0.8	4	0.549	16653
56	0.28	60	0.15	0.4	1.2	4	0.565	8480
57	0.16	50	0.25	0.8	1.2	4	0.585	15115

Table 17 Continued

trial	alh	aps	aid	arw	awt	rep	cost	time
58	0.28	50	0.25	0.8	0.8	4	0.779	10676
59	0.16	60	0.25	0.8	0.8	4	0.796	16507
60	0.28	60	0.25	0.8	1.2	4	0.566	8580
61	0.16	50	0.15	0.8	0.8	4	0.591	17065
62	0.28	50	0.15	0.8	1.2	4	0.567	8944
63	0.16	60	0.15	0.8	1.2	4	0.570	13478
64	0.28	60	0.15	0.8	0.8	4	0.568	9448
65	0.16	50	0.25	0.4	0.8	5	0.532	17634
66	0.28	50	0.25	0.4	1.2	5	0.536	8736
67	0.16	60	0.25	0.4	1.2	5	0.583	14360
68	0.28	60	0.25	0.4	0.8	5	0.540	10200
69	0.16	50	0.15	0.4	1.2	5	0.585	15026
70	0.28	50	0.15	0.4	0.8	5	0.531	10422
71	0.16	60	0.15	0.4	0.8	5	0.549	16565
72	0.28	60	0.15	0.4	1.2	5	0.565	8538
73	0.16	50	0.25	0.8	1.2	5	0.585	15122
74	0.28	50	0.25	0.8	0.8	5	0.591	10579
75	0.16	60	0.25	0.8	0.8	5	0.797	16836
76	0.28	60	0.25	0.8	1.2	5	0.566	8582

Table 17 Continued

trial	alh	aps	aid	arw	awt	rep	cost	time
77	0.16	50	0.15	0.8	0.8	5	0.591	17058
78	0.28	50	0.15	0.8	1.2	5	0.567	8958
79	0.16	60	0.15	0.8	1.2	5	0.570	13462
80	0.28	60	0.15	0.8	0.8	5	0.568	9459

Table 18: Rework Results for the SWX1

trial	alh	aps	aid	arw	awt	rep	cost	time
1	0.16	60	0.25	0.4	0.8	1	0.781	16946
2	0.28	60	0.25	0.4	1.2	1	1.368	9136
3	0.16	72	0.25	0.4	1.2	1	0.626	12906
4	0.28	72	0.25	0.4	0.8	1	1.339	9831
5	0.16	60	0.15	0.4	1.2	1	0.619	14617
6	0.28	60	0.15	0.4	0.8	1	1.320	10262
7	0.16	72	0.15	0.4	0.8	1	1.319	14615
8	0.28	72	0.15	0.4	1.2	1	0.980	7832
9	0.16	60	0.25	0.8	1.2	1	0.636	18254
10	0.28	60	0.25	0.8	0.8	1	1.201	9572
11	0.16	72	0.25	0.8	0.8	1	0.637	13550
12	0.28	72	0.25	0.8	1.2	1	0.994	9706
13	0.16	60	0.15	0.8	0.8	1	1.369	14795
14	0.28	60	0.15	0.8	1.2	1	0.607	8822
15	0.16	72	0.15	0.8	1.2	1	0.802	12605
16	0.28	72	0.15	0.8	0.8	1	1.366	8166
17	0.16	60	0.25	0.4	0.8	2	0.593	16882
18	0.28	60	0.25	0.4	1.2	2	1.368	9101
19	0.16	72	0.25	0.4	1.2	2	0.625	12872

Table 18 Continued

trial	alh	aps	aid	arw	awt	rep	cost	time
20	0.28	72	0.25	0.4	0.8	2	1.339	9827
21	0.16	60	0.15	0.4	1.2	2	0.619	14566
22	0.28	60	0.15	0.4	0.8	2	1.320	10184
23	0.16	72	0.15	0.4	0.8	2	1.319	14696
24	0.28	72	0.15	0.4	1.2	2	0.980	7843
25	0.16	60	0.25	0.8	1.2	2	0.816	14684
26	0.28	60	0.25	0.8	0.8	2	1.201	9638
27	0.16	72	0.25	0.8	0.8	2	1.387	13674
28	0.28	72	0.25	0.8	1.2	2	0.990	7834
29	0.16	60	0.15	0.8	0.8	2	0.806	14702
30	0.28	60	0.15	0.8	1.2	2	0.795	8863
31	0.16	72	0.15	0.8	1.2	2	0.802	12632
32	0.28	72	0.15	0.8	0.8	2	1.366	8234
33	0.16	60	0.25	0.4	0.8	3	0.593	16897
34	0.28	60	0.25	0.4	1.2	3	1.368	9117
35	0.16	72	0.25	0.4	1.2	3	0.625	12872
36	0.28	72	0.25	0.4	0.8	3	1.339	9825
37	0.16	60	0.15	0.4	1.2	3	0.619	14660
38	0.28	60	0.15	0.4	0.8	3	1.320	10214

Table 18 Continued

trial	alh	aps	aid	arw	awt	rep	cost	time
39	0.16	72	0.15	0.4	0.8	3	1.319	14594
40	0.28	72	0.15	0.4	1.2	3	0.980	7835
41	0.16	60	0.25	0.8	1.2	3	0.816	14606
42	0.28	60	0.25	0.8	0.8	3	1.201	9547
43	0.16	72	0.25	0.8	0.8	3	1.387	13621
44	0.28	72	0.25	0.8	1.2	3	0.990	7807
45	0.16	60	0.15	0.8	0.8	3	0.807	14712
46	0.28	60	0.15	0.8	1.2	3	0.795	8871
47	0.16	72	0.15	0.8	1.2	3	0.802	12635
48	0.28	72	0.15	0.8	0.8	3	1.369	9890
49	0.16	60	0.25	0.4	0.8	4	0.593	16913
50	0.28	60	0.25	0.4	1.2	4	1.368	9095
51	0.16	72	0.25	0.4	1.2	4	0.625	12869
52	0.28	72	0.25	0.4	0.8	4	1.339	9802
53	0.16	60	0.15	0.4	1.2	4	0.619	14664
54	0.28	60	0.15	0.4	0.8	4	1.320	10252
55	0.16	72	0.15	0.4	0.8	4	1.319	14590
56	0.28	72	0.15	0.4	1.2	4	0.980	7838
57	0.16	60	0.25	0.8	1.2	4	0.816	14659

Table 18 Continued

trial	alh	aps	aid	arw	awt	rep	cost	time
58	0.28	60	0.25	0.8	0.8	4	1.201	9549
59	0.16	72	0.25	0.8	0.8	4	1.387	13670
60	0.28	72	0.25	0.8	1.2	4	0.803	7767
61	0.16	60	0.15	0.8	0.8	4	0.807	14778
62	0.28	60	0.15	0.8	1.2	4	0.795	8866
63	0.16	72	0.15	0.8	1.2	4	0.802	12575
64	0.28	72	0.15	0.8	0.8	4	1.366	8214
65	0.16	60	0.25	0.4	0.8	5	0.593	16885
66	0.28	60	0.25	0.4	1.2	5	1.368	9101
67	0.16	72	0.25	0.4	1.2	5	0.625	12788
68	0.28	72	0.25	0.4	0.8	5	1.339	9828
69	0.16	60	0.15	0.4	1.2	5	0.619	14655
70	0.28	60	0.15	0.4	0.8	5	1.320	10143
71	0.16	72	0.15	0.4	0.8	5	1.319	14669
72	0.28	72	0.15	0.4	1.2	5	0.793	7790
73	0.16	60	0.25	0.8	1.2	5	0.816	14609
74	0.28	60	0.25	0.8	0.8	5	1.201	9537
75	0.16	72	0.25	0.8	0.8	5	1.387	13702
76	0.28	72	0.25	0.8	1.2	5	0.803	7807

Table 18 Continued

trial	alh	aps	aid	arw	awt	rep	cost	time
77	0.16	60	0.15	0.8	0.8	5	0.806	14695
78	0.28	60	0.15	0.8	1.2	5	0.795	8876
79	0.16	72	0.15	0.8	1.2	5	0.615	12591
80	0.28	72	0.15	0.8	0.8	5	1.366	8221

Table 19: Quality Score Card for the CR6

CR-6 SE Inspection Score Card												
#	Criteria	weight	Option 1		Option 2		Option 3		Option 4		Option 5	
			rating	score	rating	score	rating	score	rating	score	rating	score
1	F/ N		0	0	0	0	0	0	0	0	0	0
	Tactile	200	100%	200	100%	200	100%	200	100%	200	100%	200
	Hedonic	150	100%	150	100%	150	100%	150	100%	150	100%	150
	Visual	100	100%	100	100%	100	100%	100	100%	100	100%	100
	Totals	450		450		450		450		450		450
2	F/N		0	0	0	0	0	0	0	0	0	0
	Tactile	200	100%	200	100%	200	100%	200	100%	200	100%	200
	Hedonic	150	100%	150	100%	150	100%	150	100%	150	100%	150
	Visual	100	100%	100	100%	100	100%	100	100%	100	100%	100
	Totals	450		450		450		450		450		450
3	F/N		0	0	0	0	0	0	0	0	0	0
	Tactile	200	100%	200	100%	200	100%	200	100%	200	100%	200
	Hedonic	150	100%	150	100%	150	100%	150	100%	150	100%	150
	Visual	100	100%	100	100%	100	100%	100	100%	100	100%	100
	Totals	450		450		450		450		450		450
4	F/N		0	0	0	0	0	0	0	0	0	0
	Tactile	200	100%	200	100%	200	100%	200	100%	200	100%	200
	Hedonic	150	100%	150	100%	150	100%	150	100%	150	100%	150
	Visual	100	100%	100	100%	100	100%	100	100%	100	100%	100
	Totals	450		450		450		450		450		450

Table 19 Continued

#	Criteria	weight	Option 1		Option 2		Option 3		Option 4		Option 5	
			rating	score	rating	score	rating	score	rating	score	rating	score
5	F/N		0	0	0	0	0	0	0	0	0	0
	Tactile	200	50%	100	75%	150	100%	200	100%	200	100%	200
	Hedonic	150	50%	75	100%	150	100%	150	100%	150	100%	150
	Visual	100	75%	75	100%	100	100%	100	100%	100	100%	100
	Totals	450		250		400		450		450		450
6	F/N		0	0	0	0	0	0	0	0	0	0
	Tactile	200	100%	200	75%	150	100%	200	100%	200	100%	200
	Hedonic	150	100%	150	100%	150	100%	150	100%	150	100%	150
	Visual	100	100%	100	100%	100	100%	100	100%	100	100%	100
	Totals	450		450		400		450		450		450
7	F/N		0	0	0	0	0	0	0	0	0	0
	Tactile	200	100%	200	100%	200	100%	200	100%	200	100%	200
	Hedonic	150	100%	150	100%	150	100%	150	100%	150	100%	150
	Visual	100	100%	100	100%	100	100%	100	100%	100	100%	100
	Totals	450		450		450		450		450		450
8	F/N		0	0	0	0	0	0	0	0	0	0
	Tactile	200	100%	200	100%	200	100%	200	100%	200	100%	200
	Hedonic	150	100%	150	100%	150	100%	150	100%	150	100%	150
	Visual	100	100%	100	100%	100	100%	100	100%	100	100%	100
	Totals	450		450		450		450		450		450
9	F/N		0	0	0	0	0	0	0	0	0	0

Table 19 Continued

#	Criteria	weight	Option 1		Option 2		Option 3		Option 4		Option 5	
			rating	score	rating	score	rating	score	rating	score	rating	score
	Tactile	200	100%	200	100%	200	100%	200	100%	200	100%	200
	Hedonic	150	100%	150	100%	150	100%	150	100%	150	100%	150
	Visual	100	100%	100	100%	100	100%	100	100%	100	100%	100
	Totals	450		450		450		450		450		450
10	F/N		0	0	0	0	0	0	0	0	0	0
	Tactile	200	100%	200	75%	150	100%	200	100%	200	100%	200
	Hedonic	150	100%	150	100%	150	100%	150	100%	150	100%	150
	Visual	100	100%	100	100%	100	100%	100	100%	100	100%	100
	Totals	450		450		400		450		450		450
11	F/N		0	0	0	0	0	0	0	0		0
	Tactile	200	100%	200	100%	200	75%	150	75%	150	100%	200
	Hedonic	150	100%	150	100%	150	100%	150	100%	150	100%	150
	Visual	100	100%	100	100%	100	75%	75	100%	100	100%	100
	Totals	450		450		450		375		400		450
12	F/N		0	0	0	0	0	0	0	0	0	0
	Tactile	200	75%	150	100%	200	100%	200	75%	150	75%	150
	Hedonic	150	100%	150	100%	150	100%	150	100%	150	100%	150
	Visual	100	100%	100	100%	100	100%	100	100%	100	100%	100
	Totals	450		400		450		450		400		400
13	F/N		0	0	0	0	0	0	0	0	0	0
	Tactile	200	100%	200	100%	200	100%	200	100%	200	100%	200

Table 19 Continued

#	Criteria	weight	Option 1		Option 2		Option 3		Option 4		Option 5	
			rating	score	rating	score	rating	score	rating	score	rating	score
	Hedonic	150	100%	150	100%	150	100%	150	100%	150	100%	150
	Visual	100	100%	100	100%	100	100%	100	100%	100	100%	100
	Totals	450		450		450		450		450		450
14	F/N		0	0	0	0	0	0	0	0	0	0
	Tactile	200	100%	200	100%	200	100%	200	100%	200	100%	200
	Hedonic	150	100%	150	100%	150	100%	150	100%	150	100%	150
	Visual	100	100%	100	100%	100	100%	100	100%	100	100%	100
	Totals	450		450		450		450		450		450
15	F/N		0	0	0	0	0	0	0	0	0	0
	Tactile	200	100%	200	100%	200	100%	200	100%	200	100%	200
	Hedonic	150	100%	150	100%	150	100%	150	100%	150	100%	150
	Visual	100	100%	100	100%	100	100%	100	100%	100	100%	100
	Totals	450		450		450		450		450		450
16	F/N		0	0	0	0	0	0	0	0	0	0
	Tactile	200	100%	200	100%	200	100%	200	100%	200	100%	200
	Hedonic	150	100%	150	100%	150	100%	150	100%	150	100%	150
	Visual	100	100%	100	100%	100	100%	100	100%	100	100%	100
	Totals	450		450		450		450		450		450
17	F/N		0	0	0	0	0	0	0	0	0	0
	Tactile	200	100%	200	100%	200	100%	200	100%	200	100%	200
	Hedonic	150	100%	150	100%	150	100%	150	100%	150	100%	150

Table 19 Continued

#	Criteria	weight	Option 1		Option 2		Option 3		Option 4		Option 5	
			rating	score	rating	score	rating	score	rating	score	rating	score
	Visual	100	100%	100	100%	100	100%	100	100%	100	100%	100
	Totals	450		450		450		450		450		450
Functional (F) 0												
Nonfunctional (N) 1												

Table 20: Quality Score Card for the SWX1

SWX1 Inspection Score Card												
Run	Criteria	weight	Option 1		Option 2		Option 3		Option 4		Option 5	
			rating	score	rating	score	rating	score	rating	score	rating	score
1			0	0	0	0	0	0		0		0
	Tactile	200	100%	200	100%	200	100%	200	100%	200	100%	200
	Hedonic	150	100%	150	100%	150	100%	150	100%	150	100%	150
	Visual	100	100%	100	100%	100	100%	100	100%	100	100%	100
	Totals	450		450		450		450		450		450
2				0		0		0		0		0
	Tactile	200	75%	150	100%	200	100%	200	100%	200	100%	200
	Hedonic	150	100%	150	100%	150	100%	150	100%	150	100%	150
	Visual	100	100%	100	100%	100	100%	100	100%	100	100%	100
	Totals	450		400		450		450		450		450
3				0		0		0		0		0
	Tactile	200	25%	50	25%	50	25%	50	25%	50	25%	50
	Hedonic	150	25%	37.5	25%	37.5	25%	37.5	25%	37.5	25%	37.5
	Visual	100	25%	25	25%	25	25%	25	25%	25	25%	25
	Totals	450		112.5		112.5		112.5		112.5		112.5
4				0		0		0		0		0
	Tactile	200	100%	200	100%	200	100%	200	100%	200	100%	200
	Hedonic	150	100%	150	100%	150	100%	150	100%	150	100%	150
	Visual	100	100%	100	100%	100	100%	100	100%	100	100%	100
	Totals	450		450		450		450		450		450

Table 20 Continued

Run	Criteria	weight	Option 1		Option 2		Option 3		Option 4		Option 5	
			rating	score	rating	score	rating	score	rating	score	rating	score
5				0		0		0	0	0	0	0
	Tactile	200	25%	50	25%	50	25%	50	25%	50	25%	50
	Hedonic	150	25%	37.5	25%	37.5	25%	37.5	25%	37.5	25%	37.5
	Visual	100	25%	25	25%	25	25%	25	25%	25	25%	25
	Totals	450		112.5		112.5		112.5		112.5		112.5
6				0		0		0		0	0	0
	Tactile	200	100%	200	100%	200	100%	200	100%	200	100%	200
	Hedonic	150	100%	150	100%	150	100%	150	100%	150	100%	150
	Visual	100	100%	100	100%	100	100%	100	100%	100	100%	100
	Totals	450		450		450		450		450		450
7				0		0		0		0	1	0
	Tactile	200	25%	50	25%	50	25%	50	25%	50	25%	50
	Hedonic	150	25%	37.5	25%	37.5	25%	37.5	25%	37.5	25%	37.5
	Visual	100	25%	25	25%	25	25%	25	25%	25	25%	25
	Totals	450		112.5		112.5		112.5		112.5		112.5
8				0		0		0		0		0
	Tactile	200	25%	50	25%	50	25%	50	25%	50	25%	50
	Hedonic	150	25%	37.5	25%	37.5	25%	37.5	25%	37.5	25%	37.5
	Visual	100	25%	25	25%	25	25%	25	25%	25	25%	25
	Totals	450		112.5		112.5		112.5		112.5		112.5
9				0		0		0		0		0

Table 20 Continued

Run	Criteria	weight	Option 1		Option 2		Option 3		Option 4		Option 5	
			rating	score	rating	score	rating	score	rating	score	rating	score
	Tactile	200	75%	150	75%	150	75%	150	75%	150	75%	150
	Hedonic	150	75%	112.5	75%	112.5	75%	112.5	75%	112.5	100%	150
	Visual	100	75%	75	75%	75	75%	75	75%	75	100%	100
	Totals	450		337.5		337.5		337.5		337.5		400
10				0		0		0		0		0
	Tactile	200	100%	200	75%	150	75%	150	75%	150	75%	150
	Hedonic	150	100%	150	100%	150	100%	150	100%	150	100%	150
	Visual	100	100%	100	100%	100	100%	100	100%	100	100%	100
	Totals	450		450		400		400		400		400
11				0		0		0		0		0
	Tactile	200	50%	100	50%	100	50%	100	50%	100	50%	100
	Hedonic	150	75%	112.5	75%	112.5	50%	75	50%	75	50%	75
	Visual	100	75%	75	75%	75	75%	75	75%	75	75%	75
	Totals	450		287.5		287.5		250		250		250
12				0		0		0		0		0
	Tactile	200	100%	200	50%	100	50%	100	50%	100	50%	100
	Hedonic	150	100%	150	50%	75	50%	75	50%	75	50%	75
	Visual	100	100%	100	50%	50	50%	50	50%	50	50%	50
	Totals	450		450		225		225		225		225
13				0		0		0		0		0
	Tactile	200	50%	100	50%	100	50%	100	75%	150	75%	150

Table 20 Continued

Run	Criteria	weight	Option 1		Option 2		Option 3		Option 4		Option 5	
			rating	score	rating	score	rating	score	rating	score	rating	score
	Hedonic	150	100%	150	100%	150	100%	150	100%	150	100%	150
	Visual	100	100%	100	100%	100	100%	100	100%	100	100%	100
	Totals	450		350		350		350		400		400
14				0		0		0		0		0
	Tactile	200	50%	100	75%	150	75%	150	75%	150	75%	150
	Hedonic	150	50%	75	100%	150	100%	150	100%	150	100%	150
	Visual	100	50%	50	100%	100	100%	100	100%	100	100%	100
	Totals	450		225		400		400		400		400
15				0		0		0		0		0
	Tactile	200	100%	200	75%	150	75%	150	75%	150	75%	150
	Hedonic	150	100%	150	100%	150	100%	150	100%	150	100%	150
	Visual	100	100%	100	100%	100	100%	100	100%	100	100%	100
	Totals	450		450		400		400		400		400
16				0		0		0		0		0
	Tactile	200	75%	150	75%	150	75%	150	75%	150	100%	200
	Hedonic	150	100%	150	100%	150	100%	150	100%	150	100%	150
	Visual	100	100%	100	100%	100	100%	100	100%	100	100%	100
	Totals	450		400		400		400		400		450
17				0		0		0	0	0		0
	Tactile	200	25%	50	25%	50	25%	50	25%	50	25%	50
	Hedonic	150	25%	37.5	25%	37.5	25%	37.5	25%	37.5	25%	37.5

Table 20 Continued

Run	Criteria	weight	Option 1		Option 2		Option 3		Option 4		Option 5	
			rating	score	rating	score	rating	score	rating	score	rating	score
	Visual	100	25%	25	25%	25	25%	25	25%	25	25%	25
	Totals	450		112.5		112.5		112.5		112.5		112.5
Functional (F) 0												
Nonfunctional (N) 1												

APPENDIX B - REPEATABILITY

Prerequisites

Install Docker

- See Install Docker Engine (https://docs.docker.com/engine/install/)

Installation

10. Clone the repo

```
git clone https://github.com/wilsongis/3DP_Experiments.git
```

2. Enter workspace folder

```
cd 3DP-Experiments
```

3. Create ML Workspace

```
docker run -d \
    -p 8080:8080 \
   --name "3DP-workspace" \
   -v "$(PWD):/workspace" \
   --env AUTHENTICATE_VIA_JUPYTER="mytoken" \
    --shm-size 512m \
   --restart always \
```

mltooling/ml-workspace:0.12.1

4. Install Python Packages

pip install -U pip setuptools wheel pip install -r requirements.txt conda install -c conda-forge pyomo conda install -c conda-forge ipopt glpk conda install -c r r-irkernel

Updating

This will override your existing requirements.txt. If you want to append, use >> instead of >

pip list --format=freeze > requirements.txt

VITA

Originally from Pennsylvania, Mike Wilson grew up in Philadelphia, Pennsylvania. After High School, Mike attended Kutztown University and received a Bachelor of Science degree in Geology. Upon graduation, Mike was accepted to the Master of Science in Geosciences at Murray State University where he received his degree in 2003. In 2014, Mike applied and was accepted to the graduate program at the University of Tennessee, Knoxville to pursue a Doctor of Philosophy degree in Industrial Engineering with a concentration in Engineering Management. His research interests include GIS, 3D printing, VR. And STEM. Upon graduation, Mike will continue his position at the Austin Peay State University GIS Center as Director.